

**Aus dem Institut für Immunologie und Transfusionsmedizin
(Direktorin Prof. Dr. Christine Schütt)
der Medizinischen Fakultät der Ernst-Moritz-Arndt-Universität Greifswald**

Expression of the T cell regulatory molecule ICOS (CD278) and LICOS (CD275) on human blood cells

**Inaugural Dissertation
zur
Erlangung des akademischen Grades
Doktor der Naturwissenschaften in der Medizin (Dr. rer. med.)
der
Medizinischen Fakultät
der
Ernst-Moritz-Arndt-Universität
Greifswald
2006**

vorgelegt von: Ionela Moanta
geb. am: 10.03.1976
in: Craiova, Rumänien

Dekan: Prof. Dr. H. K. Kroemer

1. Gutachter: Frau Prof. Dr. B. Bröker (Greifswald)

2. Gutachter: Herr Prof. Dr. R. E. Schmidt (Hannover)

(3. Gutachter:) Frau PD Dr. E. Kauschke (Giessen)

Ort, Raum: Greifswald, Fleischmannstr. 6, Seminarraum 305

Tag der Disputation: 13. August 2007

Table of Contents

1. Introduction.....	1
1.1 The innate immunity.....	1
1.2 The adaptive immunity	2
1.2.1 B-cells and T-cells	3
1.2.2 Th1 and Th2 cells.....	4
1.2.3 T regulatory cells (T _{reg})	5
1.3 T cell response.....	6
1.3.1 TCR engagement – signal 1	6
1.3.2 Costimulation – signal 2	6
1.3.2.1 Costimulatory molecules	6
1.3.2.1.1 The Inducible Costimulator (ICOS).....	9
1.3.2.1.2 The Inducible Costimulator Ligand (LICOS).....	10
1.3.2.2 Functions of ICOS and LICOS.....	11
1.3.2.2.1 The role of ICOS and LICOS in T cell proliferation and cytokine production.....	11
1.3.2.2.2 The role of ICOS and LICOS in Th1 and Th2 responses	12
1.3.2.2.3 The role of ICOS and LICOS in humoral response.....	14
1.4 Sepsis – at the interface between innate and adaptive immunity	16
1.4.1 Trauma as risk factor for sepsis.....	18
1.4.2 Mechanisms of immunosuppression in polytrauma and sepsis.....	19
1.4.2.1 Biased Th2 responses.....	19
1.4.2.2 Loss of antigen presentation and costimulatory capacity of monocytes.....	20
1.4.2.3 Other immunosuppressive mechanisms	21
1.4.3 Mechanisms of immunosuppression in stroke	21
1.5 Aim of the study	22
2. Material and Methods.....	23
2.1 Materials.....	23
2.1.1 Laboratory equipment.....	23
2.1.2 Reagents	24
2.1.3 Consumables and kits	26
2.1.4 Biological material.....	28
2.1.5 Plasmids.....	28
2.1.6 Enzymes	29
2.1.7 Culture media	29
2.1.7.1 Media for bacteria	29
2.1.7.2 Media for cell lines and hybridoma.....	30
2.1.8 Buffers and stock solutions.....	30
2.1.8.1 Molecular biology methods	30

2.1.8.2 Biochemical Methods	31
2.1.8.3 Cell culture methods	32
2.1.9 Antibodies	33
2.1.9.1 ELISA.....	33
2.1.9.2 Western blot	33
2.1.9.3 Flowcytometry	34
2.1.9.3.1 Labelled antibodies	34
2.1.9.3.2 Labelled isotype controls.....	34
2.1.9.3.3 Primary and blocking antibodies.....	35
2.1.9.3.4 Secondary antibodies and conjugates.....	35
2.1.10 Fusion proteins	35
2.2 Methods	36
2.2.1 Molecular biology methods	36
2.2.1.1 Primers.....	36
2.2.1.2 Polymerase chain reaction (PCR).....	36
2.2.1.3 DNA gel electrophoresis.....	37
2.2.1.4 Agarose gel extraction of DNA fragments	37
2.2.1.5 Quantitation of DNA.....	37
2.2.1.6 Restriction digestion of DNA.....	38
2.2.1.7 Ligation of DNA fragments.....	38
2.2.1.8 Storage of DNA and of bacteria strains	39
2.2.1.9 Initiation of bacterial culture	39
2.2.1.10 Plasmid preparation from bacteria	39
2.2.1.10.1 Plasmid Mini Prep	39
2.2.1.10.2 Plasmid Maxi Prep.....	39
2.2.1.11 Transformation of competent bacteria	40
2.2.1.12 DNA sequencing.....	40
2.2.2 Biochemical methods.....	41
2.2.2.1 SDS-PAGE of proteins	41
2.2.2.2 Western blotting.....	41
2.2.2.3 Purification of LICOS-Ig and anti-LICOS HGW1.....	42
2.2.2.4 Estimation of the protein concentration	42
2.2.2.5 Biotinylation of LICOS-Ig fusion protein and anti-LICOS mAb HGW1 and Alexa Fluor® 647 labeling of anti-LICOS mAb HGW1.....	43
2.2.2.6 ELISA and competitive ELISA.....	43
2.2.3 Cell culture methods	44
2.2.3.1 General conditions of cell culture and sterile techniques.....	44
2.2.3.2 Cell lines culture	44
2.2.3.3 Determination of cell count and viability.....	45
2.2.3.4 Cryoconservation and recovery of cell lines.....	45

2.2.3.5 Transfection of eukaryotic cells	45
2.2.3.5.1 Transfection of COS cells with PolyFect Reagent	45
2.2.3.5.2 Transfection of COS cells with DEAE-Dextran and chloroquine	46
2.2.3.6 Stabilization of SKMel LICOS phenotype by limiting dilution	46
2.2.3.7 Isolation and PHA stimulation of PBMC	46
2.2.3.8 Cytocentrifugation and immunohistochemical staining (SKMel, PBMC)	47
2.2.3.9 Positive selection of CD19+ lymphocytes from PBMC	47
2.2.3.10 Flowcytometry	47
2.2.3.10.1 FACS staining of LICOS on the surface of SKMel LICOS cells	47
2.2.3.10.2 FACS staining of PBMC, purified CD19+ lymphocytes and Raji cells	48
2.2.3.10.3 FACS staining of whole blood cells	48
2.2.3.10.4 FACS data analysis	49
2.2.4 Patients and controls	50
2.2.5 Generation and production of an anti-LICOS mAb (HGW1) using LICOS-Ig as an antigen	51
2.2.5.1 Immunization of mice	52
2.2.5.2 Cell fusion and selection of hybridomas	52
2.2.5.3 Screening of primary hybridoma supernatants	53
2.2.5.4 Establishment of hybridoma line	54
2.2.5.5 Cultivation of hybridoma cells for high antibody production	54
3. Results	55
3.1 Cloning of the extracellular domain of LICOS and construction of the sequencing vector	55
3.2 Construction of the expression vector	60
3.3 Expression and purification of the LICOS-Ig fusion protein	63
3.4 Characterization of biotinylated LICOS-Ig fusion protein in Western Blot, ELISA, FACS analysis and microscopy	65
3.5 Generation and characterization of an anti-LICOS mAb (HGW1)	69
3.6 Binding of HGW1 Alexa 647 to whole blood cells	72
3.7 Competition assays	74
3.8 Comparison of HGW1 preparations binding to native LICOS	79
3.9 Expression of HLA-DR, CD86, LICOS and ICOS in patients with major trauma and stroke in a pilot study	83
3.9.1 Expression of HLA-DR, CD86 and LICOS on CD14+ monocytes	85
3.9.2 Expression of HLA-DR, CD86 and LICOS on CD19+ lymphocytes	86
3.9.3 Expression of HLA-DR and LICOS on CD3+ lymphocytes	86
3.9.4 Expression of ICOS and CD4 on CD3+ lymphocytes	87
3.9.5 Expression of HLA-DR on CD4+ lymphocytes	87
4. Discussion	99
4.1 Generation of the LICOS-Ig fusion protein and of an anti-LICOS mAb (HGW1)	99
4.2 Expression of HLA-DR, CD86, LICOS and ICOS in patients with major trauma and stroke	101

4.2.1 Expression of HLA-DR, CD86 and LICOS on CD14+ monocytes.....	101
4.2.2 Expression of HLA-DR, CD86 and LICOS on CD19+ lymphocytes	103
4.2.3 Expression of HLA-DR and LICOS on CD3+ lymphocytes	104
4.2.4 Expression of ICOS and CD4 on CD3+ lymphocytes	104
5. Conclusions.....	107
6. Summary	108
7. Bibliography	110

Abbreviations

AA	amino acid
Ag	antigen
Ab	antibody
AILIM	activation-inducible lymphocyte immunomediatory molecule
ah	Armenian hamster
Amp	ampicillin
APACHE II	acute physiology and chronic health evaluation
APC	antigen presenting cells
APS	ammoniumpersulfat
ATCC	American Type Culture Collection
B7-H	B7 homologous
B7RP-1	B7-related protein 1
BCA	bicinchoninic acid
BCR	B cell receptor
Bp	base pairs
BSA	bovine serum albumin
BTLA	B and T lymphocyte attenuator
CARS	compensatory anti-inflammatory response syndrome
CIA	collagen-induced arthritis
CD	cluster of differentiation
cDNA	complementary DNA
CLP	cecal ligation and puncture
CRP	C-reactive protein
CTL	cytotoxic T lymphocyte
CTLA-4	cytotoxic T lymphocyte antigen-4
DC	dendritic cell
DMSO	dimethyl-sulfoxide
DNA	deoxyribonucleic acid
dNTP	deoxynucleosid-5'-triphosphates
E. coli	Escherichia coli
EAE	experimental autoimmune encephalomyelitis
EBV	Epstein-Barr virus
ECL	enhanced chemiluminescence
EDTA	ethylenediaminetetraacetate
ELISA	enzyme-linked immunosorbent assay
FACS	fluorescence activated cell scanning
FCS	fetal calf serum

FITC	fluorescein-isothiocyanat
g	gravity force = 9,81 m/s ²
G3PDH	glyceraldehyde-3-phosphate-dehydrogenase
GCS	Glasgow Coma Score
GM-CSF	granulocyte-macrophage colony-stimulating-factor
GVHD	graft-versus-host disease
h	hour
HEPES	N-2-hydroxyethylpiperazine-N'-2-ethansulfonic acid
HGPRT	hypoxanthine-guanine phosphoribosil transferase
HLA	human leukocyte antigen
hu	human
HUVEC	human umbilical vein endothelial cells
HS	human serum
HT	hypoxanthine-thymidine
ICAM	intercellular adhesion molecule
ICOS	inducible costimulator
ICU	intensive care unit
IL	interleukin
Ig	immunoglobulin
IFN	interferon
IPTG	isopropyl β -D-thiogalacto-pyranoside
ISS	injury severity score
ITAM	immuno-receptor tyrosinebased activation motif
ITIM	immuno-receptor tyrosinebased inhibitory motif
Lck	lymphocyte cytoplasmic kinase
LCMV	lymphocytic choriomeningitis virus
kB	kilobase pairs
kDa	kilodalton
LB-medium	Luria-Bertani medium
LPS	lipopolysaccharide
mAb	monoclonal antibody
MHC I/II	major histocompatibility complex I/II
min	minute
mo	mouse
mRNA	messenger RNA
MVEC	microvascular endothelial cells
NFAT	nuclear factor for activation of T cells
NF- κ B	nuclear factor- κ B
NHS	hydroxy-succinimide ester
NK cell	natural killer cell

OD	optical density
PAGE	polyacrylamide gel-electrophoresis
PBMC	peripheral blood mononuclear cells
PBS	phosphate buffered saline
PCR	polymerase chain reaction
PD-1	programmed death-1
PE	phycoerythrin
PEG	polyethyleneglycol
PFA	paraformaldehyde
PHA	phytohemagglutinin
PMA	phorbol-12-myristate-13-acetate
PMN	polymorphonuclear cells
POD	peroxidase
RBC	red blood cells
RNA	ribonucleic acid
rpm	revolutions per minute
RPMI	Roswell Park Memorial Institute
RT-PCR	reverse-transcriptase-PCR
S	stroke
SD	standard deviation
SDS	sodiumdodecylsulphate
SIRS	systemic inflammatory syndrome
SKMEL	skin melanoma
STAT	signal transducer and activator of transcription
Strp	streptavidin
T	trauma
TBE-buffer	Tris/borat/EDTA-buffer
TGF- β	tumor-growthfactor- β
TE-buffer	Tris/EDTA-buffer
TCR	T-cell receptor
TEMED	tetramethylethylenediamine
Th	helper T cell
TLR	Toll-like receptor
TNF- α	tumor-necrosis factor- α
T _{reg}	regulatory T cell
Tris	2-amino-2-hydroxymethyl-propan-1,3-diol
TRITC	tetrametylrhodamine isothiocyanate
VSV	vesicular stomatitis virus
X-Gal	5-bromo-4-chloro-3-indolyl β -D-galactoside
wt	wild type

One-letter amino acid code

One-letter symbol	Amino acid
A	Alanine
C	Cysteine
D	Aspartic acid
E	Glutamic acid
F	Phenylalanine
G	Glycine
H	Histidine
I	Isoleucine
K	Lysine
L	Leucine
M	Methionine
N	Asparagine
P	Proline
Q	Glutamine
R	Arginine
S	Serine
T	Threonine
V	Valine
W	Tryptophan
X	unknown or 'other' amino acid
Y	Tyrosine

1. Introduction

To defend against microorganisms, vertebrates have evolved an intricate set of defense mechanisms - the immune response - carried out by cells and molecules that constitute the immune system. This system has the ability “to learn” to recognize an intruder and to discriminate between foreign and its own body cells in order to launch a specifically directed, finely tuned immune attack to kill and eliminate the invader while leaving the body intact (tolerance of self). When this discrimination fails, pathogens are enabled to proliferate leading to infection complications, or a fallacious attack might be directed against its own cells, a condition termed autoimmunity. This discrimination is also important in recognizing and eliminating the body constituents that become or are different from the rest (cancer cells, cells from transplanted tissue).

1.1 The innate immunity

The body's first level of defense against foreign agents is the innate (natural) immunity. This type of immunity has a broad specificity, no memory and it is provided by physical barriers (skin and mucous membranes), physiologic factors (pH, temperature, oxygen tension), protein secretion (lysozyme, complement system, interferons, C-reactive protein-CRP), natural-killer cells (NK cells) and phagocytic cells (macrophages and polymorphonuclear cells-PMN).

The activity of the innate immunity alone can be sufficient to destroy an invading organism. However, for an efficient elimination of the invader, its presence has to be detected early and precisely. For this purpose, mechanisms to recognize microbial molecules have evolved, such as complement system, TLR (receptors that can recognize bacterial, fungal and yeast molecules) and specialized receptors that enable NK cells to detect cells infected by intracellular pathogens. Failure to efficiently detect and/or react to the presence of a microorganism by the innate immunity as well as to interact with adaptive immunity may result in pathogen proliferation, which can lead to pathological conditions.

During the inflammatory response, the body's first response to infection and trauma, complement components and phagocytes enter the site of infection or injury. The complement system, upon its activation on the surface of certain pathogens, makes pores in the cell wall or outer membrane, leading to lysis and ultimately, to the death of the microorganism. Complement components bound on the surface of a microorganism enhance phagocytosis and pathogen elimination. Some pathogens are “sensed” through TLR receptors, phagocytosed by tissue macrophages, and destroyed intracellularly. Various mediators released during inflammation cause dilatation of blood vessels, increasing local blood flow; attract neutrophils to the site of infection; promote thrombosis in local vessels; enhance vascular permeability and leukocyte adhesion to vascular endothelium and their

diapedesis. Neutrophils are later followed by monocytes, which differentiate into macrophages, by eosinophils and lymphocytes. Activated macrophages release pro-inflammatory cytokines (TNF- α , IL-1, IL-12) and their antigen-presenting capacity is enhanced by increased expression of cell surface major histocompatibility complex molecules (MHC) class I and II and costimulatory molecules, B7.1 (CD80) and B7.2 (CD86). The functions of monocytes are further upregulated by activatory cytokines (IFN- γ , GM-CSF). The inflammatory response is then subjected to a negative regulation meant to dampen the inflammatory process. Indeed, pro-inflammatory cytokines like TNF- α trigger the release of anti-inflammatory cytokines, of which the prototype is IL-10. Furthermore, the apoptotic cells and immune complexes generated in inflamed areas limit the magnitude of pro-inflammatory reactions (Janeway Jr 2002).

1.2 The adaptive immunity

When the innate immune response does not suffice at initial stages after an infectious insult, the successful eradication of the invader is later ensured by the interaction and intimate cooperation between cells and molecules of the innate and adaptive immune systems.

Adaptive (acquired) immunity, the second level of defense, involves specific recognition and the acquisition of immunological memory after the first encounter of a foreign agent; and increases the strength and efficacy of the immune response against that agent with the next encounter. Through its specificity of response, adaptive immunity complements the protection conferred by innate immune response. Adaptive immunity is provided by lymphocyte subpopulations (predominantly B cells and T cells) and professional antigen presenting cells (APC) (macrophages and dendritic cells) and is initiated in secondary lymphoid organs by a complex interaction between B cells, T cells and APCs.

1.2.1 B-cells and T-cells

One feature of adaptive immunity is the antigen specificity of lymphocytes conferred by the expression of cell surface receptors that are able to recognize specific parts of the antigen.

The cell surface receptor of B cells (BCR) is a multisubunit transmembrane protein complex composed of a membrane form of the Ig molecule that acts as an antigen binding subunit, non-covalently associated with the accessory proteins Ig- α and Ig- β , which are responsible for the propagation of intracellular signals (Reth 1992; DeFranco 1997).

B cells arise in bone marrow and mature in bone marrow in mammals and in Bursa of Fabricius in birds. Naïve B cells specifically recognize the native, soluble antigens via their membrane bound immunoglobulins, which are internalized and degraded to antigenic peptides. These are then complexed with MHC class II molecules and presented to T cells of the same specificity. Upon recognition of their cognate antigen, T cells get activated and in turn “help” B cells to proliferate and to differentiate into either antibody-secreting plasma cells or memory B cells, in a so-called T cell-dependent B cell response. There are also antigens that can stimulate the production of antibodies by B cells without the help of peptide-specific T cells, but they are not able to induce memory B cells. These antigens induce a so-called T cell-independent B cell response (Janeway Jr 2002).

The cell surface receptor of T cells (TCR) is a disulfide-bound heterodimer composed of α and β chains (TCR $\alpha\beta$) in 95% of the T cells and of γ and δ chains (TCR $\gamma\delta$) with different antigen-recognition properties, in the rest of the T cells (Brenner, McLean et al. 1986). The TCR is non-covalently associated with four polypeptides: the heterodimers CD3 γ -CD3 ϵ , CD3 δ -CD3 ϵ and the disulfide-linked homodimer of the ζ chain, involved in transmembrane signal transduction (Samelson 2002).

T cells arise in the bone marrow and mature in the thymus. In contrast to B cells, that recognize the native, soluble form of antigens, T cells specifically recognize processed antigens as small antigenic peptides complexed with MHC molecules on the surface of APCs (MHC-restricted antigen recognition).

On the basis of co-receptor usage, MHC restriction and effector function, T cells are divided into two major subsets: CD4⁺ T cells (helper T cells) and CD8⁺ T cells (cytotoxic T cells).

Helper T cells (Th) have as coreceptor the CD4 molecule and recognize small peptides (10-20 amino acids) of exogenous origin presented, after proteolytic degradation, by MHC class II on the surface of APCs. Either by direct contact or by secretion of cytokines T helper cells promote B cell differentiation into plasma cells; CD8 maturation; and macrophage and natural killer (NK) cell activation.

Cytotoxic T cells (CTL) have as coreceptor the CD8 molecule and recognize antigen peptides (8-10 amino acids) of endogenous origin bound to MHC class I on the surface of virus infected cells or malignant transformed cells. Activated cytotoxic T cells release two types of preformed cytotoxic proteins: perforin, which makes pores into the membrane of infected/transformed cell through which granzyme enters. Alternatively, cytotoxic T cells can

induce apoptosis of target cells through Fas ligand on their surface that interacts with Fas expressed by target cells. By releasing IFN- γ , CTLs inhibit viral replication and augment MHC class I expression and macrophage activation and their recruitment to the site of infection (Janeway Jr 2002).

1.2.2 Th1 and Th2 cells

CD4⁺ T cells are able to differentiate into two distinct subsets: Th1 and Th2, with different cytokine secretion profiles. Th1 cells secrete IL-2 and IFN- γ , while Th2 cells produce IL-4, IL-5, IL-6, IL-10, IL-13 and TGF- β . Th1 or Th2 cells can derive from a common precursor cells depending on the cytokine milieu provided by dendritic cells or experimentally: Th1 cells are generated in the presence of IL-12, whereas a Th2 response is promoted by IL-4. The commitment to the Th1 or Th2 pathway can be positively influenced by autocrine production of IFN- γ and IL-4, respectively, that in the same time inhibit the development of the other subset. Alternatively, IL-10, which has a strong suppressive effect on inflammatory process, prevents Th1 differentiation by inhibiting the macrophages activation and production of IL-12. Other factors that favor CD4⁺ T cells to develop into either of these subsets *in vivo* could be antigen dose, affinity of antigen, MHC haplotypes and costimulatory factors (Liew 2002). The selective development of Th1 and Th2 cells leads to activation of two different pathways of immunity, which are associated with different antibody isotypes.

The Th1 pathway is cell mediated - through IFN- γ , Th1 enhances IgG2a production by B cells and triggers the destruction of intracellular pathogens or autoimmunity by activation of target cells (macrophages, NK cells and cytotoxic T cells) (Janeway Jr 2002).

The Th2 pathway is essentially associated with humoral immunity directed against extracellular antigens. Th2 induces B cell proliferation through IL-4 and IL-6, and IgE and IgG1 synthesis by B cells via IL-4. Th2 also stimulates effector cells (mast cells and eosinophils) through IL-4 and IL-5, which together with IgE provide an anti-helminthic effect and exacerbate allergic reactions (Janeway Jr 2002).

In the last years, the transcriptional regulation of Th1 and Th2 has been intensively studied. After binding to their receptors, IL-12 and IL-4 activate the signal transducer and activator of transcription 4 (STAT4) and STAT6, respectively. STAT4 activates the Th1-specific transcription factor T-bet, which upregulates, through NFAT and NF- κ B, the production of IFN- γ and downregulates IL-4 and IL-5 expression. Th2 differentiation is triggered by STAT6, which activates GATA3 (a zinc-finger protein) and c-Maf and promotes IL-4 and IL-5 synthesis, but inhibits IFN- γ expression. It has been suggested that GATA3 and T-bet can inhibit the development of the other subset by directly repressing each other's expression (Liew 2002).

It has been observed that each of the two subsets can be associated with certain clinical conditions: the Th1 subset predominates in inflammatory autoimmune diseases, whereas a high frequency of Th2 cells correlates with allergic reactions.

1.2.3 T regulatory cells (T_{reg})

The regulatory (suppressive) T cells (T_{reg}) are a newly defined subpopulation of CD4⁺ T cells with two subsets: naturally occurring (constitutive) and inducible (adaptive) T_{reg} . Naturally occurring T_{reg} develop in the thymus and then enter the periphery, express high level of CD25 (IL-2R α) and constitute 5-10% of all CD4⁺ T cells in healthy adult mice and humans (Hawrylowicz and O'Garra 2005). Other cell-surface markers suggested to be specific for naturally occurring T_{reg} include CTLA4 (Maloy and Powrie 2001), glucocorticoid-induced tumor-necrosis factor-receptor-related protein (GITR) (McHugh, Whitters et al. 2002; Shimizu, Yamazaki et al. 2002), low expression of CD45RB (Maloy and Powrie 2001) and CD62L (Bach 2003). A reliable intracellular marker for T_{reg} has been recently shown to be FOXP3 - the forkhead (winged helix) transcription factor (Fontenot and Rudensky 2005). Naturally occurring T_{reg} recognize and respond to self-antigens, but they may also respond to pathogen antigens (Belkaid and Rouse 2005). In contrast, inducible T_{reg} such as T_{R1} or T helper type 3 (Th3) develop from the naïve T cells in the periphery after exposure to various antigens, cytokines and drugs or after blockade of costimulatory signals (Mills 2004; Vermeiren, Ceuppens et al. 2004; Belkaid and Rouse 2005). These T_{reg} are characterized by a specific cytokine profile, rather than a cell-surface marker: Th3 are TGF- β -secreting cells, while T_{R1} are IL-10 producers (Mills 2004).

T_{reg} inhibit the proliferation of naïve T cells *in vitro* through cell-cell contact, although, *in vivo*, the secretion of inhibitory cytokines, such as TGF- β and IL-10, may also be involved. However, the mechanism of suppression by T_{reg} remains controversial (Bluestone 2005; Hawrylowicz and O'Garra 2005).

T_{reg} have been shown to regulate both Th1 and Th2 responses, maintaining peripheral self-tolerance and controlling autoimmunity and the immune response to pathogens and allergens, as reviewed by Mills and Belkaid (Mills 2004; Belkaid and Rouse 2005).

1.3 T cell response

1.3.1 TCR engagement – signal 1

The TCR recognition of specific antigenic peptides, presented in a MHC-restricted manner on the APC surface, is the triggering event of T cell activation (signal 1). Upon this interaction, the TCR, either by conformational changes or by clustering, initiates signals that are transmitted via CD3 complex into the cytoplasm (Jiang and Hunter 1999; Cochran, Cameron et al. 2000; Reth 2001). This event leads to the initiation of a phosphorylation cascade. Through various phosphotyrosinases (PTKs) and adaptor proteins, several signaling pathways are activated, enabling transcription factors to initiate the expression of genes involved in proliferation and T cell activation.

The signal delivered only through TCR engagement (signal 1) can trigger the activation of effector and memory T cells. In contrast, in naïve T cells, signaling only through TCR leads to abortion of activation; however, *in vitro* a very strong TCR signal alone could induce their proliferation. Physiologically, the threshold of TCR signal needed to trigger T cell activation is decreased by engagement of a second signal delivered by costimulatory molecule CD28 (Sharpe and Freeman 2002).

1.3.2 Costimulation – signal 2

Costimulation can be defined as an additional stimulus that cannot activate T cells on its own, but when delivered along with the TCR signal can modulate the effects of this signal (Kroczek, Mages et al. 2004).

The “two-signal” model of T cell activation proposed that, specific recognition of antigenic peptides-MHC complexes by TCR (signal 1), is complemented by a second interaction between the costimulatory molecules on T cells and APCs (signal 2), leading to an efficient T cell response. The absence of signal 2 renders the T cells unresponsive. Although this model was initially proposed for naïve T cells, it is now known that costimulation applies also to effector and memory T cells (Sharpe and Freeman 2002).

Costimulation can provide positive (activatory) second signals that promote and sustain T cell responses as well as negative (inhibitory) second signals that terminate/attenuate T cell activation and induce tolerance (Sharpe and Freeman 2002).

1.3.2.1 Costimulatory molecules

The most important costimulatory molecules belong to the B7-CD28 super-family (Fig. 1.3.2.1). Within this family, the B7.1 (CD80)/B7.2 (CD86)-CD28/CTLA4 co-stimulatory pathway is the first described and the best characterized.

CD28 is by far the most important costimulatory molecule. It is constitutively expressed as a homodimer on resting T cells and its engagement by B7.1 and B7.2 ligands, in the context of TCR ligation, initiates T cell activation and cytokine production, especially IL-2 (Carreno and Collins 2002; Greenwald, Freeman et al. 2005). IL-2 is a very important cytokine produced by proliferating T cells that acts both in an autocrine manner, regulating the proliferation process and, in paracrine manner, driving the expansion of the germinal-center B cells (Tsiagbe, Inghirami et al. 1996). CD28 signals enable effective and sustained growth of CD4 T cells and promotes important survival signals (Noel, Boise et al. 1996; Levine, Bernstein et al. 1997; Vella, Mitchell et al. 1997). Moreover, CD28 costimulation plays an important role in Th2 differentiation, as shown by studies using pathway antagonists, CD28-deficient T cells or B7-deficient APCs, and induces the expression of downstream costimulatory molecules, such as CTLA-4 and ICOS (Bour-Jordan et al. 2002).

CTLA-4, a homodimer, is rapidly upregulated after T cell activation and has a higher binding affinity for B7.1 and B7.2 than CD28. CTLA-4 engagement delivers negative second signals that terminate the T cell response by inhibiting IL-2 production and arresting the cell cycle. Its inhibitory role is clearly seen in CTLA-4-deficient mice that show lethal T cell proliferation due to uncontrolled B7-CD28 costimulation (Sharpe and Freeman 2002).

B7.1 (CD80) and B7.2 (CD86). B7.1 is a dimeric molecule that is inducibly expressed on APCs later after activation, while B7.2 is a monomer, which is expressed constitutively at low level on most APCs and upregulated after activation (Sharpe and Freeman 2002; Greenwald, Freeman et al. 2005). Indeed, on unstimulated blood monocytes, B7.1 is not present, while B7.2 is expressed constitutively at low level. IFN- γ induces monocytes to express B7.1 and to enhance the expression of B7.2. In contrast, IL-10 inhibits B7 expression. Unstimulated B cells do not express either B7.1 nor B7.2, but their expression can be induced by ligation of CD40, surface Ig, MHC class II, bacterial DNA and LPS and further increased by IL-2, IL-4, and IL-5. Moreover, B7.2 is induced more rapidly than B7.1 upon stimulation with LPS or anti-CD40 (reviewed in (Lenschow, Walunas et al. 1996; McAdam, Schweitzer et al. 1998).

B7.1 and B7.2 are bound by CTLA4 with a 20-fold higher affinity than CD28 and with a different valency: CTLA4 binds two molecules while CD28 can bind only one (Collins, Brodie et al. 2002; Sharpe and Freeman 2002; Greenwald, Freeman et al. 2005). The differences in their binding by CD28 and CTLA4, allow B7.1 to selectively recruit CTLA4 and B7.2 to selectively recruit CD28 at the interaction site between T cells and APCs (Radhakrishnan, Nguyen et al. 2003; Pentcheva-Hoang, Egen et al. 2004). This finding supported the idea that B7.2 binds preferentially CD28 and positively influences the initiation of T cell responses, while the binding of B7.1 to CTLA4 results in termination of the immune response, although some studies contradict this concept (Lenschow, Walunas et al. 1996; McAdam, Schweitzer et al. 1998; Pentcheva-Hoang, Egen et al. 2004).

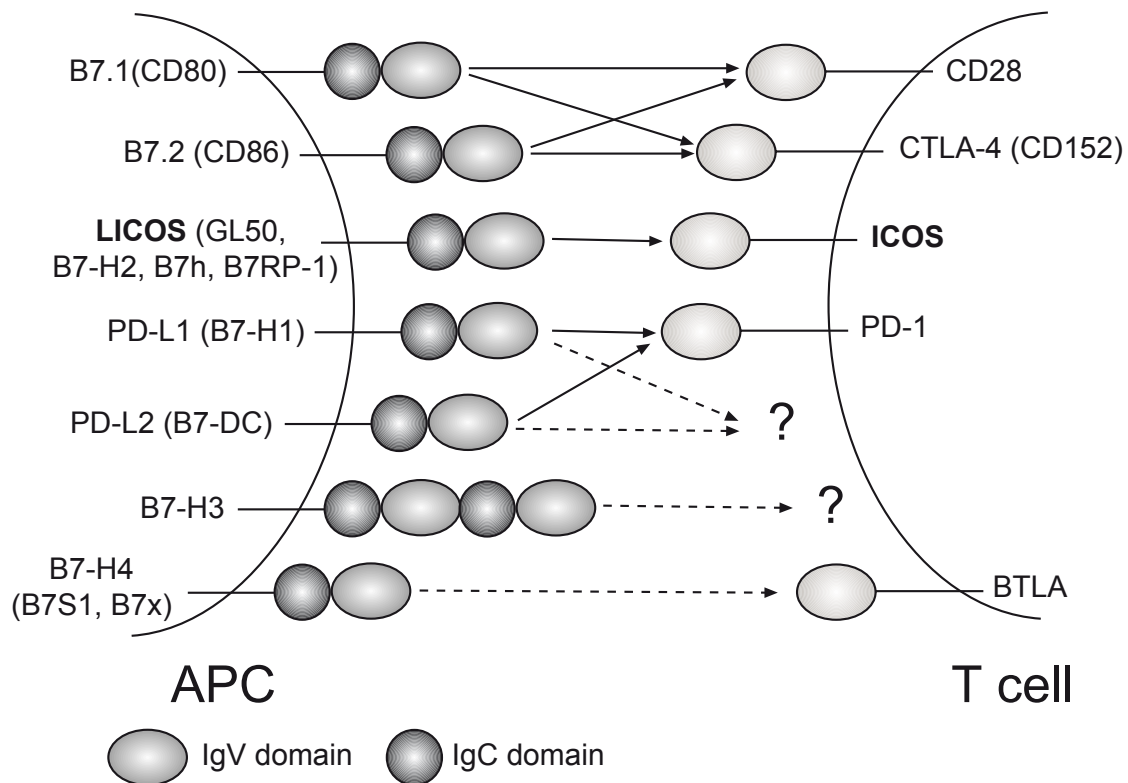


Figure 1.3.2.1. CD28-B7 super-family members. CD28 family members are receptors expressed on the surface of T cells that contain in their extracellular part a single immunoglobulin V-like domain. B7 is a family of ligands expressed by APC that contain IgV-like and IgC-like domains. B7-H3 has an extracellular domain consisting of IgV-IgC-IgV-IgC (adapted after Sharpe and Freeman 2002).

In addition to the effects exerted through CD28 and CTLA-4 engagements, new roles of B7.1 and B7.2 have been recently defined. Indeed, both B7 and CD28 are needed for the development and maintenance of CD4⁺CD25⁺ T_{reg} (Salomon, Lenschow et al. 2000; Tang, Henriksen et al. 2003). T cell interactions with different cell types are characterized by bidirectional signals delivered through both B7.1/B7.2 and CD28/CTLA4, with biological consequences on both sides. In T cell:T cell interaction, B7.1 and B7.2 engage CTLA4 and downregulate immune responses, maintaining *in vivo* T cell homeostasis (Taylor, Lees et al. 2004) and can render CD4⁺ T cells sensitive to suppressive signals from T_{reg} (Paust, Lu et al. 2004). In B cell:T cell interaction, B7.2 delivers through CD28 positive signals into T cells, but also into B cells increasing IgG1 and IgE production (Podojil and Sanders 2003; Podojil, Kin et al. 2004).

New costimulatory molecules have been defined in the last years – on the one hand, **ICOS** (Inducible Costimulator, CD278) and **PD-1** (programmed death-1) belonging to the CD28 family and, on the other hand, **LICOS** (ICOS-ligand, B7h, GL50, B7RP-1, B7-H2, AILIM/H4, CD275) and **PD-L1** (B7-H1), **PD-L2** (B7-DC) belonging to the B7 family (Fig.

1.3.2.1). Additional costimulators have been identified (**B7-H3, B7-H4, BTLA**) and their pathways are to be characterized (Greenwald, Freeman et al. 2005).

With so many costimulatory molecules, “signal 2” is a very simplified name assigned to a panel of very complex interactions of many different receptors on the surface of T cells with their ligands on APCs meant to fine-tune the immune response. In the current context, it seems more appropriate to refer to T cell activation as a “process of “multisignal integration”, with the TCR mainly responsible for the specificity of the response”, as Kroczeck et al. describes it (Kroczeck, Mages et al. 2004).

1.3.2.1.1 The Inducible Costimulator (ICOS)

In the last years, ICOS emerged as the key modulator of T cell responses and T cell-dependent B cell responses. ICOS is a glycosylated disulfide-linked homodimer (Hutloff, Dittrich et al. 1999; Beier, Hutloff et al. 2000; Mages, Hutloff et al. 2000), which lacks the MYPPPY motif, involved in the binding of CD28 and CTLA4 to their ligands (Peach, 1994 in 3Wang, 2002). Thus, ICOS can not bind to B7.1 and B7.2 and its unique ligand has been proved to be LICOS (Yoshinaga, Whoriskey et al. 1999; Beier, Hutloff et al. 2000; Brodie, Collins et al. 2000; Ling, Wu et al. 2000; Mages, Hutloff et al. 2000; Wang, Zhu et al. 2000). From the MYPPPY motif, only the PPP residues are conserved in ICOS, whose mutations could reduce or abolish ICOS-ligand binding (Wang, Zhu et al. 2002).

The ICOS gene is located on the chromosome 2q33-34, adjacent to the genes for CD28 and CTLA4 (Dariavach, Mattei et al. 1988; Lafage-Pochitaloff, Costello et al. 1990; Beier, Hutloff et al. 2000). Genetic approaches have showed that the homologous genes ICOS, CD28 and CTLA4 arose by duplication from a common ancestor gene (Beier, Hutloff et al. 2000; Mages, Hutloff et al. 2000).

Unlike CD28, ICOS is not constitutively expressed on naïve T cells; it is rather induced after T cell activation on both CD4+ and CD8+ cells (Hutloff, Dittrich et al. 1999; Beier, Hutloff et al. 2000; Buonfiglio, Bragardo et al. 2000; Coyle, Lehar et al. 2000; Mages, Hutloff et al. 2000; McAdam, Chang et al. 2000; Tezuka, Tsuji et al. 2000; Wang, Zhu et al. 2000) and it is present on effector and memory T cells (Yoshinaga, Whoriskey et al. 1999; Coyle, Lehar et al. 2000). Ligation of TCR and CD28 upregulates ICOS, which remains on the cell surface for extended periods of time (Beier, Hutloff et al. 2000; McAdam, Chang et al. 2000). In the absence of B7s, ICOS expression is reduced and can be restored by CD28 ligation (McAdam, Chang et al. 2000). However, CD28 is not absolutely needed for the expression of ICOS, as CD8+CD28- T cells could express ICOS after CD3 stimulation alone (Beier, Hutloff et al. 2000). Moreover, T cells from CD28 knock-out mice (Yoshinaga, Whoriskey et al. 1999) and B7.1/2 double knock out mice (McAdam, Chang et al. 2000) express ICOS upon activation.

ICOS has a small cytoplasmatic domain of 35 AA and contains a YMFM motif, similar to the CD28 motif YNMN, that binds p85 subunit of phosphatidylinositol 3 kinase (PI3K) (Coyle, Lehar et al. 2000). Therefore, CD28 and ICOS share a common pathway, which enables

costimulation through ICOS to occur in the absence of CD28/B7 and implies a role for ICOS also in T cell survival and enhancement of cellular metabolism. However, a single amino acid alteration in this motif in ICOS, Phenylalanine instead of Asparagine, abolishes the binding of growth-factor receptor-bound protein 2 (GRB2) and renders ICOS unable to induce the production of IL-2 (Harada, Ohgai et al. 2003). Moreover, it has been suggested that ICOS may engage multiple signaling pathways in different ways, resulting in ICOS unique effects and effects similar to those induced by CD28 ligation (Arimura, Kato et al. 2002).

In addition to T cells, ICOS is expressed at low level on freshly isolated NK cells. Its expression is upregulated upon activation of NK cells with IL-2, IL-12 and IL-15 and it augmented the cytolytic activity and IFN- γ production of these cells (Ogasawara, Yoshinaga et al. 2002).

1.3.2.1.2 The Inducible Costimulator Ligand (LICOS)

The ICOS ligand, LICOS, is a monomer that has been observed on the surface of B cells, monocytes, macrophages, monocyte-derived dendritic cells (DC) and a subset of CD3+ T cells (Swallow, Wallin et al. 1999; Yoshinaga, Whoriskey et al. 1999; Aicher, Hayden-Ledbetter et al. 2000; Ling, Wu et al. 2000; Wang, Zhu et al. 2000). In addition, LICOS is also expressed by non-immune cells: muscle fiber (Wiendl, Mitsdoerffer et al. 2003; Wiendl, Mitsdoerffer et al. 2003), glyoma cells (Schreiner, Wischhusen et al. 2003), renal tubular epithelial cells (Wahl, Schoop et al. 2002), on human umbilical vein endothelial cells (HUVEC) and microvascular endothelial cells (MVEC) (Khayyamian, Hutloff et al. 2002; Klingenberg, Autschbach et al. 2005). However, the function of LICOS on non-immune cells is not yet fully elucidated.

LICOS is expressed early during differentiation of CD34+ progenitor cells into DC, rendering the former capable to stimulate allogeneic T cell response (Richter, Hayden-Ledbetter et al. 2001). Pro-inflammatory stimuli like TNF- α and LPS enhance LICOS expression on B cells and monocytes (Yoshinaga, Zhang et al. 2000), but they inhibit it on DCs (Wang, Zhu et al. 2000; Coyle and Gutierrez-Ramos 2001). LICOS is upregulated in fibroblasts treated with TNF- α , while mRNA for LICOS is increased in non-lymphoid tissues liver, testes, kidney, peritoneum after injection of LPS (Swallow, Wallin et al. 1999).

Two splice variants of LICOS, namely B7-H2 and GL-50 that differ in their cytoplasmic tail, have been identified. B7-H2 transcripts were found in both lymphoid and non-lymphoid tissues, while GL-50 was detected only in lymph node, leukocyte and spleen samples, (Brodie, Collins et al. 2000; Wang, Zhu et al. 2000; Yoshinaga, Zhang et al. 2000; Ling, Wu et al. 2001).

1.3.2.2 Functions of ICOS and LICOS

1.3.2.2.1 The role of ICOS and LICOS in T cell proliferation and cytokine production

It is believed that CD28 plays a unique role in the initiation of immune response, while subsequent expression of ICOS and its engagement increases production of IL-10 and promotes effector functions. This hypothesis has been supported by the fact that ICOS is not expressed on naïve T cells (Hutloff, Dittrich et al. 1999). Furthermore, *in vitro* studies have shown that proliferation of naïve transgenic T cells in response to specific peptides remained intact despite the fact that ICOS-LICOS interactions were blocked with ICOS-Ig (McAdam, Chang et al. 2000). Inhibition of CD28, but not of ICOS dramatically attenuated the ability of naïve T cells to proliferate and to produce IL-2 (Coyle, Lehar et al. 2000; Gonzalo, Tian et al. 2001). Moreover, the proliferation of naïve ICOS-deficient T cells is only marginally affected by the absence of ICOS (McAdam, Greenwald et al. 2001; Tafuri, Shahinian et al. 2001).

In antigen-experienced T cells, in human and mouse systems, T-cell proliferation can be induced by ICOS engagement in the presence of suboptimal concentration of anti-CD3 antibodies, but to a lesser extent than by CD28 (Hutloff, Dittrich et al. 1999; Yoshinaga, Whoriskey et al. 1999; Coyle, Lehar et al. 2000; McAdam, Chang et al. 2000; Wang, Zhu et al. 2000). However, this ICOS-induced proliferation cannot be sustained without CD28 costimulation or exogenous IL-2 (Yoshinaga, Zhang et al. 2000; Riley, Blair et al. 2001). Antigen-experienced T cell activation and proliferation are defective in the absence of ICOS and/or LICOS, as observed in ICOS and LICOS deficient mice (Dong, Juedes et al. 2001; Tafuri, Shahinian et al. 2001; Nurieva, Mai et al. 2003; van Berkel, Schrijver et al. 2005).

ICOS is required for T cell proliferation in response to superantigen stimulation. Inhibition of ICOS suppressed the SEB-induced expansion of both CD4⁺ and CD8⁺ V β 8⁺ T cells to a degree comparable to that of CD28 blockade and had no influence on peripheral deletion or anergy induction (Gonzalo, Delaney et al. 2001).

ICOS regulates the cytokine production from recently activated T cells, but not from naïve T cells, where CD28 has the main influence. The secretion of IL-2, the feature of naïve T cell activation, is potently induced by CD28 (Yoshinaga, Whoriskey et al. 1999; Yoshinaga, Zhang et al. 2000; Gonzalo, Tian et al. 2001), although a low production of IL-2 by ICOS engagement has been reported by two groups (Wang, Zhu et al. 2000; Riley, Blair et al. 2001). ICOS ligation on human and mouse CD4⁺ T cells enhances the production of IL-4, IL-5, IL-13, IFN- γ , TNF- α and GM-CSF, but not of IL-2, and preferentially promotes IL-10 production (Hutloff, Dittrich et al. 1999; Yoshinaga, Whoriskey et al. 1999; Beier, Hutloff et al. 2000; McAdam, Chang et al. 2000; Guo, Stolina et al. 2001).

1.3.2.2.2 The role of ICOS and LICOS in Th1 and Th2 responses

Initially, because ICOS engagement resulted in high levels of IL-10 and IL-4, but not of IL-2, it was thought that ICOS had an unique role in Th2 responses (Coyle, Lehar et al. 2000; McAdam, Chang et al. 2000; Dong, Juedes et al. 2001; McAdam, Greenwald et al. 2001; Tafuri, Shahinian et al. 2001; Tesciuba, Subudhi et al. 2001). Later, the studies demonstrated that ICOS can stimulate the production of both Th1 and Th2 cytokines during the priming and the effector phase of T cell responses (Gonzalo, Tian et al. 2001; Guo, Stolina et al. 2001; Ozkaynak, Gao et al. 2001; Bertram, Tafuri et al. 2002; Greenwald, McAdam et al. 2002; Smith, Brewer et al. 2003; Suh, Tafuri et al. 2004; Wassink, Vieira et al. 2004). However, ICOS/LICOS interaction is more important for Th2 differentiation and effector functions than for Th1 responses (Mak, Shahinian et al. 2003; Nurieva, Mai et al. 2003). For a Th2 response, ICOS engagement is required immediately after immune priming; consequently, ICOS blockade at this stage may result in a Th1-biased response, while ICOS blockade during the effector phase could favor a Th2 response (McAdam, Chang et al. 2000; Gonzalo, Tian et al. 2001; Rottman, Smith et al. 2001). ICOS expression is increased on both Th1 and Th2 cells during T cell differentiation, but after multiple restimulation in the presence of IL-12, the level remains high only on Th2 (Coyle, Lehar et al. 2000; McAdam, Chang et al. 2000). However, ICOS level does not remain stable by previous polarization as addition of IL-12 and/or IL-23 have brought ICOS expression on the Th1 and Th2 cells to the same level (Wassink, Vieira et al. 2004).

In ICOS and in LICOS deficient mice, upon restimulation, differentiated Th cells produced IFN- γ and IL-10, but not IL-4 (Dong, Juedes et al. 2001; Tafuri, Shahinian et al. 2001; Nurieva, Mai et al. 2003; Wong, Oh et al. 2003). This finding suggested that ICOS is involved in regulation of IL-4 and, consequently, in Th2 differentiation and this occurs, as later demonstrated, through regulation of the c-Maf transcription factor (Nurieva, Duong et al. 2003).

The involvement of ICOS in Th1 as well as Th2 responses has been also demonstrated in various infection and disease models. ICOS induced protective Th1 response to *Toxoplasma* and to intracellular bacterium *Listeria monocytogenes*, by stimulating the production of IFN- γ (Mittrucker, Kursar et al. 2002; Villegas, Lieberman et al. 2002; Bonhagen, Liesenfeld et al. 2003). After infection with *Nippostrongylus brasiliensis*, both Th1 and Th2 responses were impaired in CD28-deficient mice as compared to wild type mice, with a further decrease in Th1 response when ICOS was blocked. Moreover, ICOS inhibition led to decreased Th1 responses after infection with vesicular stomatitis virus (VSV) of wild type mice and after infection with lymphocytic choriomeningitis virus (LCMV) of CD28-deficient mice (Kopf, Coyle et al. 2000). ICOS deficient mice infected with *Leishmania mexicana* showed reduced Th1 and Th2 cytokine production and severely defective isotype class switching (Greenwald, McAdam et al. 2002). Eight weeks after the infection with *Schistosoma mansoni*, at the height of a Th2-dominated response, ICOS expression was

enhanced on CD4⁺ T cells from liver granulomas and it positively correlated with the release of IL-10 and Th2 cytokines IL-5 and IL-13 (Bonhagen, Liesenfeld et al. 2003). Blockade of ICOS four weeks after *S. mansoni* infection resulted in enhanced hepatic immunopathology and exacerbation of IFN- γ release by *S. mansoni* egg granuloma cells and CD4⁺ T cells (Rutitzky, Ozkaynak et al. 2003).

In an EAE model (experimental allergic encephalomyelitis, an animal model for multiple sclerosis), blockade of ICOS during the effector phase ameliorated the disease, while blockade of ICOS during the priming phase led to exacerbation of the Th1-mediated disease, similarly as in ICOS deficient mice (Dong, Juedes et al. 2001; Rottman, Smith et al. 2001; Sporici, Beswick et al. 2001).

In alloimmunity models, ICOS blockade successfully inhibited Th1 responses when the blockade occurred during the effector/differentiation phase (Harada, Salama et al. 2003), promoted increased allograft acceptance (Ozkaynak, Gao et al. 2001) and suppressed graft-versus-host disease (GVHD) due to a Th2 immune deviation (Hubbard, Eng et al. 2005). Blockade of ICOS during the effector phase, in a model of rheumatoid arthritis (collagen-induced arthritis, CIA), resulted in inhibition of both Th1 and Th2 responses and in amelioration of CIA (Iwai, Kozono et al. 2002).

In the models of asthma and allergic airway disease, ICOS blockade did not affect Th1-mediated inflammation or Th2 differentiation, but Th2 effector function (Coyle, Lehar et al. 2000; Dong, Juedes et al. 2001; Gonzalo, Tian et al. 2001; Tesciuba, Subudhi et al. 2001; Coyle and Gutierrez-Ramos 2004).

Implication of ICOS in Th1 versus Th2 differentiation is not favored by the newer “release model”. This model is based on the finding that in the unbiased immune system of non-manipulated mice, T cells expressing low density of ICOS on their surface produced IL-2, IL-3, IL-6 and IFN- γ , while T cells bearing intermediate levels of ICOS, representing the large majority of ICOS⁺ T cells *in vivo*, were involved in the release of the Th2 cytokines IL-4, IL-5, IL-13. In contrast, high density of ICOS on T cells was linked to the predominant secretion of IL-10. In the release model, surface density of ICOS expression dictates the cytokine pattern released by activated T cells, depending on the degree of ICOS availability: low ICOS levels result in cytokine production from T cells with high ICOS density, while high ICOS levels trigger cytokine release from all ICOS⁺ T cells (Lohning, Hutloff et al. 2003; Kroczeck, Mages et al. 2004).

ICOS and T_{reg}. A growing body of evidence suggests that ICOS pathway is critically involved in induction and function of T_{reg}, in tolerance and autoimmune disease. ICOS costimulation and IL-10 are required for the development and functions of IL-10-secreting T_{reg} involved in inhibition of airway hyper-reactivity (Akbari, Freeman et al. 2002). Transgenic mice expressing high levels of self-antigens generated IL-10-producing T cells with regulatory activity and their IL-10 production and inhibitory functions depended on high levels of ICOS expression (Kohyama, Sugahara et al. 2004). In a murine model of type 1

diabetes, IL-10-producing T_{reg} could regulate the progression of diabetes from a prediabetic lesion in an ICOS-dependent manner (Herman, Freeman et al. 2004).

T cell activation by allogeneic costimulation-deficient APCs induced ICOS expression on a subpopulation of T cells, which, after restimulation, remained anergic but produced IL-10. This subpopulation suppressed the response of ICOS⁻ T cells and also the activation of naïve or primed T cells upon allogeneic stimulation (Vermeiren, Ceuppens et al. 2004).

ICOS in CD8⁺T cell responses. The role of ICOS in CD8⁺ T cell activity is controversial. In murine tumor models, LICOS⁺, but not LICOS⁻ tumors were rejected through enhancement of cytolytic activity of T cells driven by ICOS engagement by its ligand LICOS, (Liu, Bai et al. 2001; Wallin, Liang et al. 2001). ICOS ligation was comparable to that of CD28 in regard to CTL priming, effector functions and tumor specific memory CTLs (Zuberek, Ling et al. 2003). However, in viral infection experiments, ICOS blockade had no effect on CTL response, suggesting that lytic function of T cells is ICOS-independent (Kopf, Coyle et al. 2000; Bertram, Tafuri et al. 2002).

1.3.2.2.3 The role of ICOS and LICOS in humoral response

The ICOS/LICOS pathway has a major role in providing T cell help to B cells in the so-called T cell-dependent B cells response. ICOS is expressed predominantly on T cells in the germinal centers and T cell zone of spleen, lymph nodes and Peyer's patches (Mages, Hutloff et al. 2000; Beier, Hutloff et al. 2004; Hutloff, Buchner et al. 2004). LICOS is highly expressed on B cell-rich areas of the lymph nodes, in the follicles in the spleen and Peyer's patches (Yoshinaga, Whoriskey et al. 1999; Yoshinaga, Zhang et al. 2000).

Transgenic mice overexpressing soluble LICOS are characterized by lymphoid hyperplasia in the spleen, lymph node and Peyer's patches and hypergammaglobulinemia (Yoshinaga, Whoriskey et al. 1999). ICOS-deficient as well as LICOS-deficient mice showed defective B cell expansion, impaired germinal center formation in response to both primary and secondary immunization and defective Ig class-switching to IgG1 and IgE, (Dong, Juedes et al. 2001; Dong, Temann et al. 2001; McAdam, Greenwald et al. 2001; Tafuri, Shahinian et al. 2001; Mak, Shahinian et al. 2003; Wong, Oh et al. 2003; Loke, Zang et al. 2005).

Reduced germinal center formation and defective isotype switching have been also observed in mice deficient in CD28 or in both B7.1/B7.2, or in CD40L, suggesting a complex interplay between these costimulatory pathways not yet completely understood (Sharpe and Freeman 2002). As CD28/B7.1/B7.2 pathway signals are required for an optimal ICOS expression (Beier, Hutloff et al. 2000; McAdam, Chang et al. 2000), it has been suggested that these defects in B cell activation are due to the failure to induce ICOS (Sharpe and Freeman 2002). Furthermore, after the initial down-regulation of LICOS upon activation of naïve B cells, signals of the CD40-CD40L pathway reestablish LICOS expression on activated B cells to ensure proper specific interaction between activated T cells and B cells (Liang, Porter et al.

2002). Costimulation through CD40 reversed the defective isotype switching in ICOS-deficient mice, suggesting that ICOS induces isotype switching through activation of the CD40-CD40L pathway (McAdam, Greenwald et al. 2001). Engagement of ICOS increases CD40L expression. However, as normal levels of CD40L are detected in ICOS-deficient T cells, CD40L expression is not exclusively dependent on ICOS pathway (Dong, Temann et al. 2001; McAdam, Greenwald et al. 2001; Tafuri, Shahinian et al. 2001).

In patients with common variable immunodeficiency (CVID), it has been reported that a homozygous deletion of ICOS gene was responsible for an impaired T cell help for B cells resulting in defective late B cell differentiation, class-switch and memory B cell generation (Grimbacher, Hutloff et al. 2003).

ICOS/LICOS interactions have been proven to be important in both phases of T cell dependent B cell response: during T cell priming by APCs and during the delivery of T cell help to B cells. However, these interactions were required in primary, but not in secondary helper T cell response and controlled both T and B cell activities (Guo, Stolina et al. 2001; Mak, Shahinian et al. 2003; Smith, Brewer et al. 2003; Suh, Tafuri et al. 2004). Moreover, they had no effect on the migration of T cells into B cell follicles (Smith, Brewer et al. 2003).

1.4 Sepsis – at the interface between innate and adaptive immunity

Sepsis is a complex pathological condition characterized by a strong, unbalanced systemic immune response to infection with harmful to lethal consequences for the patient. The sepsis syndrome affects approximately 700,000 patients annually in the United States and accounts for 210,000 deaths each year with enormous costs for hospitalization (Angus, Linde-Zwirble et al. 2001). Advanced age, immuno-incompetence status, use of invasive procedures and antibiotic resistance in pathogens contribute to the increase of sepsis incidence (Rice and Bernard 2005).

Originally, sepsis was thought to result from the presence of bacteria in the blood (bacteremia). In 1972, Lewis Thomas proposed the theory that it is the overreaction of the individual - an uncontrolled inflammatory response to the presence of an invading microorganism - that causes sepsis (Riedemann, Guo et al. 2003). Based on this his theory, therapies aimed to attenuate the exacerbated inflammatory response were thought to reduce mortality caused by sepsis (Abraham 1999). Unfortunately, almost none of these therapies significantly improved the outcome in sepsis (Abraham 1999).

The failure of immunomodulatory therapies questioned the theory that high mortality rate in sepsis is due mainly to a hyperinflammatory response and prompted a critical review of the clinical approaches used. It turned out that these approaches were based on animal models, which did not accurately reflect clinical picture of human sepsis (Fink and Heard 1990; Natanson, Hoffman et al. 1994; Deitch 1998). Moreover, the lack of a clear clinical definition of sepsis resulted in the study of heterogeneous populations of septic patients (Abraham 1999). The definition of sepsis, based on specific clinical symptoms in the context of an infection, proposed by Bone et al. in 1989, was limited. It could not explain, for example, the presence of clinical sepsis symptoms in patients with no clinical evidence for infection (e.g., trauma and acute pancreatitis patients) (Bone, Fisher et al. 1989). It became clear that the sepsis definition had to be refined.

In 1992, at the Consensus Conference of the American College of Chest Physicians/Society of Critical Care Medicine the term “systemic inflammatory response syndrome” (SIRS) has been introduced. This term describes a condition that results from a systemic activation of the innate immune response that can be induced not only by infectious inflammatory processes (localized or generalized infection) but also by sterile inflammatory processes (acute pancreatitis, trauma, thermal injury). At the same conference, sepsis has been defined as a “systemic inflammatory response syndrome (SIRS) in response to infection” which, when associated with the dysfunction of least one organ has been classified as severe sepsis. Septic shock has been defined as severe sepsis with hypotension unresponsive to fluid resuscitation (Bone, Balk et al. 1992).

It is now accepted that, in sepsis, the systemic inflammatory response induces an exaggerated systemic anti-inflammatory response that results in immune paralysis, as described below. During sepsis, endotoxins, such as LPS, and other infectious stimuli (Van Amersfoort, Van Berkel et al. 2003), induce massive TNF- α release from macrophages and monocytes, which triggers a cascade of pro-inflammatory cytokines released into the circulation, including IL-1 and IL-6. This results in activation of the coagulation cascade and fibrinolysis (Rice and Bernard 2005). In addition to their beneficial effects to host defense against infection and injury, TNF- α , in concert with IL-1, are thought to trigger also systemic responses, translated into the clinical signs of the systemic inflammatory syndrome (SIRS): hypo/hyperthermia, tachycardia, tachypnea or hyperventilation, leukocytosis or leukopenia (Bone 1991). Excessive systemic release of TNF- α and IL-1 drives the release of anti-inflammatory cytokines (IL-10, IL-13 and TGF- β) from leukocytes, which in turn suppress further production of pro-inflammatory cytokines (van Dissel, van Langevelde et al. 1998; van der Poll 2001) and inhibit macrophage antigen-presentation, and T cell and B cell functions. Soluble receptors and receptor antagonists for pro-inflammatory cytokines (TNF- α and IL-1) neutralize the cytokine effects, dampening the inflammatory response (Rice and Bernard 2005). This systemic counterregulatory mechanism is meant, under normal circumstances, to counterbalance and control the proinflammatory response. However, on many occasions in sepsis, the anti-inflammatory response exceeds the pro-inflammatory response inducing a state of immunoparalysis that renders the organism unable to mount an effective immune response to new infectious challenges (Bone 1996). This state constitutes so-called compensatory anti-inflammatory response syndrome (CARS) and leads in septic patients to inhibited delayed hypersensitivity reactions (MacLean, Meakins et al. 1975), and a susceptibility to opportunistic and nosocomial infections (Hotchkiss and Karl 2003).

Little is known about how an inflammatory response is endogenously counterregulated by compensatory anti-inflammatory mechanisms to prevent unnecessary damage of distant organs and tissues. Yet, it is not clear which of these antagonistic responses predominates in different stages of sepsis or whether there is a simultaneous or sequential occurrence of them. Some researchers consider that an early, short and intense release of pro-inflammatory mediators, that can cause early mortality in septic shock, is immediately followed by an anti-inflammatory response with immunosuppression in later phases of sepsis (Natanson, Hoffman et al. 1994; Lederer, Rodrick et al. 1999; Kox, Volk et al. 2000; Oberholzer, Oberholzer et al. 2001). Munford and Pugin proposed that the body's normal response to stress (psychological trauma, strenuous exercise, cold exposure and major injury) consists of activation of a systemic anti-inflammatory response that limit the inflammatory reaction to the site of infection or injury and prevent systemic inflammation. In polytrauma, they suggest, an overactivation of the systemic anti-inflammatory response suppresses the normal local defense and allows multiplication and dissemination of microorganisms that enter the tissues through disrupted epithelia (Munford and Pugin 2001). However, clinical practice demonstrated that pro- and anti-inflammatory reactions could coexist in a so-called mixed

antagonistic response syndrome (MARS) (Bone 1996; Kox, Volk et al. 2000; Hoflich and Volk 2002; Tschakowsky, Hedwig-Geissing et al. 2002).

The balance between pro- and anti-inflammatory mechanisms in response to infection and trauma is greatly influenced by genetic factors (Hotchkiss and Karl 2003; De Maio, Torres et al. 2005). Polymorphisms in genes controlling the host response to microorganisms (TNF receptors, IL-1 receptors, Fcγ receptors or TLR receptors, cytokines) are presumed to influence the outcome in sepsis and could provide valuable information for designing appropriate treatment for each patient (Bown, Horsburgh et al. 2004; Schwacha, Holland et al. 2005).

1.4.1 Trauma and stroke as risk factors for sepsis

Major (severe/serious) injury/trauma are terms used for injuries involving different body regions or organs when at least one or a combination of more of these injuries could be potentially life threatening (Maghsudi and Nerlich 1998).

Stroke is a clinical syndrome caused by inadequate blood flow in a certain part of the brain due to hemorrhagic or ischemic causes that leads to death of the neurons in the affected area (Frizzell 2005).

Trauma and stroke induce profound, detrimental changes in immune function causing in the end a predominant anti-inflammatory response that is widely perceived as responsible for the immunosuppression that leads to increased susceptibility to infections and ultimately to septic complications. Both aspects are well documented in the literature, both in animal models and in patients (Molloy, O'Riordain et al. 1993; Wu, Ogle et al. 1995; Hensler, Hecker et al. 1997; Kelly, Lyons et al. 1997; Heidecke, Hensler et al. 1999; Lederer, Rodrick et al. 1999; Shahbazian, Jeevanandam et al. 1999; Weighardt, Heidecke et al. 2000; Angele and Faist 2002; Paterson, Murphy et al. 2003; Menger and Vollmar 2004).

In humans, systemic inflammatory response (SIRS) manifests itself as a clinical phenomenon with high prevalence in ICU patients (>50% of all ICU patients), affecting 50 to 88% of the trauma patients of which approx. 48% developed septic complications (Smail, Messiah et al. 1995; Muckart and Bhagwanjee 1997; Brun-Buisson 2000). Infection is considered to be the third most common complication in stroke, with chest and urinary tract infections occurring in the first days after stroke (12% and 13-18%, respectively) and pneumonia being the main cause of death in the postacute phase (5-14%) (Kalra, Yu et al. 1995; Davenport, Dennis et al. 1996; Johnston, Li et al. 1998; Aslanyan, Weir et al. 2004; Hanchaiphiboolkul 2005; Hung, Tsay et al. 2005). Moreover, the severity of injury correlates with the incidence of trauma-induced sepsis, while the stroke severity correlates with the extent of infectious complications (Hilker, Poetter et al. 2003; Katzan, Cebul et al. 2003; Osborn, Tracy et al. 2004).

1.4.2 Mechanisms of immunosuppression in polytrauma and sepsis

Immunosuppression in polytrauma and sepsis may result in depressed function of monocytes, but also the activity of the adaptive immunity is affected as shown by the loss of Th1, but an increase of Th2 responses.

In trauma, circulating monocytes express reduced levels of MHC class II molecules (HLA-DR) and costimulatory molecules (CD80, CD86) resulting in loss of antigen-presentation function and ineffective immune responses. Moreover, the depression of monocyte function was correlated with loss of Th1 response and IFN- γ production (Heidecke, Weighardt et al. 2000; Brunner, Krenn et al. 2004).

1.4.2.1 Biased Th2 responses

It has recently emerged that T-cells also play a critical role in the systemic response to infection. Cytokines produced during SIRS may affect the Th1/Th2 balance and subsequent immune responses. Many studies have shown that susceptibility to sepsis after major trauma correlated with low production of Th1 cytokines (IL-2, IFN- γ), impaired antigen-specific Th1 function and dominance of Th2 cytokines (IL-4 and IL-10). In mice, for example, burn injury resulted in depressed levels of Th1-dependent antigen-specific IgG2a antibodies, whereas levels of Th2-dependent antigen-specific antibodies (IgG and IgE) remained unchanged. Th1-dependent response could be restored with anti-IL-10 mAb (Kelly, O'Sullivan et al. 1997) or by IL-12 (O'Sullivan, Lederer et al. 1995; Kelly, O'Suilleabhain et al. 1999) and prevented injury-induced immunosuppression and improved mice survival in polymicrobial sepsis (Gennari, Alexander et al. 1994; Kobayashi, Kobayashi et al. 1999; Lyons, Goebel et al. 1999; Goebel, Kavanagh et al. 2000). Reduced production of IFN- γ and IL-12 and enhanced production of IL-10 early after a *Pseudomonas aeruginosa* challenge was associated with impaired bacterial clearance after cecal ligation and puncture (CLP) (Murphey, Lin et al. 2004). Sublethal doses of staphylococcal enterotoxins A and B (SEA, SEB) administered immediately after injury caused high mortality in mice, whereas no mortality was recorded when administered 7 days after injury. At the latter time point, the low mortality rate correlated with high levels of Th2 cytokines (IL-4 and IL-10) and it was increased by blocking IL-10 (Zang, Dolan et al. 2004).

In humans, severe trauma induced the loss of circulating CD4⁺ and CD8⁺ T cells with progressive decrease of IFN- γ and IL-2 production and was followed by an increased capacity of stimulated CD4⁺ T cells to produce IL-10 that correlated with subsequent septic complications (Lyons, Kelly et al. 1997; Murphy, Paterson et al. 2003). Immunosuppressive effects of IL-10 have been also revealed in a clinical trial of IL-10 in humans, where Chernoff et al. have reported marked reduction in circulating lymphocytes expressing CD3, CD4, CD8 markers and also in mitogen-induced T cell proliferation, and significant dose-

dependent inhibition of pro-inflammatory cytokines IL-1 β and TNF- α production after endotoxin challenge *in vitro* (Chernoff, Granowitz et al. 1995). Enhanced soluble ST2 (a specific marker expressed on Th2 but not on Th1 cells) and IgG1 production, accompanied by marked decrease of Th1-cytokine synthesis, have been reported in patients with sepsis and trauma (Brunner, Krenn et al. 2004).

1.4.2.2 Loss of antigen presentation and costimulatory capacity of monocytes

Low HLA-DR expression. A decrease in monocyte HLA-DR expression has been shown to accompany surgical and accidental trauma (Giannoudis, Smith et al. 1999). Moreover, a low monocyte HLA-DR level was correlated with post-traumatic septic morbidity and mortality and it has been used as a prognostic parameter in patients with infection and sepsis (Livingston, Appel et al. 1988; Hershman, Cheadle et al. 1990; Cheadle, Hershman et al. 1991; Saenz, Izura et al. 2001). Whether this marker of monocyte function is suitable as a predictive parameter for clinical outcome in sepsis is still under debate as apparently conflicting data have been reported (Perry, Mostafa et al. 2003; Spittler and Roth 2003).

The mechanism of HLA-DR downregulation on monocytes is not yet clear, although it may be linked to release of anti-inflammatory cytokines, such as IL-10 (de Waal Malefyt, Abrams et al. 1991; Klava, Windsor et al. 1997). IL-10 may cause the decrease in HLA-DR expression either by blocking the trafficking of MHC class II molecules from the intracellular compartment to the cell surface (Cheadle, Hershman et al. 1991; Klava, Windsor et al. 1997; Giannoudis, Smith et al. 2000) or by inducing reendocytosis and intracellular sequestration of surface HLA-DR molecules (Fumeaux and Pugin 2002). Immediately after trauma, patients who subsequently developed sepsis exhibited persistent high levels of IL-10 that negatively correlated with HLA-DR expression during hospitalization (Klava, Windsor et al. 1997; Giannoudis, Smith et al. 2000). Moreover, sera from trauma-induced septic patients or plasma from patients with septic shock, collected on admission, had inhibitory effect on HLA-DR expression in monocytes, suggesting the presence of a soluble, HLA-DR-downregulation inducing factor (Mueller, Kreuzfelder et al. 2003).

Low costimulatory molecules expression. The costimulatory molecule CD86 appeared to contribute to macrophage dysfunction through regulation of the IL-10 response. Normal mouse peritoneal macrophages displayed, after the onset of sepsis, low expression of CD86 and MHC class II, but not of CD40 or CD80. After the septic challenge, the serum IL-10 concentrations and the IL-10 release capacity of peritoneal macrophages were increased in the background controls, but not in the CD86-deficient mice, showing that IL-10 release is modulated by CD86 (Newton, Ding et al. 2004). MHC class II molecules and CD86 were downregulated following *in vitro* LPS-priming of PBMC in an endogenous IL-10-dependent manner. These changes were followed by diminished T-cell proliferation and IFN- γ release in response to different recall antigens (Wolk, Docke et al. 2000).

1.4.2.3 Other immunosuppressive mechanisms

Other potential mechanisms of immune suppression, including anergy, apoptosis and mechanisms involving T_{reg} have been reported in patients with trauma and sepsis (Lederer, Rodrick et al. 1999; Oberholzer, Oberholzer et al. 2001; Murphy, Choileain et al. 2005). Low density of MHC class II molecules on APCs is responsible for a defective interaction with T cells that renders the latter anergic, namely unable to proliferate and secrete cytokines in response to stimulation via TCR (De, Kodys et al. 2000; Perry, Mostafa et al. 2003). In addition, the inability of lymphocytes to react to mitogens in trauma and septic patients has been recognized for a long time (Dawson, Ledgerwood et al. 1982; Wolfe, Wu et al. 1982). T cell apoptosis is increased in trauma and sepsis (Hotchkiss, Tinsley et al. 2001; Le Tulzo, Pangault et al. 2002) and apoptotic cells are presumed to have a potential immunosuppressive effect on the cells of the immune system (Hotchkiss, Chang et al. 2003).

1.4.3 Mechanisms of immunosuppression in stroke

The increased susceptibility to infection complications after stroke appears to be associated with a state of immunosuppression (Howard and Simmons 1974). However, the study of the mechanisms leading to poststroke decreased resistance to infections is in its infancy. In a mouse model, cerebral ischemia (stroke) has been associated with impaired cell-mediated immune response that results in spontaneous systemic bacterial infections. A poststroke shift from Th1 to Th2 cytokine production with loss of IFN- γ , but increased IL-4 secretion; apoptosis-induced lymphopenia; as well as monocyte deactivation, in terms of low endotoxin-induced TNF- α production, have been described as mechanisms of stroke-induced immunosuppression, which were neuroendocrine mediated (Prass, Meisel et al. 2003).

1.5 Aim of the Study

In the last years, costimulatory molecule interactions and their effects on the T cell arm of the immune response have been a focus of immunological research. The CD28/B7.1/B7.2 pathway is involved in the regulation of Th1/Th2 balance. In this context, CD86 (B7.2) has been suggested to act as a regulator of anti-inflammatory IL-10 response. Signaling through the ICOS/LICOS pathway, while it can enhance both Th1 and Th2 cytokine production, is particularly important for the induction of IL-10 production. In addition, ICOS/LICOS interactions are required for Th2 differentiation and effector functions as well as for T cell-dependent B cell responses.

Severe trauma and stroke lead to immunosuppression and thus carry a high risk of infection complications such as sepsis. In trauma, defects in antigen-presentation (low level of HLA-DR on monocytes) and costimulation as well as a bias towards Th2 responses with high IL-10 secretion have been reported to characterize these situation. Therefore, the aim of this study was the investigation of ICOS and LICOS expression in trauma and stroke patients.

In a first step, recombinant LICOS needed to be generated as an antigen for the development of anti-LICOS mAbs. The goal was to employ these mAbs in an orienting investigation of the expression of HLA-DR and costimulatory molecules (CD86, LICOS, ICOS) by different immune cell populations in patients suffering from major trauma and stroke.

2. Materials and Methods

2.1 Materials

2.1.1 Laboratory equipment

Autoclave 2540 EL	Huttner Systec, Wettenberg
Bacterial incubator	Binder Labortechnik, Tuttlingen
Biofuge fresco/pico	Heraeus Instruments, Hanau
Blotter (Desablot 160)	Desaga, Heidelberg
Bunsen burner	Merck, Darmstadt
Bürker counting chamber	OptikLabor, Friedrichsdorf
CO ₂ -Incubator	Binder Labortechnik, Tuttlingen
Cytocentrifuge (Cytospin 3)	Shandon, Frankfurt
Digital Weighters BP121S and BP1200	Sartorius Ag, Göttingen
DNA gel electrophoresis apparatus	Bio-Rad, München
DNA/RNA Spectrophotometer	Pharmacia Biotech, Uppsala, Sweden
Electronic pipette	Eppendorf, Hamburg
ELISA-Reader	SLT Labinstrument, Crailsheim
FACS Calibur Flow Cytometer	Becton Dickinson, Mountain View, CA, USA
FACSScan Flow Cytometer	Becton Dickinson, Mountain View, CA, USA
Film Case (18x24cm)	Dr. Goos suprema
Fluorescence microscope	Olympus, Japan
Gel dryer M543	BioRad, München
Glass syringes Fortuna Optima (1 ml, with Luer-Lok tip)	Roth, Karlsruhe
Heating block (ML 100)	Kleinfeld, Labortechnik
Ice mashine AF100	Scotsman, Milan, Italy
Incubator shaker Innova 4000	New Brunswick Scientific, Edison, NJ, USA
Inverted microscope	Hund Wetzlar, Wetzlar
Laminar flow hood	Heraeus Instruments, Hanau
Light microscope	Carl Zeiss, Jena
Magnet stirrer MR-3001	Heildolph, Schwabach
Megafuge1.0/1.0R	Heraeus Instruments, Hanau
Microcuvette	Greiner, Frickenhausen
Microwave oven	Bosch, München

Orbital shaker for bacterial culture	Sternkopf, Lübeck
PCR-cycler	Biometra, Göttingen
Peristaltic pump P-1	Pharmacia Biotech, Uppsala, Sweden
pH-meter	WTW, Weilheim
Pipette aid	Hirtschmann Laborgeräte
Pipettes	Eppendorf, Hamburg
Quartzcuvette	Biometra, Göttingen
Darkroom lamp Model A	Eastman Kodak Company, Rochester, NY, USA
SDS electrophoresis apparatus	Bio-Rad, München
Shaker KL-2	Merck, Darmstadt
Spectrophotometer Genesis 5	Omnilab, Hamburg
Surgical scalpel	Becton Dickinson, NJ, USA
Ultracentrifuge Sorvall RC 5B	Kendro Laboratory Products
Ultrasound apparatus Sonorex TK52	Bandelin, Berlin
UV Photometer GeneRay	Biometra, Göttingen
UV transilluminator	Fluco-Link
UV transilluminator with digital camera	MWG Biotech, Ebersberg
Vortex mixer	Heidolph, Schwabach
Waterbath	Haake, Karlsruhe
Wax pen	DAKO, Glostrup, Danmark

2.1.2 Reagents

β -mercaptoethanol	Roche Diagnostics, Mannheim and Gibco BRL, Eggenstein
1 Kb DNA-ladder	MBI, Fermentas, St. Leon-Rot
100 bp Plus DNA-ladder	MBI, Fermentas, St. Leon-Rot
2N H ₂ SO ₄	Sigma, Deisenhofen
Acetone	Hedinger, Stuttgart
Acrylamid/Bisacrylamid 30%-0.8% (29:1)	Roth, Karlsruhe
Agar	Gibco BRL, Eggenstein
Amonium persulfate	Roth, Karlsruhe
Ampicillin	Sigma, Deisenhofen
Blocking reagent for ELISA	Boehringer Mannheim
BM Blue POD Substrate for ELISA	Boehringer Mannheim
Boric acid	Sigma, Deisenhofen
Bradford Reagent	Merck, Darmstadt

Bromphenolblue	SERVA Electrophoresis, Heidelberg
BSA (Bovine Serum Albumine)	ICN Biomedicals, Costa Mesa, USA
Carbonate buffer (coating buffer pH 9,6)	Boehringer Mannheim
Chloroquine	Sigma, Deisenhofen
Cohn II g-Globuline	Sigma, Deisenhofen
Coomassie Brilliant Blue	Merck, Darmstadt
DABCO	Merck, Darmstadt
DEAE-Dextran	Sigma, Deisenhofen
D-Glucose	Sigma, Deisenhofen
DMSO (dimethyl-sulphoxid)	Sigma, Deisenhofen
dNTP	Roche Diagnostics, Mannheim
EDTA	Sigma, Deisenhofen
Ethanol	J. T. Baker, Deventer, Holland
Ethidium bromide	Boehringer Mannheim
FACS sheath buffer	Becton Dickinson, MountainView, CA, USA
FCS (Fetal calf serum)	Gibco BRL, Eggenstein
Ficoll (Density 1.077)	Biochrom AG, Berlin
G418 (Geneticin, Neomycin)	Gibco BRL, Eggenstein
Gentamycin	Gibco BRL, Eggenstein
Glycerin	AppliChem, Darmstadt
Glycerol	FERAK, Berlin
Glycin	Riedel-de-Haen, Seelze
HEPES (N-2-hydroxyethylpiperazine-N'-2ethanesulfonic acid)	Sigma, Deisenhofen
HT Media Supplement	Sigma, Deisenhofen
IPTG (isopropyl β -D-thiogalacto-pyranoside)	peqLab, Erlangen
Iscove's medium	Sigma, Deisenhofen
Isopropanol	Sigma-Aldrich, Steinheim and Roth, Karlsruhe
L-Glutamine	Biochrom AG
Ligase buffer (10x)	Roche Diagnostics, Mannheim
MgSO ₄	Sigma, Deisenhofen
MgCl ₂	Sigma, Deisenhofen
Milk powder	Saliter, Obergrünzburg
Na ₂ HPO ₄	Merck, Darmstadt
NaCl	Sigma, Deisenhofen
NaOH	Sigma, Deisenhofen
Natrium acetate	Sigma-Aldrich, Steinheim

Natrium azide	VWR, Buffalo Grove, IL, USA
Paraformaldehyde	Sigma, Deisenhofen
PBS (cell culture grade)	Sigma, Deisenhofen
PBS	BioChem KG, Berlin
Penicillin-Streptomycin	Gibco BRL, Eggenstein
PHA (Phytohemagglutinin)	Abbot, Wiesbaden
Polyethyleneglycol (PEG 30 000)	Fluka Chemika, Buchs, Austria
Polyethyleneglycol (PEG 1450)	Sigma, Deisenhofen
Protein marker	Roth, Karlsruhe
Restriction enzyme buffers A, B and H (10x)	Roche Diagnostics, Mannheim
RPMI 1640 (L-Glutamine free)	Sigma, Deisenhofen and PAA Laboratories, Pasching, Austria
SDS (Sodiumdodecylsulphate)	AppliChem, Darmstadt
Select peptone	Gibco BRL, Eggenstein
Select yeast extract	Gibco BRL, Eggenstein
T4-ligase buffer (10x)	Roche Diagnostics, Mannheim
Taq buffer (10x)	Promega, Madison, WI, USA
TEMED	Serva, Heidelberg
Tris-base	Sigma, Deisenhofen
Trypan Blue	Sigma, Deisenhofen
Trypsin/EDTA (10x)	Biochrom, Berlin
Tween 20	Serva, Heidelberg
X-Gal (5-bromo-4-chloro-3-indolyl β-D-Galactoside)	peqLab, Erlangen
Hydrogen peroxid	Merck, Darmstadt

2.1.3 Consumables and kits

3-way stopcock	Braun, Melsungen
Cell culture flasks (25 cm ² , 75 cm ² and 175 cm ²)	Nunc, Roskilde, Denmark
Cell culture plates (6-, 48-, 96-well plates, flat bottom)	Nunc, Roskilde, Denmark and Greiner, Frickenhausen
Coverslides	Superior, Marienfeld
Cryotubes	Nunc, Roskilde, Denmark
Dialysis membrane VISKING, 36/32	Serva, Heidelberg
ECL-Western Blotting Detection Reagents	Pierce, Rockfort IL, USA
EDTA Vacutainers	Becton Dickinson, Heildelberg
FACS tubes	Becton Dickinson, Heidelberg
Falcon tubes (15 and 50 ml)	Sarstedt, Nürnberg
Hybond-ECL-Nitrocellulose membrane	Schleicher & Schuell, Dassel

Hyperfilm ECL	Amersham Pharmacia, Piscataway, NJ, USA
Microtiterplates (96-well, MaxiSorp)	Nunc, Roskilde, Denmark
MiniPERM bioreactor	Vivascience, Hannover
PCR-tubes (0.2ml)	peqLab, Erlangen
Petri dishes	Greiner, Frickenhausen
Pipette tips	Eppendorf, Hamburg and Greiner, Frickenhausen
Protein G Sepharose 4 Fast Flow	Amersham Biosciences, Amersham, UK
Reaction tubes (0.5 ml, 1.5 ml, 2.0 ml)	Eppendorf, Hamburg
Saran wrap	Dow Chemical Company, Hamburg
Sterile filters (0.22 μ m; 0.4 μ m)	Schleicher&Schuell, Dassel and Nalgene, Neerijse, Belgium
Sterile needles	Sarstedt, Nürnberg and Becton Dickinson, Heidelberg
Sterile pipettes (5 ml, 10 ml, 25 ml)	Sarstedt, Nürnberg
Sticky cover for microtiterplates	Roth, Karlsruhe
Syringes (2 ml, 10 ml, 50 ml)	Becton Dickinson, Heidelberg
TiterMax Gold Adjuvant	Sigma, Deisenhofen
Tubes (5 ml and 10 ml)	Greiner, Frickenhausen
Alexa Fluor® 647 Protein Labeling Kit	Molecular Probes, Eugene, OR, USA
Biotin Labeling Kit	Roche Diagnostics, Mannheim
Gel-Extraction Kit QIAEX II	QIAGEN, Hilden
MACS CD19 MicroBeads	Miltenyi Biotec, Bergisch Gladbach
Mouse Isotyping Kit	Roche Diagnostics, Mannheim
Plasmid Maxi-preparation Kit “Endofree”	QIAGEN, Hilden
Plasmid Maxi-preparation Kit	QIAGEN, Hilden
Plasmid Mini-preparation Kit	peqLab, Erlangen
Polyfect Transfection Kit	QIAGEN, Hilden
Super Signal Chemiluminiscent Substrate	Pierce, Rockford, IL, USA

2.1.4 Biological material

E. coli XL1-Blue Subcloning Grade

Stratagene, La Jolla, CA, USA

SKMel wt -adherent, human skin melanoma cells,
SKMel B7.1 -adherent, human skin melanoma cells,
 -transfected with B7.1 (CD80),
 -Neomycin (G418) resistant

Dr. Wolfgang Rudy,
 Deutschen
 Krebsforschungszentrum,
 Heidelberg

SKMel B7.2 -adherent, human skin melanoma cells,
 -transfected with B7.2 (CD86),
 -Neomycin (G418) resistant

SKMel LICOS -adherent, human skin melanoma cells,
 -transfected with LICOS,
 -Neomycin (G418) resistant

S. Hardtke,
 University of Greifswald

COS-7 -adherent African green monkey kidney cells

ATCC

X63AG8.653 -non-adherent mouse myeloma ATCC

Raji -non-adherent human Burkitt's lymphoma

ATCC

Animals: pathogen-free Balb/c female mice,

Animal Facility,
 University of Greifswald

Blood („buffy coat“)

Institut für Transfusionsmedizin,
 University of Greifswald

2.1.5 Plasmids

pBluescript KS+

Invitrogen, Groning, Holland

pcDNA1.1

Invitrogen, Groning, Holland

pcDNA1.1-CTLA4Ig

Dr. U. Speck,
 Bernhard Nocht Institute for
 Tropical Medicine, Hamburg

pcDNA3-LICOS

S. Hardtke,
 University of Greifswald

2.1.6 Enzymes

BamHI	Roche Diagnostics, Mannheim
HindIII	Roche Diagnostics, Mannheim
BssHII	MBI, Fermentas, Hanover, MD, USA
PvuI	Pharmacia Biotech, Uppsala, Sweden
EagI	New England Biolabs, Frankfurt a. M.
KpnI	Boehringer Mannheim
XbaI	Boehringer Mannheim
T4 ligase	Roche Diagnostics, Mannheim
Taq polymerase	Promega, Madison, WI, USA
RNase	Promega, Madison, WI, USA

2.1.7 Culture media

Unless otherwise specified, the media and the buffers were made in deionized water.

2.1.7.1 Media for bacteria

LB-Medium: 1% Peptone
0.5% Yeast extract
1% NaCl
0.001M NaOH
the pH adjusted to 7.5, autoclaved

LB- agar plates: 1.5 g Agar in 100 ml LB-Medium
After autoclavation, 15 ml medium were distributed per Petri dish. The plates were dried under the laminar flow hood and stored at 4°C.

SOC-Medium: 2% Peptone
0.5% Yeast extract
0.05% NaCl
2.5 M KCl
pH adjusted to 7.0, autoclaved and then added
20 µM Mg²⁺ stock and 20 µM Glucose
filter-sterilized

DNA loading buffer: 1% SDS
9.7% EDTA
0.1% Bromphenolblue
50% Glycerol
in 10 ml TBE

Ampicillin stock solution: 100 mg/ml Ampicillin, filter sterilized
IPTG stock solution: 0.1M in Aqua bidest., filter sterilized
X-Gal stock solution: 50 mg/ml in N, N'-dimethylformamide, filter sterilized

2.1.8.2 Biochemical methods

Stacking gel: 4% Acrylamid/Bis
0.125 M Tris/HCl pH 6.8
0.1% SDS
0.05% APS
0.001% TEMED

Resolving gel: 8%-12% Acrylamid/Bis
0.375 M Tris/HCl pH 8.8
0.1% SDS
0.05% APS
0.01% TEMED

Amonium persulphate (APS) 100 mg/ml

2x loading buffer (SDS-PAGE): 20 mM Tris
0.8% SDS
2% Glycerin
0.1 M DTT
0.03% Bromphenol Blue
the pH adjusted to 6.8

Running buffer for SDS-PAGE: 25 mM Tris
250 mM Glycine
0.1% SDS

20x Transfer buffer pH 8.3: 0.25 M Tris
2 M Glycine

Washing solution: 0.05% Tween 20
in PBS

Blocking solution: 4% dry milk powder
in 0.05% Tween20 PBS

20 mM Sodium phosphate buffer pH 7.0 5.77 ml 1M $\text{NaH}_2\text{PO}_4 \cdot \text{H}_2\text{O}$
4.23 ml 1M $\text{Na}_2\text{HPO}_4 \cdot 2\text{H}_2\text{O}$
the pH adjusted to 7.0

ELISA-Buffers:

Coating buffer: 0.1 M Carbonate buffer pH 9.6
Blocking buffer: Boehringer Blocking reagent 1:10
Dilution buffer: Boehringer Blocking reagent 1:10
Wash buffer: 0.05% Tween 20 in PBS

2.1.8.3 Cell culture methods

G418 stock solution: 50mg/ml, final concentration 1mg/ml, filter sterilize

Trypan Blue stock solution: 0.02mg/ml in PBS

10X PBS, pH 7.4: 26mM KCl
14mM KH_2PO_4
1.4M NaCl
81mM $\text{Na}_2\text{HPO}_4 \cdot 2\text{H}_2\text{O}$
the pH adjusted to 7.4

DEAE Dextran stock solution: 10 mg/ml
in PBS

Cloroquine stock solution: 5.6 mg/ml in PBS

FACS buffer: 2% FCS
0.1% NaN_3
in PBS

RBC Lysis buffer (10x): 1.5M NH_4Cl
100mM NaHCO_3
10mM EDTA
the pH adjusted to 7.2-7.4

<u>CohnII stock solution:</u>	10 mg/ml in PBS
<u>Fixation solution (PFA):</u>	2% paraformaldehyde (PFA) in PBS
<u>Normal mouse serum</u>	Caltag Laboratories Burlingame, CA, USA

2.1.9 Antibodies

2.1.9.1 ELISA

goat anti-mouse IgG	Dianova, Hamburg
sheep anti-human IgG	Dianova, Hamburg
goat anti-human IgG	Dianova, Hamburg
goat anti-mouse IgG-POD	Dianova, Hamburg and Sigma, Deisenhofen
mouse anti-human LICOS (clone HIL131)	Dr. R. A. KroczeK Robert Koch Institute, Berlin
mouse anti-human CTLA4 (clone BNI3)	Bernhard Nocht Institute for Tropical Medicine, Hamburg
mouse anti-human LICOS (clone HGW1)	see Chapter 3
biotinylated mouse anti-human LICOS (HGW1)	see Chapter 3
standard mouse IgG	Frau B. Füll, University of Greifswald

2.1.9.2 Western blot

goat anti-human-IgG-POD	Sigma, Deisenhofen
streptavidin-POD	Sigma, Deisenhofen

2.1.9.3 Flowcytometry

All the antibodies for flow cytometric analysis were directed against human antigens.

2.1.9.3.1 Labeled antibodies

Antigen	Antibody	Fluorochrome	Isotype	Reference
CD14	M ϕ P9	FITC	mo*IgG2b	BD-Pharmingen
CD19	HIB19	FITC	moIgG1	BD-Pharmingen
CD3	UCHT1	FITC	moIgG1	DAKO
CD3	UCHT1	PE	moIgG1	BD-Pharmingen
CD3	UCHT1	Alexa 647	moIgG1	BD-Pharmingen
CD4	RPA-T4	Alexa 647	moIgG1	BD-Pharmingen
CD86	IT2.2	PE	moIgG2b	BD-Pharmingen
HLA-DR	G46-6	APC	moIgG2a	BD-Pharmingen
HLA-DR	G46-6	PE	moIgG2a	BD-Pharmingen
ICOS	C398.4A	FITC	ah*IgG	eBioscience
LICOS	HGW1	Alexa 647	moIgG1	See Chapter 3
LICOS	HIL131	PE	moIgG1	Dr.R. A. Krocze [†]
LICOS	MIH12	PE	moIgG1	eBioscience

ah* =Armenian Hamster; mo* =mouse; [†] Robert Koch Institute, Berlin

2.1.9.3.2 Labelled isotype controls

Antibody	Isotype	Fluorochrome/ conjugate	Reference	Isotype control for:
MPC-11	mo*IgG2b	FITC	BD-Pharmingen	CD14
MOPC-21	moIgG1	FITC	BD-Pharmingen	CD19
MOPC-21	moIgG1	Alexa 647	BD-Pharmingen	CD3
G155-178	moIg2a	APC	BD-Pharmingen	HLA-DR
G155-178	moIg2a	PE	BD-Pharmingen	HLA-DR
n/a	ah*IIgG1	FITC	eBioscience	ICOS
MOPC 31C	moIgG1	biotin	Ancell	LICOS
P3	moIgG1	PE	eBioscience	LICOS

ah* =Armenian Hamster; mo* =mouse

2.1.9.3.3 Primary and blocking antibodies

LICOS clone HGW1	see Chapter 3
Biotinylated LICOS clone HGW1	see Chapter 3
LICOS (clone HIL131)	Dr. R. Kroczeck Robert Koch Institute, Berlin

2.1.9.3.4 Secondary antibodies and conjugates

rat anti-mouse IgG1 PE (clone A85-1)	BD-Pharmingen
goat anti-mouse IgG1 FITC	Southern Biotechnology Associates, Birmingham, AL, USA
streptavidin PE	BD-Pharmingen

2.1.10 Fusion proteins

LICOS-Ig	see Chapter 3
CTLA4-Ig	Bernhard Nocht Institute for Tropical Medicine, Hamburg
B7.1-Ig	Bernhard Nocht Institute for Tropical Medicine, Hamburg

2.2 Methods

The molecular biology, biochemical and cell culture methods used for this work were based on those described in the following laboratory manuals:

Ausubel, F.M., ed (1995). Current Protocols in Molecular Biology, vol. 1-4, Wiley and Sons, New York, USA

Sambrook, J.; Russel, D.W., (2001). Molecular Cloning: A Laboratory Manual, 3.Edition, Cold Spring Harbour Laboratory Press, New York, USA

Current Protocols in Molecular Biology (1997)

Current Protocols in Immunology (1992)

2.2.1 Molecular biology methods

2.2.1.1 Primers

The primers were designed for the extracellular domain of human LICOS molecule (the GL50 splice variant) and they contained restriction sites for either HindIII or BamHI.

Primers sequence:

-forward primer 5'CGC CCG CAA GCT TAC CAT GCG GCT GGG CAG TCC T 3'

-reverse primer 5' GAT CGG ATC CGC GTT TTT CTG GCC GGT ACT GAC TGG 3'.

The sequence from which the primers were derived can be found in the NCBI database, under the accession number AF199028.

2.2.1.2 Polymerase chain reaction (PCR)

Polymerase Chain Reaction (PCR) is a cyclic reaction that allows the *in vitro* amplification of a small quantity of a polynucleotide sequence. PCR requires the presence of a template sequence of DNA, two oligonucleotide primers and a thermostable DNA polymerase (for example, Taq polymerase from *Thermus aquaticus*). The reaction takes place in three steps: template denaturation, primer annealing, and the extension of the annealed primers by DNA polymerase.

The PCR reaction was performed in 0.5 ml Eppendorf tubes, as follows:

dNTP (10X)	2.0 µl
Taq buffer (10X)	2.5 µl
DNA (1 mg/ml)	1.0 µl
Primer forward (20 µM)	1.0 µl
Primer reverse (20 µM)	1.0 µl
Taq Polymerase (5 U/µl)	0.5 µl
dH ₂ O	17.0 µl

PCR steps included:

Hot start	60°C	30 sec
Denaturation	95°C	30 sec
Annealing	60°C	30 sec
Synthesis	72°C	1min 15 sec
Elongation	72°C	5 min

2.2.1.3 DNA gel electrophoresis

By the means of electrophoresis, DNA fragments of different sizes loaded on an agarose gel can be separated by applying an electric field. The mixture of DNA and loading buffer was run on an 1% agarose gel, in TBE (1X), for 50-70 min at 100 V, or on 0.8% agarose gel, for 60 min at 75 V. To visualize the DNA fragments, ethidium bromide was incorporated into the gels at a final concentration of 0.5 µg/ml (10 mg/ml stock). As molecular weight markers “100 bp ladder” and “1 Kb ladder” (10 µl per slot) were used.

2.2.1.4 Agarose gel extraction of DNA fragments

After PCR (see section 2.2.1.2) or restriction reaction (see section 2.2.1.6), the resulting DNA fragments were separated on a gel of agarose of appropriate concentration and the desired DNA bands were excised from the gel with a sharp scalpel under the UV light of the transilluminator.

The extraction and purification of various DNA fragments were performed using QiaexII Gel Extraction Kit (QIAGEN), according to the manufacturer protocol. After the last centrifugation step, the supernatant containing the purified DNA fragment was transferred into a clean tube and the DNases were inactivated by incubating the tube at 65°C for 10 min.

2.2.1.5 Quantitation of DNA

DNA concentration was determined by spectrophotometric measurement of the absorption at 260 nm (A_{260}), according to the formula:

DNA concentration (µg/ml) = $A_{260} \times 50 \times \text{dilution factor}$, when one absorption unit at 260 nm corresponds to a concentration of 50 µg DNA/ml.

Because the absorption of nucleic acids depends on the pH and ionic strength of the solvent (Wilfinger, Mackey et al. 1997), to obtain reliable results, the DNA was resuspended in low-salt buffer, at low ionic strength, alkaline pH, such as Tris·Cl 10 mM, pH 8.5. The values of A_{260} were between 0.2 and 0.9, which ensured the exact determination of the concentration

(Sauer, Philippe et al., 1998*). The DNA contained no RNA contamination, as shown by agarose gel analysis.

The contamination of plasmid DNA with residual proteins was determined by measuring the absorption at 280 nm (A_{280}). The ratio A_{260}/A_{280} was in the range of 1.8 and 2.00, showing that DNA solution was 90% to 100% protein free.

2.2.1.6 Restriction digestion of DNA

The restriction reactions were performed according to the producer's indications, using the appropriate buffer for the highest enzymatic activity. When a double restriction was performed, the buffer was chosen to provide the best reaction conditions (pH, Mg^{2+} , salt concentration) and the maximum enzymatic activity (usually more than 75%) for both enzymes. The corresponding buffer was diluted 1:10 in the final volume. Bovine Serum Albumin (BSA) was added to digestion reactions to stabilize the enzyme at 1 mg/ml. To digest contaminant RNA, RNase was added at a final concentration of 0.01 mg/ml. Based on unit definition, an excess of 2- to 3-fold of restriction enzyme over DNA, depending on the enzyme and the context in which it was used with regards to its level of activity, was added to the reaction mix. The amount of DNA to be digested depended on the purpose of its usage, usually between 0.2 and 3.5 μ g, with the proportionately scaled final volume of the basic reaction (20 μ l).

Most restriction enzymes used had maximum activity at 37°C (BamHI, HindIII, PvuI, EagI, KpnI, XbaI). One enzyme required higher temperature for its optimal activity (BssHII, 50°C). Typically, the restriction reaction lasted 2-3h. After the appropriate incubation time, the restriction enzymes were inactivated with EDTA 10 mM final concentration, or when appropriate, by heat (EagI, 15min. at 65°C).

2.2.1.7 Ligation of DNA fragments

The cohesive ended fragments (LICOS, Ig) resulted after restriction reaction (see section 2.2.1.6 and Fig. 1) were ligated with T4 ligase in a molar ratio of 1:1, following the manufacturer recommendations. However, when an insert was ligated into a vector (pBluescript or pcDNA1.1), the molar ratio of vector : insert used was 1:3. Ligation reaction was performed in the presence of 2 Weiss units T4 DNA ligase and 1 μ l ligase buffer per 10 μ l final volume of reaction mix. The reaction was incubated at room temperature for 4h or at 4°C overnight, then the enzyme was inactivated by heating to 70°C for 10 min.

*Sauer, Philippe; Muller, Markus; Kang, Jie, (1998). Quantitation of DNA. Qiagen Corporation

2.2.1.8 Storage of DNA and of bacteria strains

Plasmid DNA, DNA fragments, or ligated DNA fragments were stored at 4°C or -20°C. For bacteria strains storage, 1 ml of a freshly saturated culture was added to 1 ml of glycerol solution and stored at -70°C.

2.2.1.9 Initiation of bacterial culture

From glycerol stock, stored at -70°C, or from transformation plates, *E. coli* containing pBluescript, or recombinant vectors (pBluescript-LICOSIg, pcDNA1.1-LICOSIg and pcDNA1.1-CTLA4Ig, respectively), was inoculated on LB agar plates supplemented with ampicillin (Amp) 100 µg/ml and incubated at 37°C over night. Next day, one medium-sized isolated colony was inoculated into 5 ml (for MiniPrep) or 2 ml (for the starter culture of the Maxi Prep) liquid LB medium supplemented with ampicillin 100 µg/ml and grown at 37°C either over night with shaking at 250 rpm (for MiniPrep) or for 8h at 300 rpm (for the starter culture for the Maxi Prep).

2.2.1.10 Plasmid preparation from bacteria

2.2.1.10.1 Plasmid Mini Prep

The plasmid DNA was isolated with PeqLab Plasmid miniprep kit. Bacteria were pelleted for 1 min at 10.000xg and further processed after the recommendation of the manufacturer.

The plasmid purification procedure was based on the alkaline lysis method of Birnboim and Doly (Birnboim and Doly 1979). Briefly, the bacterial cells were lysed under alkaline conditions resulting in denaturation of both nucleic acids and proteins. Then, the solution was neutralized and chromosomal DNA and proteins precipitated. Plasmids renatured correctly and remained in solution allowing their separation from chromosomal DNA and proteins by centrifugation. The supernatant was loaded on a column, where the DNA bound to a silicium membrane and the contaminants were washed away. The DNA was eluted with Tris-Cl buffer 10 mM, pH 8.5.

2.2.1.10.2 Plasmid Maxi Prep

When a greater amount of DNA was needed for further applications, it was obtained with Qiagen Plasmid Maxi kit. 100 ml of LB Amp medium were inoculated with 200 µl of starter culture (8h old) (see section 2.2.1.9) and grown overnight (16h) at 37°C, 250 rpm. The bacteria were centrifuged at 6 000xg for 15 min at 4°C and further processed by the producer recommendation. For the principle of the method, see section 2.2.1.10.1. In addition, filtering the bacterial lysate through a provided cartridge enabled a rapid plasmid isolation without

centrifugation. The filtered lysate was further cleared by passing it through a column; the DNA was eluted in a high-salt buffer. Precipitation of plasmid DNA with isopropanol led to its concentration when resuspended in low-salt Tris·Cl buffer 10 mM, pH 8.5.

For the transfection of eukaryotic cells, high amounts of ultrapure, endotoxin-free DNA were needed and they were obtained with Qiagen EndoFree Plasmid kit, which includes an supplementary endotoxin-removal step.

2.2.1.11 Transformation of competent bacteria

To 50 µl competent bacteria (*E. coli* XL1-Blue Subcloning Grade competent cells - Stratagene) were added approx. 50 ng ligated DNA and incubated on ice for 20 min. Thereafter, the bacteria cells were subjected to a thermic shock by transferring them from ice on a water bath (42°C) for 45 sec and then back on ice, for another 2 min. Next, 900 µl LB medium warmed up at 42°C, were added to the cells and incubated at 37°C with shaking at 225 rpm for 60 min. The transformed bacteria were plated at 1:10 dilution (200 µl) either on LB Amp (100 µg/ml), when the bacteria were transformed with pcDNA1.1, pcDNA1.1-CTLA4Ig, pcDNA1.1-LICOSIg or on X-Gal/IPTG LB Amp plates, when bacteria received pBluescript-LICOS.

For the preparation of X-Gal/IPTG LB Amp plates, LB agar plates were spread with a mixture of 100 µl LB medium, 40 µl X-Gal (stock 40 mg/ml) and 40 µl IPTG (stock 0.1M). The X-Gal/IPTG LB Amp plates were incubated at 37°C for 17h. Colonies containing plasmids without inserts were blue after a 17-hour incubation time, while colonies containing the plasmid with insert remained white. The blue color was enhanced by additionally incubating the plates at 4°C for 2h. Transformed bacteria plated on LB Amp plates were grown at 37°C overnight.

2.2.1.12 DNA sequencing

The pBluescript-LICOS was sequenced between T3 and T7 promoters, a region that covers a multiple cloning site in which the LICOS fragment was inserted, by SeqLab (Göttingen, Germany).

The pcDNA1.1-LICOSIg was sequenced with primers that cover the joining of LICOS and Ig, the two fragments cloned. Primers' sequence:

-forward primer 5'GTCGTCAGCGCCCCCACA 3'

-reverse primer 5'GATCCCGAGGGTGAGTACTAAGCTTCA 3'

2.2.2 Biochemical methods

2.2.2.1 SDS -PAGE of proteins

SDS-PAGE is a one-dimensional gel electrophoresis, which under denaturing conditions (boiling in the presence of SDS, treatment with β -mercaptoethanol) and in a discontinuous buffer system allows the separation of proteins function of their molecular size.

The SDS-PAGE was performed either in an 8% or 12% polyacrylamide gels. The resolving gel was allowed to polymerize by covering it with ethanol, which was washed away after 30 min. Then, the stacking gel was poured, the comb immersed and the gel was allowed to polymerize for 30 min. Next, the comb was removed and the polymerized gel wells washed and the gel assembled into the electrophoresis device. The samples were mixed with loading buffer and denatured by boiling at 95°C for 5 min. The gel was run at 30 mA per gel (15 V/cm) for 1h. In order to determine the molecular size of sample proteins, a protein marker was run along with them.

2.2.2.2 Western blotting

The protein mixture separated previously by SDS-PAGE (see section 2.2.2.1) was electrophoretically transferred onto a nitrocellulose membrane using a semidry transfer apparatus. The current was applied at 0.8 mA/cm² for 1h. To prevent the unspecific binding of the Ab, the membrane was next incubated for 1h in blocking buffer (0.05% Tween20/4% nonfat dry milk/PBS), at room temperature with agitation on an orbital shaker, or, alternatively, at 4°C overnight. The membrane was briefly rinsed and extensively washed in 0.05% Tween20/PBS several times and then incubated with the POD-coupled antibody (goat anti-human IgG-POD 1:2000) diluted in 0.05% Tween20/1% nonfat dry milk/PBS at 4°C over night or at room temperature for 1h. After washing, bound POD-coupled Ab were detected by providing the enzyme with the chemiluminescent substrate. For that purpose, the two components of the ECL system were mixed in a 1:1 ratio, poured over the membrane and incubated for 1 min at room temperature. The membrane was wrapped in SaranWrap and, in a dark room, placed face down onto an ECL-sensitive film. Depending on the strength of the signal, the film was exposed for various time frames, ranging from 1 min to overnight and developed automatically.

2.2.2.3 Purification of LICOS-Ig and anti-LICOS HGW1

For increased yields of LICOS-Ig, Protein G Sepharose was used. All the solutions that run through the column (supernatant, washing buffer, elution buffer) were filter sterilized (0.45 μm), degassed and at the same temperature as the column (4°C). Protein G Sepharose 4 Fast Flow, was packed in a 10 cm high column and equilibrated with washing buffer until reached the pH 7.0. The cell culture or hybridoma supernatant was applied on the column and the unbound proteins of the supernatant were washed away until Bradford test was negative. Next, the matrix-coupled protein was eluted as 0.5-ml fractions with an acidic glycine solution (0.1M, pH 2.7) and neutralized with 50 μl 1M Tris-Cl pH 9.0 to avoid damaging the protein. The eluted fractions were assayed for protein content by Bradford test and those containing proteins were pooled. The protein solution was concentrated by removal of the water with PEG 30.000 and dialyzed against PBS (200X volumes or more) several times at 4°C.

2.2.2.4 Estimation of the protein concentration

Different protein concentrations were estimated by three methods: the absorption at 280nm, ELISA and Bradford assay.

Absorption at 280 nm (A_{280}). For pure protein of known absorbance coefficient (1.4 for antibodies) and for a path length of 1 cm, the following formula was used:

Concentration (mg/ml) = A_{280} : absorbance coefficient. This method was used to ascertain the concentration of the purified LICOS-Ig fusion protein.

ELISA. A standard curve was drawn using the OD values of a serial dilution between 5 ng/ml and 0.078 ng/ml of mouse IgG, from which the concentration of the protein of interest was determined. ELISA was used to determine the concentration of the hybridoma supernatant.

Bradford assay. In the present work, the Bradford assay was used just to assess the presence or the absence of the protein in a given volume. In the case of protein purification, 10 μl flow-through or eluate was added to 90 μl of Bradford solution, and the presence of the protein was indicated by the corresponding change of the mix color.

2.2.2.5 Biotinylation of LICOS-Ig fusion protein and anti-LICOS mAb HGW1 and Alexa Fluor® 647 labeling of anti-LICOS mAb HGW1

Roche's "Biotin labeling kit" was used for the biotinylation of LICOS-Ig fusion protein. The protein to Biotin-7-NHS ratios used were 1:10, 1:20, 1:40. The proteins were labeled in concordance with producer's protocol.

Alexa Fluor® 647 Protein Labeling Kit (Molecular Probes) enabled the tagging of anti-LICOS mAb. The procedure was executed in conformity with manufacturer's recommendation.

2.2.2.6 ELISA and competitive ELISA

ELISA was the method of choice to estimate the concentration of mAbs, to confirm the presence of LICOS-Ig in COS-7 transfected supernatant, to screen the hybridoma supernatants for the production of monoclonal Ab and to assess the binding capacity of two anti-LICOS mAb - one reference, namely HIL131 and the other one produced in our lab, HGW1.

First, a 96-well Nunc Maxisorb Immunoplate was coated with sheep anti-human IgG or goat anti-mouse IgG diluted 1:520 (2.5 µg/ml final concentration), and 1:720 (2.5 µg/ml final concentration), respectively, in coating buffer pH 9.6 and incubated at 4°C over night. After washing in 0.05% Tween20/PBS, 200 µl/well blocking buffer was incubated for 1h to avoid the unspecific binding of Ab. The next steps were performed differently, as follows:

- a. For determination of Ab concentration, 50 µl of a series of dilutions of hybridoma supernatants and a series of dilutions of standard mouse IgG solution of known concentration (between 5 ng/ml and 0.078 ng/ml), were incubated at room temperature, for 1h, with gentle shaking.
- b. To detect the presence of LICOS-Ig in the supernatant, 50 µl of serial dilutions of LICOS-Ig supernatant and, as a negative control, CTLA4-Ig supernatants at optimal dilution were incubated for 1h. Following the washing steps, 50 µl of anti-CTLA4 mAb (BNI3) and anti-LICOS mAb (HIL131) of optimal dilution were added and incubated for 1h as described above.
- c. To screen the hybridoma supernatants for the production of mAb, the procedure was identical to b., excepting that LICOS-Ig was added at optimum dilution and the undiluted hybridoma supernatant was used instead of anti-LICOS mAb (HIL131) at different stages of cloning and screening.
- d. For competitive ELISA, 50 µl of LICOS-Ig and, as a negative control, CTLA4-Ig supernatants at optimal dilution, and incubated for 1h. Then the specific binding sites were blocked progressively with increasing concentration of purified anti-LICOS HIL131 mAb, starting at 0.003 µg/ml up to 60 µg/ml, for 15min. 50 µl of biotinylated HGW1 suboptimal

concentration (1/625 or 1/3125) were added and incubated for 1h at room temperature. The next steps were again common for all four cases.

After unbound proteins were removed by washing with 0.05% Tween20/PBS, the conjugated antibody (goat anti-mouse IgG-POD) was added at 0.8 µg/ml and incubated for 1h. All the incubation times, except for the overnight incubation, were carried out at room temperature and with mild shaking. After the washing step, 50 µl BM Blue POD substrate solution was added and the reaction was allowed to develop for maximum 15 min. The color reaction was stopped with 100 µl of 2M H₂SO₄. The absorption at 450 nm was measured using an ELISA reader.

2.2.3 Cell culture methods

2.2.3.1 General conditions of cell culture and sterile techniques

The handling of cultured cells was performed under a laminar flow hood. The cells were grown in incubators at 37°C, in a humidified atmosphere containing 5% CO₂. All the materials that came into contact with the cultures were sterilized before usage by autoclaving or by dry heat. All the solutions, except for the basic culture media purchased already sterile, were added to the culture after filter sterilization through 0.22 or 0.45 µm filters. The cultured cells were pelleted by 300xg centrifugation, for 6 min, if not otherwise specified. The basic culture medium was RPMI 1640.

2.2.3.2 Cell lines culture

The cell lines used in this work were: COS-7 (adherent, African green monkey kidney cells), SKMel (adherent, human skin melanoma cells), Raji (non-adherent, human Burkitt's lymphoma), X63AG8.653 (non-adherent, mouse myeloma).

SKMel cell line that was transfected to express on the cell surface either LICOS, B7.1 or B7.2. The transfected cell lines SKMel LICOS, SKMel B7.1 and SKMel B7.2 were cultivated in R10F supplemented with 1 mg/ml G418 (Geneticin, Neomycin), as selection marker, whereas the wild-type cell lines – COS, SKMel wt and Raji – were cultured in R10F medium.

Typically, when the culture was 80-95% confluent or the medium color turned yellow, the adherent COS and SKMel cells were detached with Trypsin/EDTA 1X, incubated for 2 min at room temperature, washed one time in PBS and then plated at 1-5x10⁵ cells/ml. After need. COS cells were maintained at 3x10⁴ cells/ml and split 1:3 to 1:5, two or three times a week. SKMel wt, B7.1 and B7.2 were maintained at 1-3x10⁵ cells/ml and split 1:10 once a week, while SKMel LICOS, growing slower, was maintained at 5x10⁵ cells/ml and split every 10th day.

Raji cells were maintained at 5x10⁵ cells/ml and split 1:4 two times a week.

Mouse X63-Ag8.658 myeloma cells (Kearney, Radbruch et al. 1979), cultured in Iscove's+ medium, were maintained at 10^6 cells/ml and split 1:20 every second day.

2.2.3.3 Determination of cell count and viability

The viability of the cells was estimated by Trypan-Blue exclusion. One aliquot of cell suspension was diluted 1:10 in Trypan-Blue solution, the cell number counted and the cell concentration calculated.

2.2.3.4 Cryoconservation and recovery of cell lines

For long-term storage, the cell lines were frozen in liquid nitrogen (-196°C). To avoid cell damage, DMSO was used as cryoprotective agent. Between 2×10^6 and 1×10^7 cells per ml freezing medium were aliquoted in cryotubes, stored at -70°C for 24h and then transferred into liquid nitrogen.

When a cryopreserved cell line was needed, it was rapidly thawed at 37°C , washed with 20% FCS RPMI to remove residual DMSO, and plated in the appropriate culture medium at high density to ensure recovery.

2.2.3.5 Transfection of eukaryotic cells

The COS-7 cell line was transiently transfected with pcDNA1.1-LICOSIg vector to produce high amounts of fusion protein in two ways: with PolyFect Reagent (Qiagen) (see section 2.2.3.5.1) and with DEAE-Dextran and chloroquine (see section 2.2.3.5.2). COS-7 cell line was transfected with high purity, endotoxin-free plasmid DNA (see section 2.2.1.10.2).

2.2.3.5.1 Transfection of COS cells with PolyFect Reagent

The day prior to transfection, 4.5×10^5 COS cells/well were cultivated in R10F medium, in a 6 well-plate, so that in the moment of transfection they achieved approx. 80% confluence. 1.5 μg DNA (pcDNA1.1-LICOSIg) in Tris-Cl buffer were diluted in RPMI to a final volume of 100 μl . Next, 10 μl of PolyFect Reagent were added to the DNA solution, mixed and incubated at room temperature for 5-10 min. Cells were washed one time with PBS and fed with R10F. 0.6 ml R10F were added to DNA- PolyFect Reagent mixture and the total volume obtained was transferred immediately to the cells and incubated at 37°C , in a humidified atmosphere containing 5% CO_2 , for 72h. The supernatant was recovered and assayed for LICOS-Ig fusion protein presence (see sections 2.2.2.1 and 2.2.2.2).

2.2.3.5.2 Transfection of COS cells with DEAE-Dextran and chloroquine

30 µg plasmid DNA (pcDNA1.1-LICOSIg) were diluted in 15 ml 2% FCS RPMI. 240 µl DEAE Dextran (10 mg/ml), 600 µl chloroquine (5.6 mg/ml) and 14 ml 2% FCS RPMI were mixed together and added to the endotoxin-free DNA solution (see section 2.2.1.10.2). 80% confluent COS cells were washed with RPMI, covered with the transfection mixture and incubated at 37°C for 4h. After the removal of transfection medium, the cells were incubated for 8 min in RPMI containing 10% DMSO. After a washing step, the cells were fed with R10F medium and incubated for 7 days at 37°C, in a humidified atmosphere containing 5% CO₂. The supernatant was recovered and assayed for LICOS-Ig fusion protein presence (see sections 2.2.2.1 and 2.2.2.2).

2.2.3.6 Stabilization of SKMel LICOS phenotype by limiting dilution

The SKMel LICOS cell line, previously obtained in our laboratory by S. Hardtke, showed a progressive loss of LICOS phenotype after several passages after thawing, rendering it unreliable for experiments. The best method to obtain a stable cell line was selection by limiting dilution, but this method was time-consuming (approx. 3 month needed to obtain a sufficient number of cells). Briefly, a culture of instable SKMel LICOS, in the log growth phase, was trypsinized as described above (see section 2.2.3.2) and resuspended at 1.5×10^3 cells/ml, in complete standard growth medium, yet containing 20%FCS. From the initial suspension a dilution of 1:100 (about 15 cells/ml), and from this further serial dilutions were prepared at approximately 5 cells/ml and 1 cell/ml, of which 200 µl/well were plated in a flat-bottom 96-well plate. The plate was incubated 2 months in a humidified 37°C, 5% CO₂ incubator. After approx. 5 weeks, monoclonality became observable by inspection with an inverted microscope, in the wells seeded with the 1 cell/ml dilution. Polyclonal growth, which was evidenced by more than one cluster of cells per well, appeared earlier. All the wells showing monoclonal growth were expanded, tested for a high level of LICOS expression on the cell surface by FACS analysis (see section 2.2.3.10.1) and frozen.

2.2.3.7 Isolation and PHA stimulation of PBMC

Peripheral blood mononuclear cells (PBMC) were isolated from buffy coats or EDTA whole blood, by gradient-density centrifugation in Ficoll-Hipaque (density 1.077 g/ml). The blood was diluted 1:2 in PBS and added slowly over Ficoll in a ratio of 2.5:1. The tubes were centrifuged at 1.600xg without brake, for 15 min, at room temperature. The mononuclear cell ring was collected and washed three times with PBS. After the last wash, the cells were resuspended in R10F, counted and the concentration adjusted after need. A suspension of 10^6 cells/ml was cultivated in the presence of PHA (1.5µg/ml) for 24, 48 or 72h.

2.2.3.8 Cytocentrifugation and immunohistochemical staining (SKMel, PBMC)

By immunohistochemical staining that follows cytocentrifugation, the antigens on the cell surface as well as intracellular proteins become visible under the fluorescent microscope. Approx. 2×10^4 cells per 100 μ l medium were spun down onto a glass slide by centrifugation (800 rpm, 8 min) and dried over night, at room temperature. The cells on the slides were then fixed in acetone for 5 min and then dried for at least 2h before the slides were stained or stored at -70°C . All incubation times were carried out in a wet chamber. When appropriate, the dilutions were performed in PBS containing 20% human serum. The slides were rinsed and washed with PBS for 5 min. The unspecific binding sites were blocked using 20 μ l/slide of human gamma globulin fraction II (Cohn II, 10mg/ml) for 15 min. After a washing step, the cells were incubated with the first antibody (UCHT1 supernatant 50 μ l/slide, biotinylated LICOS-Ig 1.5 μ g/slide, or HGW1 hybridoma supernatant 50 μ l/slide) for 90 min. Following a 90 min-incubation with goat anti-mouse FITC-labeled antibody (1 μ g/slide) and/or streptavidin-TRITC (Strp-TRITC) (dilution 1:100) the cells were covered with 10 μ l of antifadent solution (DABCO).

2.2.3.9 Positive selection of CD19+ lymphocytes from PBMC

CD19+ lymphocytes were isolated from PBMC by means of magnetic cell sorting using CD19+ MACS MicroBeads (Miltenyi Biotec). Briefly, after PBMC isolation (see section 2.2.3.7), the cells were magnetically labeled with CD19 MicroBeads and loaded on a column placed in the magnetic field of a MACS separator. The magnetically labeled cells were retained on the column, then eluted as the positively selected cell fraction and stained for FACS analysis (see section 2.2.3.10.2).

2.2.3.10 Flowcytometry

2.2.3.10.1 FACS staining of LICOS on the surface of SKMel LICOS cells

Following trypsinization, SKMel LICOS cells were resuspended at 5×10^6 cells/ml in RPMI and from this suspension, 50 μ l containing 2.5×10^5 cells were distributed per tube and washed once in 1 ml FACS buffer. Either of the following antibodies were added to the cells and incubated for 30 min, at 4°C , in the dark: 4 μ l anti-LICOS PE (HIL131), HGW1 Alexa 647 (1:3), 50 μ l of HGW1 hybridoma supernatant, purified HGW1 (50 μ g/ml), biotinylated HGW1 (9 μ g/ml), or the isotype control (mo-IgG1 Alexa 647). After the washing step, the cells incubated with primary Abs were stained with either anti-moIgG1 FITC (1:25) or

streptavidin PE (1:500) and incubated as described above. After washing, the cells were resuspended in 2% PFA and analyzed next day on a FACSCalibur Flow Cytometer.

2.2.3.10.2 FACS staining of PBMC, purified CD19+ lymphocytes and Raji cells

5x10⁵ cells/tube were washed with 1ml FACS buffer. The Fc receptors were blocked with 20 µl of human gamma globulin fraction II (Cohn II, 10 mg/ml), for 15 min, at 4°C. The primary antibodies – 5µl anti-CD3 (FITC or PE coupled), biotinylated LICOS-Ig (60 µg/ml), or anti-LICOS FITC (10 µg/ml) and combination of these – streptavidin PE (1:500) and 50 µl FACS buffer were added to the PBMC and incubated for 30 min, at 4°C, in the dark.

To the purified CD19+ lymphocytes and the Raji cells were added the following Abs: HIL 131 PE, unlabeled HGW1, HGW1 Alexa 647, biotinylated HGW1 and incubated as mentioned above. The cells were washed with FACS buffer and incubated with streptavidin PE or anti-moIgG1 PE (1:10). After washing, the cells were resuspended either in FACS buffer or 2% PFA and analyzed immediately or next day, respectively, on a FACScan Flow Cytometer.

2.2.3.10.3 FACS staining of whole blood cells

To block Fc receptor binding of antibody to human cells and to reduce non-specific binding in general, 50 µl of whole blood collected on EDTA were pre-incubated for 10 min on ice with normal serum from the same species as the specific antibody (10 µl/tube mouse serum) or with 200 µg/ml human gamma globulin fraction II (Cohn II).

For direct staining, the matched isotype controls or specific antibodies (HIL 131 PE, HGW1 Alexa 647, unlabeled HGW1, biotinylated HGW1) were added to each tube directly to the mixture and incubated for 30 min, at 4°C, in the dark. The monoclonal antibody and their isotype control combinations used in the patient study are listed in Table 2.2.3.10.3. All of these mAbs were purchased from Becton-Dickinson, except for anti-huLICOS MIH12 mAb, which was purchased from eBioscience. Lysis of erythrocytes was performed by incubating the cells with 3 ml of RBC lysis solution per tube for 10 min, at room temperature, in the dark. The cells were pelleted and washed with FACS buffer.

For indirect staining (HGW1 supernatant, biotinylated HGW1), the appropriate amount of fluorochrome coupled secondary antibody (anti-moIgG1 PE) or streptavidin PE was added, incubated for 30 min, at 4°C, in the dark, then washed with FACS buffer. Cells were resuspended in FACS buffer and analyzed on a FACSCalibur Flow Cytometer.

In the blocking experiments, the following Ab concentrations were used: HIL131 PE suboptimal concentration 1 µl/tube (1:50), HGW1 Alexa 647 (1:50), unlabeled HGW1 blocking concentration (0.5 mg/ml), unlabeled HIL131 blocking concentration (0.5 mg/ml), biotinylated HGW1 suboptimal concentration (0.5 µg/ml).

Table 2.2.3.10.3. Combinations of monoclonal antibody used in the patients' study.

Fluorescence 1	Fluorescence 2	Fluorescence 4
CD19 FITC	CD86 PE	HLA-DR APC
CD19 FITC	LICOS PE	HLA-DR APC
CD3 FITC	LICOS PE	HLA-DR APC
ICOS FITC	CD3 PE	CD4 Alexa 647
ICOS FITC	HLA-DR PE	CD4 Alexa 647
CD14 FITC	CD86 PE	HLA-DR APC
CD14 FITC	LICOS PE	HLA-DR APC
Isotype control γ 1 FITC	Isotype control γ 1 PE	Isotype control γ 2a APC
Isotype control γ 1 FITC	Isotype control γ 2a PE	Isotype control γ 1 Alexa 647
Isotype control γ 2b FITC	Isotype control γ 1 PE	Isotype control γ 2a APC

2.2.3.10.4 FACS data analysis

FACS measurements were performed on FACS Calibur (Becton-Dickinson) equipped with an argon laser at 488nm, plus a secondary laser with red emission at around 630 nm. Patients' FACS data were processed using CellQuest software (Becton-Dickinson) on a minimum of 25 000 peripheral blood cells. The rest of the data shown in this work were processed using WinMDI 2.8 software and displayed as histograms.

In patients, lymphocyte and monocyte gates were defined on a Forward Scatter/Side Scatter dot-plot. CD19, CD3, CD4 populations were analyzed in the lymphocyte gate, while CD14 population in the monocyte gate. LICOS, CD86 levels were measured in the CD19 and CD14 population as defined above and highlighted in Table 2.2.3.10.4 LICOS level was also determined in the CD3 population, while ICOS expression in both CD3 and CD4 populations. HLA-DR was defined in all populations – CD19, CD3, CD4, CD14 (Table 2.2.3.10.4 and Fig. 33).

Table 2.2.3.10.4 Gates and plots on lymphocyte and monocyte populations used in the patients' study.

Cell population	Gates	2-D Dot-Plots
		CD14+ HLA-DR+
Monocytes	CD14+	CD14+CD86+
		CD14+LICOS+
		CD14+CD86+HLA-DR+
		CD14+LICOS+HLA-DR+
Lymphocytes	CD19+	CD19+HLA-DR+
		CD19+CD86+
		CD19+LICOS+
		CD19+CD86+HLA-DR+
		CD19+LICOS+HLA-DR+
	CD3+	CD3+HLA+
		CD3+LICOS+
		CD3+ICOS+
		CD3+LICOS+HLA-DR+
		CD3+ICOS+HLA-DR+
	CD4+	CD4+HLA-DR+
		CD4+ICOS+
		CD4+ICOS+HLA-DR+

2.2.4 Patients and controls

This pilot study was approved by the local Ethics Board (Ethikkommission der Ärztekammer Mecklenburg-Vorpommern bei der Ernst-Moritz-Arndt Universität Greifswald). The criteria for study enrollment of polytrauma patients were: patient age ≥ 16 years, injury severity score (ISS) ≥ 20 . Sepsis was diagnosed when at least 2 of 4 criteria for systemic inflammatory response syndrome (SIRS) in combination with a septic focus or a positive blood culture. Severe sepsis was defined, in addition, by acute organ dysfunction according to American College of Chest Physicians/Society of Critical Care Medicine Consensus Conference*.

Whole blood collected on EDTA from 6 polytrauma and 10 stroke patients from Intensive Care Unit 2 (ICU2) of University of Greifswald was purchased after the routine clinical parameters were determined. First sample was obtained, for the polytrauma patients, within the first 18h following admission to the ICU; for stroke patients, blood samples were

* American College of Chest Physicians/Society of Critical Care Medicine Consensus Conference: definition for sepsis and organ failure and guidelines for the use of innovative therapies in sepsis. Crit Care Med 20: 864-874, 1992

obtained at variable time points after the admission in ICU, but not later than third day. The analysis was performed for as many days as the patients remained in the ICU or as the blood samples were available. For control, blood samples from 32 healthy donors, mean age 33 years, were included in the study. The clinical and demographic profile of the patients as well as the controls is shown in Table 2.2.4.

Table 2.2.4. Clinical and demographic profile of polytrauma, stroke patients and controls.

Group	Patients with polytrauma	Patients with stroke	Healthy donors Controls
Number of persons	6	9	32
ISS mean	42.33 (SD: 12.12)	-	-
ISS range	29-57	-	-
APACHE II mean	19 (SD: 4.3)	-	-
APACHE II range	13-24	-	-
GCS score mean	-	12 (SD: 4.65)	-
GCS score range	-	6-15	-
NIH score mean	-	6.6 (SD: 0.58)	-
NIH score range	-	6-7	-
Age in years mean	43.33 (SD: 23.95)	62.11 (SD: 13.9)	33.41 (SD: 11.37)
Age in years range	18-70	44-77	19-53
Ratio male:female	4:2	4:5	17:15
Deceased	1	0	0

2.2.5 Generation and production of an anti-LICOS mAb (HGW1) using LICOS-Ig as an antigen

To obtain highly specific antibodies against extracellular domain of LICOS, B cells from mouse spleen were fused to tumor cells (myeloma) to produce hybrid cells or hybridoma (see Fig. 2.2.5). Because hybridoma cells have usually a very low plating efficiency, after fusion they were cultured in the presence of feeder cells (i.e., normal mice splenocytes) that produce growth factors and also provide cell contact for hybridoma. The desired antibody-producing hybridoma was identified by a screening process and further subcloned, eventually resulting in a stable mAb producing clone. To avoid contamination, during the screening and subcloning processes a cell-free mice splenocyte-conditioned medium was used instead of feeder cells. To produce this special medium, after sacrificing the mice, the spleens were aseptically removed, a single cell suspension prepared and grown for several days in Iscove's+ medium. Next, the supernatant was harvested, filter sterilized and stored at -20°C.

2.2.5.1 Immunization of mice

Female BALB/c mice, 10 weeks old were immunized three times as follows. The primary immunization was accomplished using 50-100 µg LICOS-Ig in TiterMax Gold Adjuvant administered intraperitoneally. An intraperitoneal booster injection with 50-100 µg LICOS-Ig in TiterMax Gold Adjuvant followed after 3-4 weeks from priming. After another 3-4 weeks 50 µg LICOS-Ig (without adjuvant) per mouse were injected intravenously (tail vein).

2.2.5.2 Cell fusion and selection of hybridomas

Three days after the last booster injection, the animal was sacrificed by cervical dislocation. The spleen was aseptically drawn, recovered in PBS and squashed between two slides to tease the cells out of the tissue structure into a single cell suspension. The debris were removed and cells further dispersed by passing the suspension through a fine-mash screen and washed with PBS. 1/10 of mouse spleen cells were used for fusion, the rest were frozen in liquid nitrogen (see section 2.2.3.4).

Mouse P3/X63-Ag8.658 myeloma cells cultured in Iscove's+ medium were split on the previous day to be in the logarithmic growth phase by the day of fusion. 3×10^7 myeloma cells and spleen cells from immunized mice were separately washed three times in RPMI (200xg, for 6 min), mixed in a 50 ml tube in a proportion 1:2 and sedimented at 500xg, for 10 min. The mixed-cell pellet was completely drained and gently resuspended in 1ml warm (37°C) PEG 1500 added drop by drop and incubated for exactly 1 min. Next, 11 ml of warm (37°C) serum free medium were added drop by drop, in the following sequence:

1 ml RPMI within 1 min.

2 ml RPMI within 1 min.

4 ml RPMI within 2 min.

4 ml RPMI within 4 min.

The volume was brought up to 50 ml with Iscove's+ and split into two volumes: one volume of 12.5 ml (1/4) and the other of 37.5 ml (3/4) were subsequently brought again to 50 ml. The cells were centrifuged at 500xg, for 10 min.

Normal mouse spleen cells, used as feeder cells, were washed in RPMI and resuspended in 200 ml of Iscove's+ medium, of which 100 ml were added to either of the two sedimented cell mixtures. Next, the mixtures containing the three cell types were plated at 100 µl per well in ten 96-well-flat-bottom plates for each mixture. After 24h, 100 µl/well of Iscove's+ medium enriched with 2X HT (Thymidine Hypoxantine, Sigma), as selection factor, were added.

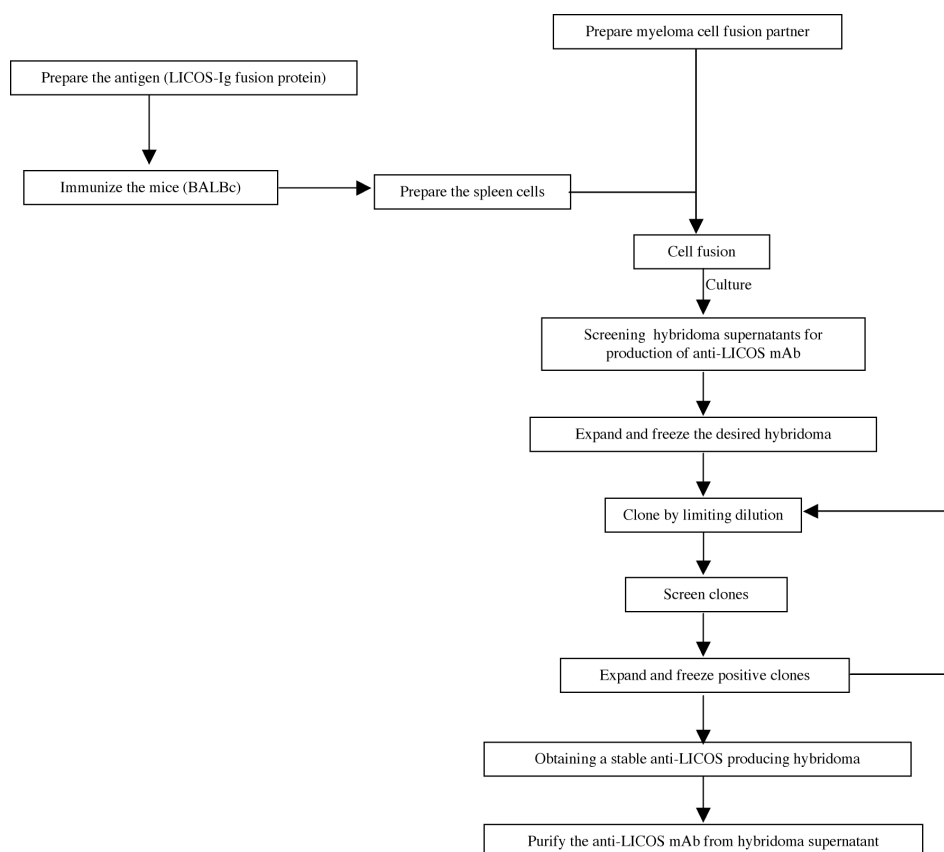


Figure 2.2.5. Flow chart for preparation of the monoclonal antibody.

In the first seven days after fusion, when the color of the medium turned yellow (acidic), the cells were fed with Iscove's+ medium enriched with 1X HT. After 14 days from fusion, the cells were ready for the first screening – most of the wells containing growing cells showed 10 to 25% confluence; some wells with denser cell population turned yellow within 2 days after feeding.

2.2.5.3 Screening of primary hybridoma supernatants

The purpose of screening was to identify the wells with hybridomas that secreted the antibody of desired specificity. The first screening was performed by ELISA (see section 2.2.2.6) when most of the wells containing one cell cluster/well, as determined by inspection with an inverted microscope, turned yellow, i.e., on the 14th day after fusion. The yellow medium was drawn from the wells and replaced with an equal volume of fresh medium. Slowly growing wells, the most likely to originally contain one single cell (clone), were screened later. The screening procedure was performed also after every subcloning (see section 2.2.5.4), to further identify the desired mAb-producing clones, in the process of stabilizing the hybridoma line.

2.2.5.4 Establishment of hybridoma line

Once hybridomas of desired specificity were identified, they were expanded and fed, then the cells were concomitantly frozen and subcloned by limiting dilution in order to obtain homogenous clones derived from a single progenitor. This process was repeated until the great majority of the derived clones gave positive results when assessed for the presence of anti-LICOS mAb by ELISA.

When the positive hybridoma, detected by ELISA in the initial screening, showed 25% to 50% confluence in the master well, the cells were resuspended and a volume containing approx. 400 cells depending on the density of the grown cells per well was taken up into 4 ml 1xHT Iscove's+ medium. From this suspension, a series of eight two-fold dilutions were made and plated on each row of a 96-well plate, at 100 μ l per well. The screening described above was carried out when most of the wells turned yellow, i.e., usually, after 2 to 3 days. Slowly growing wells were screened later. The remained medium in the master well was transferred to a well in 24-well plate. The master well, still containing sufficient numbers of cells to serve as a second back-up to the expanded cells, was refilled with fresh medium. The positive subclones identified later among the screened clones were expanded, frozen and subjected to another subcloning by limiting dilution, as for the primary hybridoma. When the cells in the 24-well plate reached 50% confluence, they were resuspended and centrifuged at 300xg, for 5min, at room temperature. The supernatant was kept as a control and the cell pellet was frozen as a back up (see section 2.2.3.4).

2.2.5.5 Cultivation of hybridoma cells for high antibody production

To produce enough amount of HGW1 mAb supernatant for the purification step (see section 2.2.2.3), hybridoma cells at 90% or more viability (see section 2.2.3.3), were cultured in a miniPERM bioreactor (Vivascience, Hannover). Principally, miniPERM unit consists of a production module and a nutrient module, separated by a semi-permeable dialysis membrane that selectively allows the nutrients and the dissolved gases to diffuse into production module and the metabolites secreted by cells to diffuse into nutrient module. Hybridoma cells were seeded at about $1-3 \times 10^6$ cells/ml ($7-10 \times 10^7$ cells/production unit) in a mixture of Iscove's+ medium and mouse splenocyte-conditioned supernatant in a ratio of 35:1 (see section 2.2.5.4).

Due to the special growth conditions and culture high density, the medium in the nutrient compartment of the miniPERM bioreactor was changed first after 3 days, then again after two days and then every day as the density reached 10×10^6 cells/ml, for a total of 10-13 days. The cell viability was determined at each medium changing point and the culture was stopped when viability was under 30%. The supernatant was centrifuged at 20,000xg for 20 min, filter sterilized and subjected to purification (see section 2.2.2.3).

3. Results

This chapter contains two parts. The first part deals with the cloning, production and purification of a human LICOS-Ig fusion protein and the generation of an anti-huLICOS monoclonal antibody (mAb). For this purpose, the following strategy was adopted. The PCR-amplified DNA fragment coding for the extracellular domain of LICOS costimulatory molecule was cloned into the pBluescript KS + vector (Fig. 1) and then sequenced. After the huLICOS DNA sequence was proven to be in frame and free of mutations, the huLICOS DNA fragment was excised from pBluescript KS + vector and inserted into pcDNA1.1 together with the DNA fragment encoding for the Fc part of human IgG1 (referred herewith as Ig fragment). pcDNA1.1 is a shuttle vector that can be used both as a cloning vector, in prokaryotic systems, and as an expression vector, in eukaryotic systems. This allowed the huLICOS-Ig base sequence to be translated into protein after the transfection of recombinant pcDNA1.1 vector into COS-7 cells. The huLICOS-Ig fusion protein was purified and further used for the immunization of mice, and monoclonal antibody (mAb) production.

In the second part of this chapter, the results of a preliminary study on the expression analysis of ICOS, LICOS, CD86 and HLA-DR on the surface of different immune cells in critically ill patients (major trauma and stroke) are reported.

3.1 Cloning of the extracellular domain of LICOS and construction of the sequencing vector

Full length LICOS cDNA had been previously cloned into pcDNA3.1 in our lab (see Svenja Hardke's work). The cDNA fragment for the extracellular domain of LICOS was amplified with specific primers designed to introduce restriction sites for BamHI and HindIII into the PCR product. The amplified fragment was 787 bp on an agarose gel (Fig. 2).

The amplified product was then extracted from the agarose gel, purified and digested with BamHI and HindIII, which generated a DNA fragment of 774bp, and subsequently cloned between BamHI and HindIII sites of linearized pBluescript KS+ (Fig. 3). The high quality of the pBluescript DNA preparation was demonstrated by the supercoiled form, devoid of covalent circular closed or covalent open forms, of the intact vector (Fig. 3, lane 2).

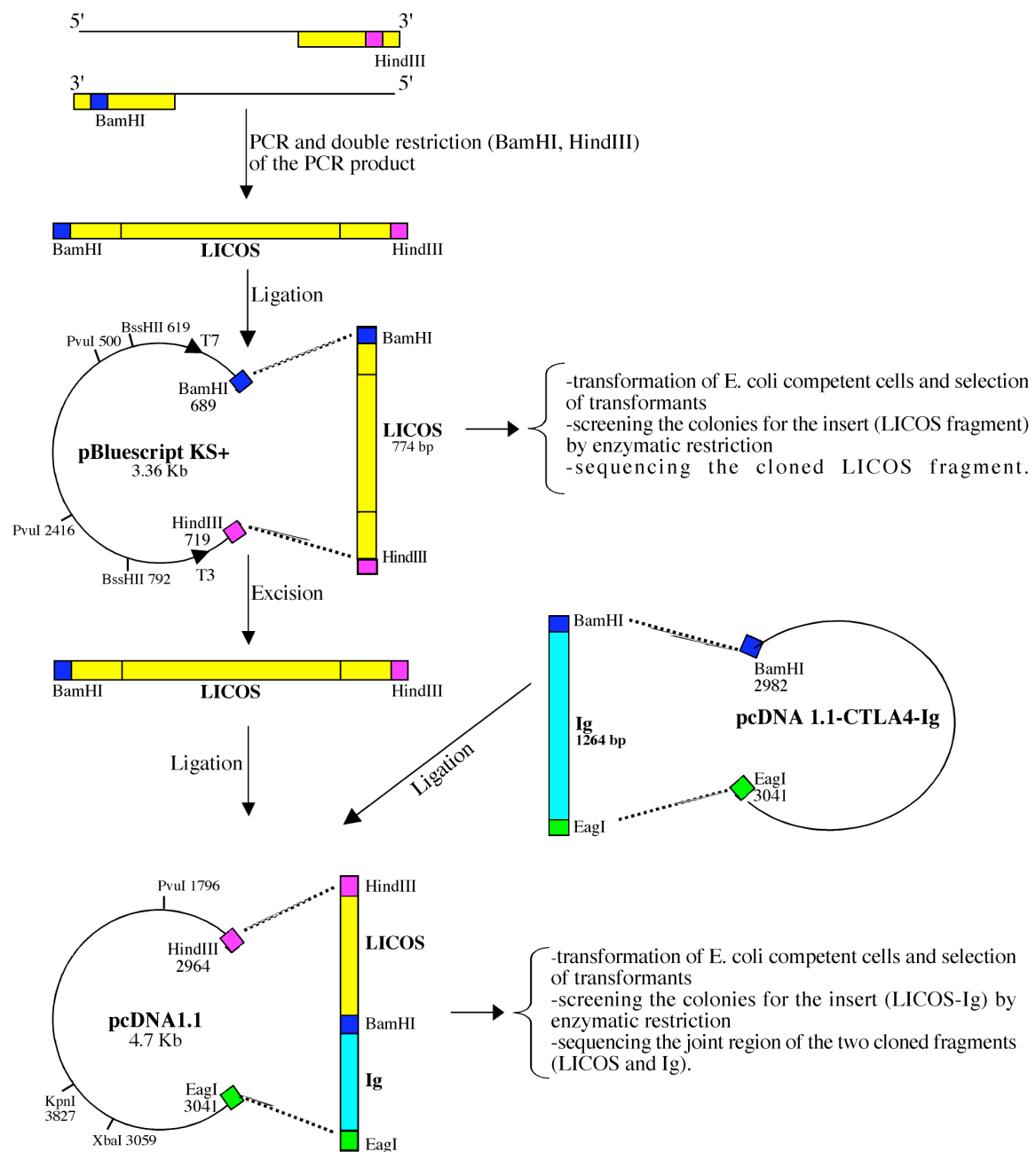


Figure 1. The cloning strategy of huLICOS-Ig fusion protein. The DNA fragment encoding the extracellular domain of LICOS was obtained by PCR amplification of cDNA using specific primers designed to introduce restriction sites for BamHI and HindIII (depicted as blue and pink squares, respectively, in the primers). The restriction enzyme-digested PCR product was ligated into pBluescript KS+ vector and the LICOS insert sequenced. After excision from pBluescript, the LICOS fragment was ligated along with hulg fragment from another vector, into pcDNA1.1. The resulting vector was transfected into COS-7 cells and the LICOS-Ig fusion protein was purified from the supernatant of transfected cells. The positions of the restriction sites of various enzymes used throughout this experiment are given on both pBluescript and pcDNA1.1 vectors.

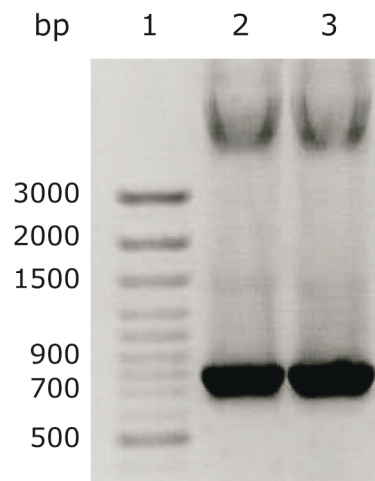


Figure 2. PCR amplification of LICOS extracellular-domain cDNA fragment (787bp). Lane 1, DNA marker (100bp DNA ladder); lanes 2, 3, the amplified DNA fragment for extracellular domain of huLICOS. The amplified DNA fragment for extracellular domain of huLICOS (lanes 2, 3) was located between 700 bp and 800 bp, corresponding to the expected length of 787 bp.

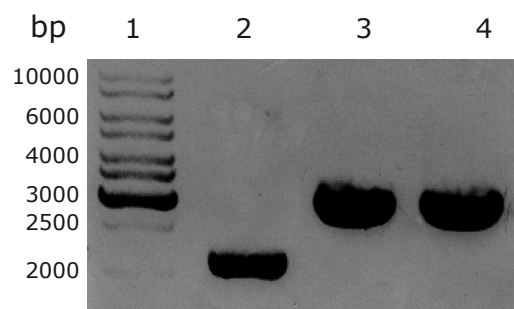


Figure 3. Restriction enzyme digestion of pBluescript with BamHI and Hind III. Lane 1, DNA marker (1Kb DNA ladder); lane 2, intact pBluescript vector (supercoiled form); lanes 3 and 4, linearized pBluescript vector by restriction digestion with BamHI and Hind III; the bands visible around 3500 bp were consistent with the calculated digested-vector size of 3429 bp.

After the restricted pBluescript vector and the LICOS fragment (774 bp) were ligated, competent bacteria were transformed with the resulting recombinant vector. The transformants (19 clones) were screened by restriction enzyme digestion with PvuI to identify those containing the vector with the insert (Fig. 4). PvuI was chosen because it generates the largest size difference between the two resulting fragments of clones that contain and do not contain the insert. If the plasmid had not contained the insert, DNA fragments of 1084 bp and 1916 bp would have been expected after the PvuI digestion. Conversely, if the plasmid had contained the insert, two other segments of 2660 bp and 1038 bp, respectively, would have been generated. Ten clones displayed the 2660 bp band, indicating that they contained the insert (Fig. 4, lanes 1, 2, 3, 9, 10, 11, 12, 13, 14, 17). Nine clones presented the 1916 bp band, and therefore they did not contain the insert (Fig. 4, lanes 4, 5, 6, 7, 8, 15, 16, 18, 19).

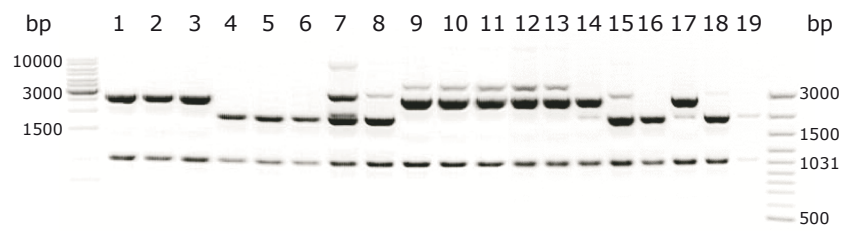


Figure 4. The screening of transformed bacterial colonies for the LICOS insert by restriction digestion of their plasmid DNA with PvuI. As DNA markers, 1Kb DNA ladder (left side) and 100bp DNA ladder (right side) were used. Lanes 1-19 represent plasmid DNA extracted from individual bacterial colonies. Lanes 1, 2, 3, 9, 10, 11, 12, 13, 14 and 17 display the 2660 bp band indicating that the corresponding clones contained the LICOS insert. Lanes 4, 5, 6, 7, 8, 15, 16, 18, and 19 present the 1916 bp band, consequently the corresponding clones did not contain the insert.

To confirm the presence of the LICOS insert, one of the ten positive clones detected by screening with PvuI was subjected to restriction digestion with another enzyme, BssHII (Fig. 5). If the insert had been present, segments of 919 bp and 2788 bp should have been generated. In the absence of the insert, BssHII digestion would have yielded segments of 173 and 3226 bp. Agarose gel analysis of the digestion products revealed two bands, at around 1000 bp and 3000 bp, respectively (Fig. 5, lane 3), similar to the expected size in the case the clone contained the insert.

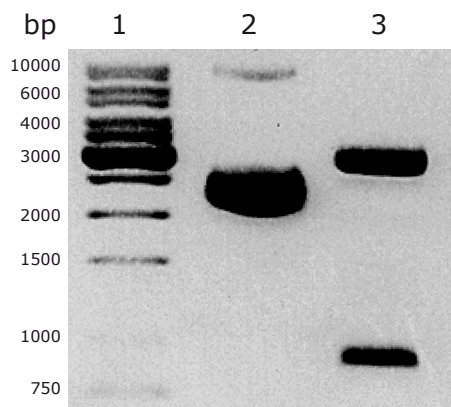


Figure 5. Confirmation of the LICOS insert presence in one positive bacterial clone by restriction digestion with BssHII. Lane 1, DNA marker (1Kb DNA ladder); lane 2, intact pBluescript-LICOS vector (supercoiled form and concatemers); lane 3, the BssHII digestion of pBluescript-LICOS vector yielded two bands, at around 1000 bp and 3000 bp, respectively, consistent with the expected band size (919 bp and 2788 bp, respectively) and confirming the presence of LICOS insert in the vector.

After amplification in bacteria, the pBluescript-LICOS vector was isolated and the LICOS insert sequenced with the T3 and T7 promoter primers of pBluescript vector (Fig. 6). The consensus between the NCBI database sequence of LICOS (AF199028) and the LICOS insert sequence was 100%.

NCBI	1	-----GGCCTCAGGTCCTCCCGC--ACCATGCGGCTGGGCA
T3	9	TGGGTACCGGGCCCCCTCGAGGTCGACGGTATCGATAGGCTTACCATGCGGCTGGGCA
T7	301	TGGGTACCGGGCCCCCTCGAGGTCGACGGTATCGATAGGCTTACCATGCGGCTGGGCA
consensus	301	tgggtaccgggccccctcgaGGTCgacGGTaTCgataaGcttACCATGCGGCTGGGCA
NCBI	37	GTCCTGGACTGCTCTTCTGCTCTTCAGCAGCCTTCGAGCTGATACTCAGGAGAAGGAAG
T3	69	GTCCTGGACTGCTCTTCTGCTCTTCAGCAGCCTTCGAGCTGATACTCAGGAGAAGGAAG
T7	361	GTCCTGGACTGCTCTTCTGCTCTTCAGCAGCCTTCGAGCTGATACTCAGGAGAAGGAAG
consensus	361	GTCCTGGACTGCTCTTCTGCTCTTCAGCAGCCTTCGAGCTGATACTCAGGAGAAGGAAG
NCBI	97	TCAGAGCGATGGTAGGCAGCGACGTGGAGCTCAGCTGCGCTTGCCCTGAAGGAAGCCGTT
T3	129	TCAGAGCGATGGTAGGCAGCGACGTGGAGCTCAGCTGCGCTTGCCCTGAAGGAAGCCGTT
T7	421	TCAGAGCGATGGTAGGCAGCGACGTGGAGCTCAGCTGCGCTTGCCCTGAAGGAAGCCGTT
consensus	421	TCAGAGCGATGGTAGGCAGCGACGTGGAGCTCAGCTGCGCTTGCCCTGAAGGAAGCCGTT
NCBI	157	TTGATTTAAATGATGTTTACGTATATTGGCAAACCAAGTGAAGTGAAGAACCGTGACCT
T3	189	TTGATTTAAATGATGTTTACGTATATTGGCAAACCAAGTGAAGTGAAGAACCGTGACCT
T7	481	TTGATTTAAATGATGTTTACGTATATTGGCAAACCAAGTGAAGTGAAGAACCGTGACCT
consensus	481	TTGATTTAAATGATGTTTACGTATATTGGCAAACCAAGTGAAGTGAAGAACCGTGACCT
NCBI	217	ACCACATCCCACAGAACAGCTCCTTGGAAAACGTGGACAGCCGCTACCGGAACCGAGGCC
T3	249	ACCACATCCCACAGAACAGCTCCTTGGAAAACGTGGACAGCCGCTACCGGAACCGAGGCC
T7	541	ACCACATCCCACAGAACAGCTCCTTGGAAAACGTGGACAGCCGCTACCGGAACCGAGGCC
consensus	541	ACCACATCCCACAGAACAGCTCCTTGGAAAACGTGGACAGCCGCTACCGGAACCGAGGCC
NCBI	277	TGATGTCACCGGGCGGCATGCTGCGGGGCGACTTCTCCCTGCGCTTGTTCACAGTCACCC
T3	309	TGATGTCACCGGGCGGCATGCTGCGGGGCGACTTCTCCCTGCGCTTGTTCACAGTCACCC
T7	601	TGATGTCACCGGGCGGCATGCTGCGGGGCGACTTCTCCCTGCGCTTGTTCACAGTCACCC
consensus	601	TGATGTCACCGGGCGGCATGCTGCGGGGCGACTTCTCCCTGCGCTTGTTCACAGTCACCC
NCBI	337	CCCAGGACGAGCAGAAGTTTCACTGCCTGGTGTGAGCCAATCCCTGGGATTCCAGGAGG
T3	369	CCCAGGACGAGCAGAAGTTTCACTGCCTGGTGTGAGCCAATCCCTGGGATTCCAGGAGG
T7	661	CCCAGGACGAGCAGAAGTTTCACTGCCTGGTGTGAGCCAATCCCTGGGATTCCAGGAGG
consensus	661	CCCAGGACGAGCAGAAGTTTCACTGCCTGGTGTGAGCCAATCCCTGGGATTCCAGGAGG
NCBI	397	TTTTGAGCGTTGAGGTTACACTGCATCTGCGCAGCAAACTTCAGCGTGCCCGTCTGAGCG
T3	429	TTTTGAGCGTTGAGGTTACACTGCATCTGCGCAGCAAACTTCAGCGTGCCCGTCTGAGCG
T7	721	TTTTGAGCGTTGAGGTTACACTGCATCTGCGCAGCAAACTTCAGCGTGCCCGTCTGAGCG
consensus	721	TTTTGAGCGTTGAGGTTACACTGCATCTGCGCAGCAAACTTCAGCGTGCCCGTCTGAGCG
NCBI	457	CCCCCAGAGCCCTCCAGGATGAGCTCACCCTTACGCTGTACATCCATAAACGGCTACC
T3	489	CCCCCAGAGCCCTCCAGGATGAGCTCACCCTTACGCTGTACATCCATAAACGGCTACC
T7	781	CCCCCAGAGCCCTCCAGGATGAGCTCACCCTTACGCTGTACATCCATAAACGGCTACC
consensus	781	CCCCCAGAGCCCTCCAGGATGAGCTCACCCTTACGCTGTACATCCATAAACGGCTACC
NCBI	517	CCAGGCCAACGCTGTACTGGATCAATAAGACGGACAACAGCCTGCTGGACAGGCTCTGC
T3	549	CCAGGCCAACGCTGTACTGGATCAATAAGACGGACAACAGCCTGCTGGACAGGCTCTGC
T7	841	CCAGGCCAACGCTGTACTGGATCAATAAGACGGACAACAGCCTGCTGGACAGGCTCTGC
consensus	841	CCAGGCCAACGCTGTACTGGATCAATAAGACGGACAACAGCCTGCTGGACAGGCTCTGC
NCBI	577	AGAATGACACCGCTCTTCTTGAACATGCGGGGCTTGTATGACGTGGTCAGCGTGTGAGGA
T3	609	AGAATGACACCGCTCTTCTTGAACATGCGGGGCTTGTATGACGTGGTCAGCGTGTGAGGA
T7	901	AGAATGACACCGCTCTTCTTGAACATGCGGGGCTTGTATGACGTGGTCAGCGTGTGAGGA
consensus	901	AGAATGACACCGCTCTTCTTGAACATGCGGGGCTTGTATGACGTGGTCAGCGTGTGAGGA
NCBI	637	TCGCACGGACCCCGAGCGTGAACATTGGCTGCTGCATAGAGAAGCTGCTTCTGCAGCAGA
T3	669	TCGCACGGACCCCGAGCGTGAACATTGGCTGCTGCATAGAGAAGCTGCTTCTGCAGCAGA
T7	961	TCGCACGGACCCCGAGCGTGAACATTGGCTGCTGCATAGAGAAGCTGCTTCTGCAGCAGA
consensus	961	TCGCACGGACCCCGAGCGTGAACATTGGCTGCTGCATAGAGAAGCTGCTTCTGCAGCAGA
NCBI	697	ACCTGACTGTGCGCAGCCAGACAGGAAATGACATCGGAGAGAGAGACAAGATCACAGAGA
T3	729	ACCTGACTGTGCGCAGCCAGACAGGAAATGACATCGGAGAGAGAGACAAGATCACAGAGA
T7	1021	ACCTGACTGTGCGCAGCCAGACAGGAAATGACATCGGAGAGAGAGACAAGATCACAGAGA
consensus	1021	ACCTGACTGTGCGCAGCCAGACAGGAAATGACATCGGAGAGAGAGACAAGATCACAGAGA
NCBI	757	ATCCAGTCAGTACCGGCGAGAAAAACGCGC--CCAGCTT----GAGCTTCTTCTGTCT
T3	789	ATCCAGTCAGTACCGGCGAGAAAAACGCGCAGTCTTCTAGAGCGGCC--GCCACCG
T7	1081	ATCCAGTCAGTACCGGCGAGAAAAACGCGCAGTCTTCTAGAGCGGCC--GCCACCG
consensus	1081	ATCCAGTCAGTACCGGCGAGAAAAACGCGGatCCActaGttctaGAGCgGCC GcCa

Figure 6. The alignment of LICOS sequence from NCBI database (AF199028) with the LICOS insert sequence determined between T3 and T7 promoters of pBluescript vector. AAGCTT represents the HindIII restriction site and AAGCTTACCATGCGGCTGGGCAGTCTCT the sense primer sequence, while ATG represents the start codon, GGATCC the BamHI restriction site and CCAGTCAGTACCGGCGAGAAAAACGCGGATCC the antisense primer sequence.

3.2 Construction of the expression vector

After the LICOS sequence in pBluescript was shown to be correct, it was excised from this vector using BamHI and Hind III (Fig. 7), with expected resulting fragment sizes of 3369 bp and of 774 bp. The latter band corresponded to the LICOS insert size of 774 bp and was extracted from the gel (Fig. 7, lanes 2, 3).

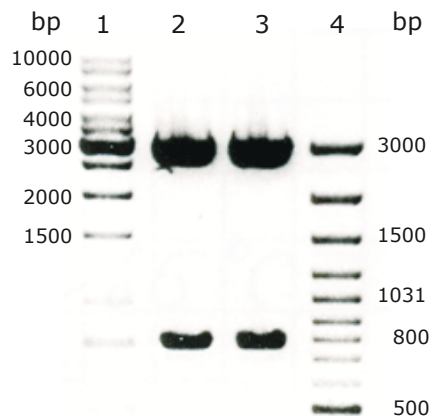


Figure 7. Excision of the LICOS insert from pBluescript-LICOS vector by restriction digestion with BamHI and Hind III. Lane 1, DNA marker (1Kb DNA ladder); lane 2, 3, BamHI and Hind III digested pBluescript-LICOS vector; the band at around 800 bp corresponded to the insert length of 774 bp; lane 4, DNA marker (100 bp DNA ladder).

pcDNA1.1 was digested with the enzymes HindIII and EagI (Fig.8), to render it able to receive the LICOSIg insert. The expected size of the linearized vector was 4690 bp. The restricted vector DNA migrated at around 5000 bp, corresponding to the expected size (Fig.8, lanes 3, 4).

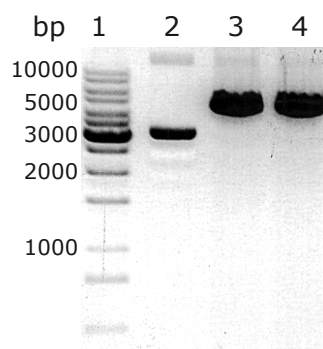


Figure 8. Restriction digestion of the pcDNA1.1 vector with Hind III and EagI. Lane 1, DNA marker (1Kb DNA ladder); lane 2, intact pcDNA1.1 vector (supercoiled form); lanes 3, 4, HindIII and EagI digested pcDNA1.1 vector; the bands migrated at around 5000 bp were equivalent to the length of linearized vector (4690 bp).

The Fc part of human IgG1 (Ig fragment), previously cloned along with the extracellular domain of CTLA4 in pcDNA1.1 vector, was excised using BamHI and EagI (Fig. 9). The resulting fragment migrating at 1300 bp corresponded to the calculated Ig fragment length of 1264 bp (Fig. 9, lanes 2, 3).

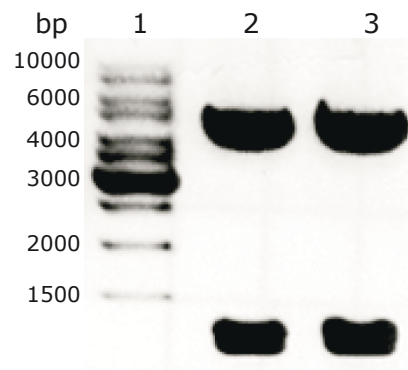


Figure 9. Excision of the Ig fragment from pcDNA1.1-CTLA4Ig vector by restriction digestion with BamHI and EagI. Lane 1, DNA marker (1Kb DNA ladder); lane 2 and 3, HindIII and EagI digested pcDNA1.1-CTLA4Ig vector; the bands migrated at 1300 bp were consistent with the calculated Ig fragment length of 1264 bp.

The ligation of the three DNA fragments – LICOS, Ig and the vector – was carried out sequentially, in two ways:

1. The two inserts, LICOS and Ig fragment, were ligated first and the resulting LICOSIg segment was then ligated into the HindIII/EagI-restricted pcDNA1.1 vector (Fig. 10, lanes 2–9).
2. the LICOS fragment was ligated into HindIII/EagI-restricted pcDNA1.1 vector and the resulting construct further received the Ig fragment (Fig. 10, lanes 11–13).

Both strategies were successful (Fig. 10). In both cases, competent bacteria *E. coli* were transformed with the ligation mix and selected on growth medium.

To identify the clones containing the LICOSIg insert, plasmid DNA from 25 colonies was isolated and digested with XbaI and BamHI. If the plasmid had not contained the LICOSIg insert, a DNA fragment of 4749 bp would have been expected after enzymatic restriction with XbaI and BamHI. On the other hand, if the vector had contained the LICOSIg insert, two fragments, of 1296 bp and 5452 bp, would have been generated. Four clones displayed a band at around 1300 bp, indicating that the plasmids contained the LICOSIg insert (Fig. 10, lanes 2, 7, 9 and 11), while the rest showed only the 4800 bp band, corresponding to a plasmid without insert (Fig. 10, lanes 3, 4, 5, 6, 8, 12 and 13).

To further confirm the presence of the LICOSIg insert, two of the four positive colonies selected by restriction with XbaI-BamHI, were enzymatically digested with PvuI-KpnI and with PvuI-XbaI (Fig.11). The two expected DNA fragment sizes resulting from each restriction reaction were of 4002 bp, 2746 bp, and 3252 bp, 3496 bp, respectively. Agarose gel analysis of the restriction products exhibited bands of about 4000 bp and 2700 bp,

corresponding to the PvuI-KpnI digestion products (Fig.11, lanes 2 and 3), and two close bands between 3000 and 4000 bp, corresponding to the PvuI-XbaI digestion products (Fig.11, lanes 4 and 5), similar to the expected sizes in the case the clones contained the insert.

DNA derived from the positive colonies was sequenced using primers designed to amplify a segment that covers the joining of the two fragments. The sequences were in frame and without any mutation.

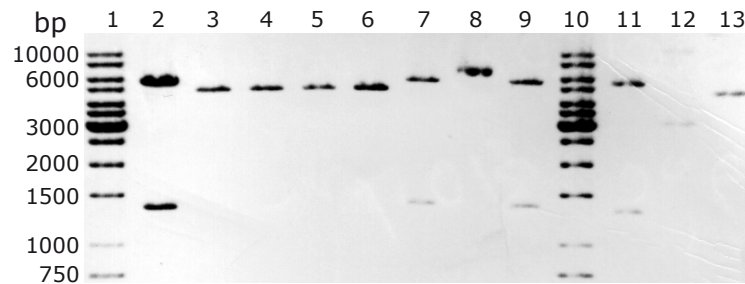


Figure 10. The screening of transformed bacterial colonies for the LICOSlg insert by restriction digestion of their plasmid DNA with XbaI and BamHI. Lanes 1 and 10, DNA marker (1Kb DNA ladder); lanes 2–9 and 11–13 represent plasmid DNA extracted from individual bacterial colonies. The lanes 2, 7, 9 and 11 display a band at around 1300 bp, indicating the presence of the LICOSlg insert in the corresponding clones, while the lanes 3, 4, 5, 6, 8, 12, 13 showed only the 4800 bp band, expected from a vector devoid of the insert. Recombinants in the lanes 2 to 9 were generated by ligation of LICOSlg segment into pcDNA1.1, while those in the lanes 11-13 were formed by ligation of lg fragment into pcDNA1.1-LICOS.

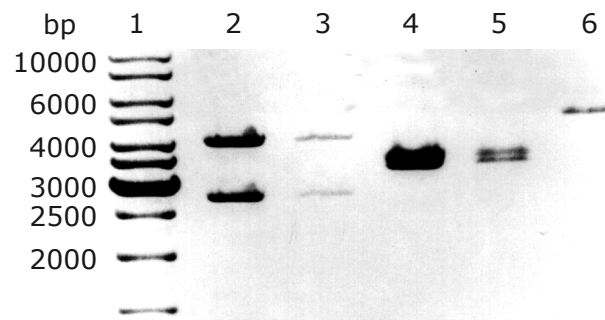


Figure 11. Confirmation of the LICOSlg insert presence in two positive bacterial clones by restriction digestion with PvuI-KpnI and PvuI-XbaI. Lane 1, DNA marker (1Kb DNA ladder); lane 2, 3, the PvuI-KpnI digestion of pcDNA1.1-LICOSlg vector yielded two bands of about 4000 bp and 2700 bp, respectively; lane 4, 5, the PvuI-XbaI digestion of pcDNA1.1-LICOSlg yielded bands of about 3200 bp and 3500 bp, respectively. The sizes of these bands agreed with the calculated size (4002 bp, 2746 bp, and 3252 bp, 3496 bp, respectively) and confirmed that the vectors contained LICOSlg insert. Lane 6, linearized pcDNA1.1 vector obtained with BamHI.

3.3 Expression and purification of the LICOS-Ig fusion protein

The extracellular domain of LICOS, encoded by 762 bp, contains 254 amino acids. The 234 amino acids of Fc part of human IgG are encoded by 702 bp, the remaining base pairs up to 1278 bp represents non-coding DNA. The extracellular domain of LICOS was fused immediately after the Ala²⁵⁴ to the human IgG1 Fc domain containing the hinge, CH2 and CH3 domains. The amino acid sequence predicted at the fusion junction was: *STGEKNA*¹*DPE*²*EPKSC*³. The resulting LICOS-Ig fusion protein contains an IgG hinge region, including the two cysteine residues, which in IgG are involved in the formation of disulfide bridges (Fig. 12). Therefore, the resulting LICOS-Ig fusion protein is expected to form a covalently linked homodimer with a calculated molecular weight of approx. 109 kDa.

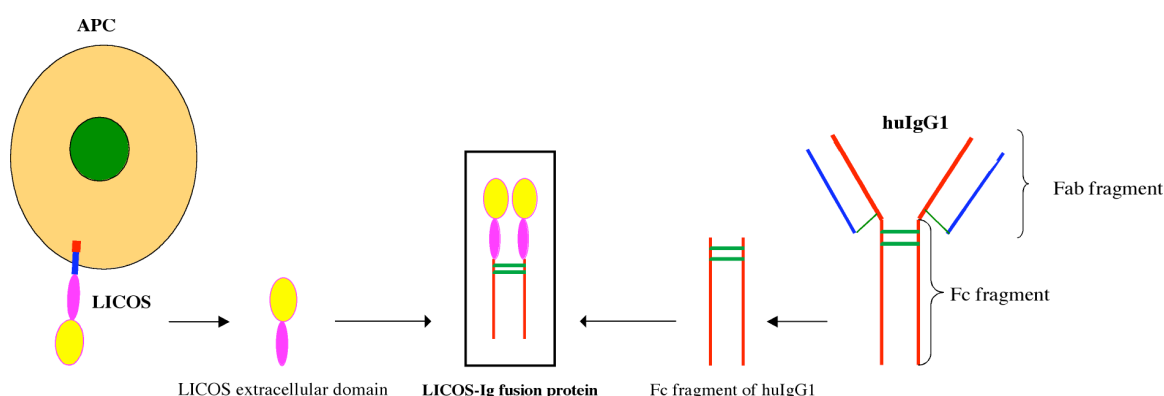


Figure 12. Scheme for production of LICOS-Ig fusion protein. At the DNA level, the extracellular domain of LICOS, which is expressed on the surface of APCs, was fused to Fc fragment of huIgG1. The resulting chimeric protein is a disulfide-linked homodimer formed by the cysteine residues in the hinge region of Fc fragment.

COS-7 cell line was transiently transfected (14 days) with the recombinant vector pcDNA1.1-LICOSIg or pcDNA1.1-CTLA4Ig used as a positive control. The LICOS-Ig fusion protein was purified from the cell culture supernatant of transfected COS-7 cells by affinity chromatography using a Protein G column. After purification, the eluate was concentrated with PEG 30 000 and then dialyzed against PBS.

The cell culture supernatant and the purified fusion protein were tested for the presence of LICOS-Ig by SDS-PAGE under non-reducing conditions followed by Western blotting using a goat anti-huIgG Ab coupled with peroxidase (POD) (Fig. 13). Additionally, to evaluate the efficiency of the purification process, fractions of the flow-through, wash and eluate were also assayed for LICOS-Ig.

¹ belonging to LICOS

² introduced at BamHI site

³ belonging to the hinge region

CTLA4-Ig supernatant obtained after transfection of COS cells with pcDNA1.1-CTLA4Ig vector was used as a positive control for the amount of the LICOS-Ig protein secreted in supernatant (Fig. 13). LICOS-Ig was detected in the LICOS-Ig-transfected COS cell culture supernatants, in amounts comparable to those of CTLA4-Ig, but at a higher molecular weight than expected (around 150 kDa), probably due to spontaneous formation of LICOS-Ig higher order multimers (Fig. 13, lanes 2, 3, 4).

No detectable LICOS-Ig was present in the flow-through and wash fractions (Fig. 13, lanes 5 and 6). However, in the eluate, one band was revealed at 110 kDa, corresponding to expected molecular weight of dimeric LICOS-Ig (Fig. 13, lane 7). Again, the band at around 150 kDa, representing trimers of LICOS-Ig was detected.

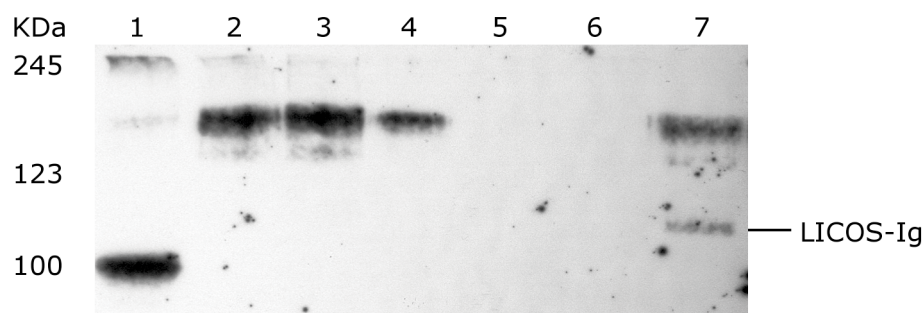


Figure 13. Western blot analysis of LICOS-Ig fusion protein in the COS-7 cell culture supernatant at various stages in the purification process. The protein samples were separated by SDS-PAGE (8%) under non-reducing conditions and analyzed by Western blotting using a goat anti-huIgG coupled with peroxidase (POD). Lane 1, CTLA4-Ig supernatant (positive control); Lanes 2, 3, 4, LICOS-Ig supernatant; Lane 5, a flow-through fraction; Lane 6, a wash fraction; Lane 7, eluate. The electrophoretic mobility of molecular mass standards is indicated on the right side of the panel. CTLA4-Ig from the transfected cell supernatant had the expected molecular weight of ca. 100kDa (Aicher et al. 2000) (lane 1). LICOS-Ig was detected in the LICOS-Ig transfected COS supernatants at a higher molecular weight than expected (at around 150 kDa instead of 109 kDa), probably due to spontaneous formation of LICOS-Ig multimers (lanes 2, 3, 4). No protein content was revealed in the flow-through and wash solutions (lanes 5, 6, respectively). In turn, only in the eluate a band at around 100 kDa corresponding to the expected molecular weight of dimeric LICOS-Ig (109 kDa) was detectable.

To determine whether LICOS-Ig had the right conformation, the specific recognition of LICOS-Ig by an anti-LICOS mAb (HIL131) was examined in ELISA assay. Wells were coated with anti-huIgG: half of them were covered with LICOS-Ig supernatant and the other half with CTLA4-Ig supernatant, as a negative control, and each half was incubated either with anti-LICOS mouse mAb (HIL131) or with anti-CTLA4 mouse mAb (BNI3). Finally, an anti-moIgG coupled with POD was added and the reaction developed in the presence of a POD substrate. The results of the ELISA assay indicated that LICOS-Ig was specifically recognized by anti-LICOS mAb (HIL131) while the negative control, i.e., CTLA4-Ig was not (Fig. 14). This implied that the conformation of epitopes in LICOS moiety of LICOS-Ig

fusion protein resembled the epitope conformation of a huLICOS-rabbitIg used as an antigen in HIL131 production (Khayyamian et al. 2002).

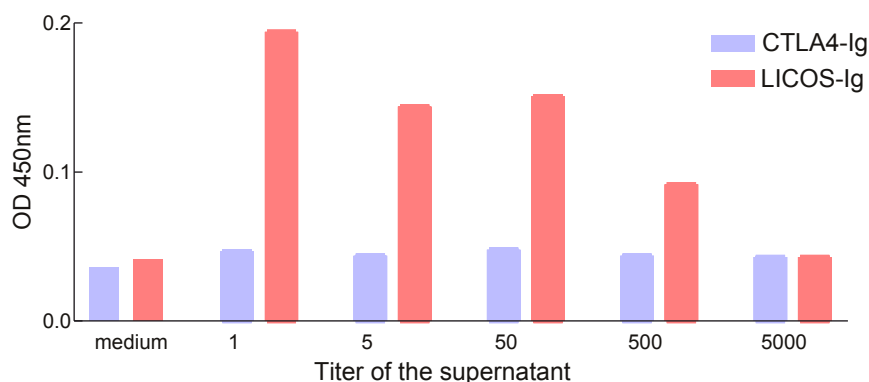


Figure 14. Specific recognition of LICOS-Ig by an anti-LICOS mAb (HIL131), in ELISA assay. One plate was coated with anti-huIgG and half of it was incubated with different titers of LICOS-Ig supernatant and the other half with different titers of CTLA4-Ig supernatant as a negative control. Next, to each half of the plate either a mouse anti-huLICOS mAb (HIL131) or a mouse anti-huCTLA4 mAb (BNI3) were added and each half was incubated with an anti-molIgG coupled with POD, which was then detected with a POD substrate. Different dilutions of LICOS-Ig supernatant showed specific recognition by HIL131 when compared to the negative control, i.e., CTLA4-Ig supernatant suggesting that LICOS moiety in LICOS-Ig fusion protein had the right conformation.

3.4 Characterization of biotinylated LICOS-Ig fusion protein in Western Blot, ELISA, FACS analysis and microscopy

After the purification, the LICOS-Ig fusion protein was biotinylated (Fig. 15) and tested in Western Blot, ELISA, FACS analysis and microscopy to determine its potential use in these assays.

First, in Western blot analysis, the binding of biotinylated LICOS-Ig was compared to that of unbiotinylated fusion protein using two different developing reagents: streptavidin-POD and anti-IgG-POD, respectively (Fig.15). For this purpose, both biotinylated and unbiotinylated proteins were separated by SDS-PAGE under non-reducing conditions followed by Western blotting with the two detection reagents. The biotinylated LICOS-Ig was detected with both developing reagents (Fig. 15, lanes 2 and 4), while unlabeled LICOS-Ig was identified only by anti-IgG-POD as expected (Fig. 15, lane 1). This result showed that biotinylated LICOS-Ig could be detected by streptavidin-POD and, implicitly, it is a suitable reagent for Western blot analysis.

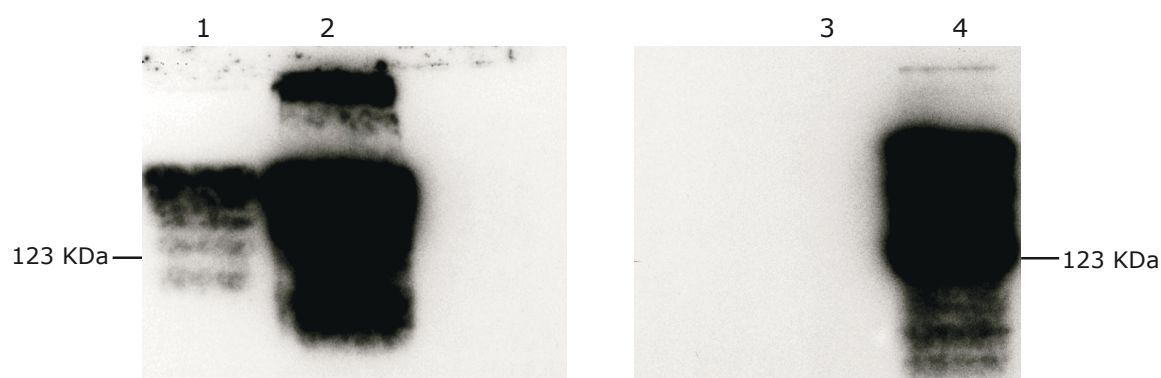


Figure 15. Western blot analysis of unbiotinylated and biotinylated LICOS-Ig fusion proteins detected either with anti-hulgG-POD or with streptavidin-POD. The unbiotinylated and biotinylated LICOS-Ig fusion proteins were analyzed by SDS-PAGE under non-reducing conditions followed by Western blotting. Two different reagents were used to visualize the protein (anti-hulgG-POD and streptavidin-POD, respectively). Lanes 1 and 3, unbiotinylated LICOS-Ig; lanes 2 and 4 biotinylated LICOS-Ig. Lanes 1 and 2, developed with anti-hulgG-POD; lanes 3 and 4, developed with streptavidin-POD. Biotinylated LICOS-Ig was detected by both developing reagents, while unlabeled LICOS-Ig was identified only by anti-IgG-POD.

Second, in ELISA assay, the binding of biotinylated LICOS-Ig was compared to that of unbiotinylated fusion protein again using two different developing reagents: streptavidin-POD and anti-IgG-POD, respectively. Plates coated with anti-huIgG were covered with different dilutions either of biotinylated or of unlabeled LICOS-Ig. The unbiotinylated LICOS-Ig was additionally incubated with anti-LICOS mAb (HIL131). Finally, biotinylated and unlabeled fusion proteins were detected with streptavidin-POD and anti-IgG-POD, respectively. ELISA assay showed that biotinylated LICOS-Ig was detected by streptavidin-POD in a similar manner to unbiotinylated LICOS-Ig was detected by anti-LICOS mAb (HIL131) in conjunction with anti-IgG-POD (Fig. 16). Therefore, biotinylated LICOS-Ig appeared to be a reliable reagent for ELISA assay.

Third, in FACS analysis, biotinylated LICOS-Ig was tested for its ability to bind to its natural receptor ICOS on the surface of CD3⁺ cells. A commercially available FITC-coupled anti-huICOS mAb (C398.4A) was used as a positive control. Briefly, isolated PBMC were stimulated with PHA for 48h, to induce the expression of ICOS on the activated T cells or were left unstimulated for the same time period. Then, both stimulated and unstimulated PBMC were double-stained either with biotinylated LICOS-Ig, in conjunction with streptavidin-PE or with FITC-coupled anti-huICOS mAb (C398.4A), and with anti-CD3 FITC or anti-CD3 PE, respectively. After 48h, unstimulated PBMC exhibited an upregulated ICOS expression on CD3⁺ cells, but to a lesser extent compared to PHA stimulated PBMC, as determined with the anti-ICOS mAb (54% versus 78%) (Fig. 17, upper row). More importantly, biotinylated LICOS-Ig in conjunction with streptavidin-PE was able to detect ICOS on T cells in a similar manner to the commercially available anti-ICOS FITC mAb, used as positive control, although the background staining was higher (Fig. 17, lower row

compared to upper row). Thus, biotinylated LICOS-Ig fusion protein seemed to be a suitable reagent for FACS analysis.

Finally, I determined whether biotinylated LICOS-Ig was capable of binding to denatured receptor ICOS in cytospin preparations. 48h unstimulated and PHA stimulated PBMC were centrifuged onto glass slides, fixed in acetone and stained with anti-CD3 FITC mAb and biotinylated LICOS-Ig, the latter being secondarily stained with streptavidin TRITC. The ICOS presence on T cells, as detected by biotinylated LICOS-Ig staining on stimulated PBMC, was colocalized with CD3 (Fig. 18). That is, biotinylated LICOS-Ig specifically bound to its receptor ICOS, when the latter was denatured during the fixation step of cytospin preparation.

Together, the results obtained in PBMC showed that biotinylated LICOS-Ig specifically bound to its native receptor ICOS in both biological active and denatured forms.

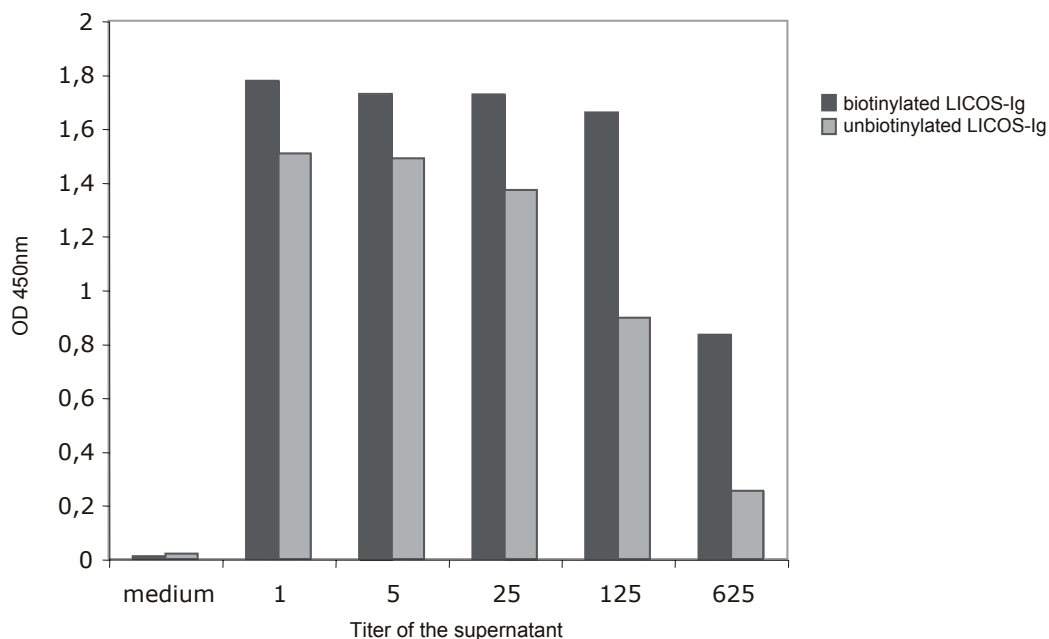


Figure 16. Detection of biotinylated and of unbiotinylated (purified) LICOS-Ig by streptavidin-POD and anti-LICOS mAb (HIL131) in conjunction with anti-IgG-POD, respectively, in ELISA assay. Plates coated with sheep anti-huIgG were covered with different dilutions of biotinylated or unlabeled LICOS-Ig. The unbiotinylated LICOS-Ig was additionally incubated with anti-huLICOS mouse mAb (HIL131). Finally, biotinylated and unlabeled fusion proteins were detected with streptavidin-POD and anti-molIgG-POD, respectively. Biotinylated LICOS-Ig fusion protein was detected by streptavidin-POD in a similar manner to unbiotinylated LICOS-Ig that was detected by anti-huLICOS mouse mAb (HIL131) in combination with anti-molIgG-POD.

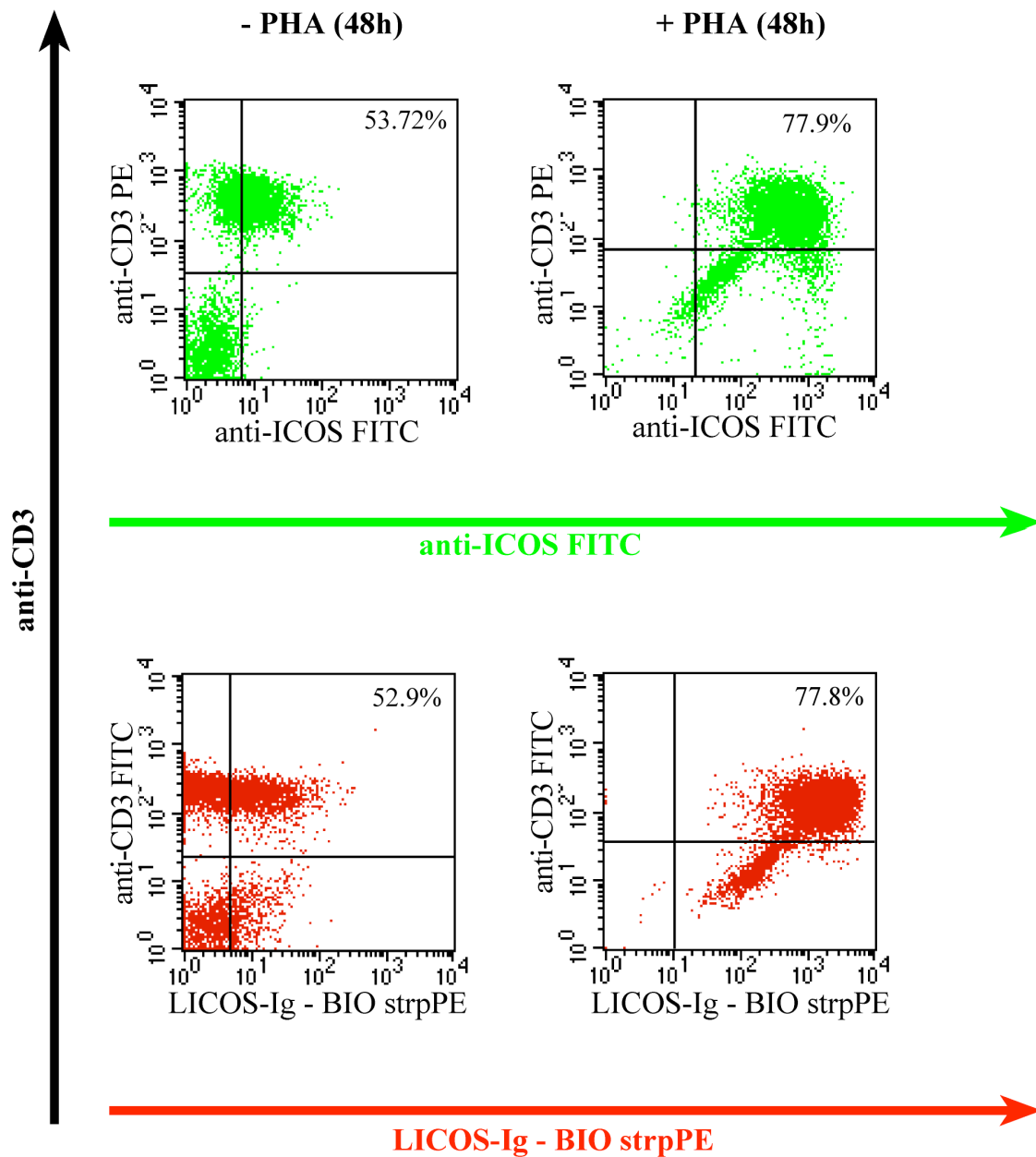


Figure 17. Similar binding pattern of biotinylated LICOS-Ig to that of a commercially available anti-ICOS FITC in FACS analysis of unstimulated and PHA stimulated PBMC. Unstimulated (left panels) or 48h PHA stimulated PBMC (1 μ g/ml) (right panels) were stained either with biotinylated LICOS-Ig in conjunction with streptavidin-PE (lower panels) or with FITC-coupled anti-huICOS mAb (upper panels) and with anti-CD3 FITC (lower panels) or anti-CD3 PE (upper panels). Biotinylated LICOS-Ig, in combination with streptavidin-PE, was able to detect ICOS on PHA stimulated T cells in a similar manner to commercially available anti-ICOS FITC mAb

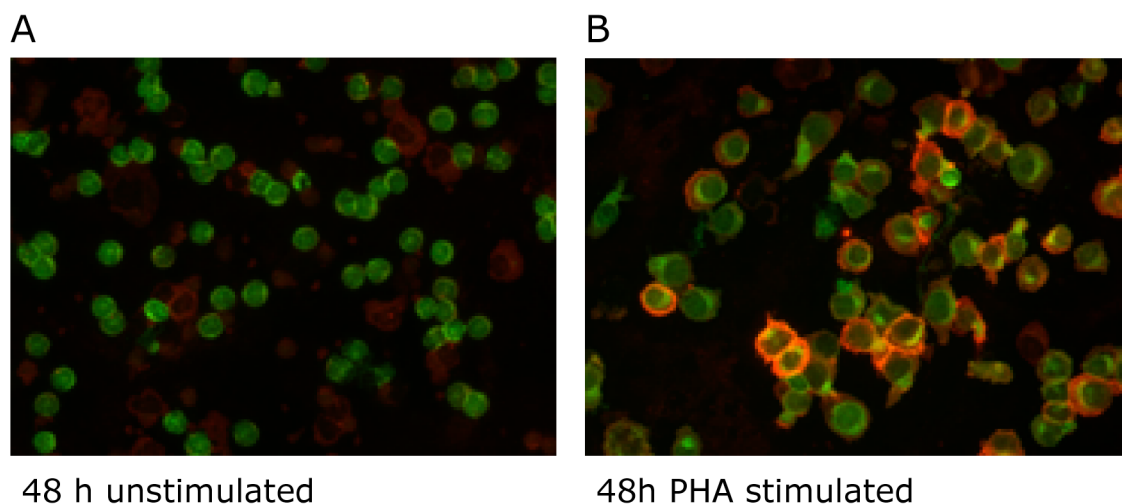


Figure 18. Cytospin preparations of unstimulated and PHA stimulated PBMC stained with biotinylated LICOS-Ig. 48h unstimulated (A) and PHA stimulated PBMC (1 μ g/ml) (B) were centrifuged down onto slides, fixed in acetone and stained with anti-CD3 FITC mAb and biotinylated LICOS-Ig; the latter was detected with streptavidin-TRITC.

3.5 Generation and characterization of an anti- LICOS mAb (HGW1)

The utility of monoclonal antibodies derives from their binding specificity and their homogeneity. In addition, their ability to be produced in unlimited quantities is closely connected to low costs. Thus, having a mAb producing hybridoma offers important advantages.

At the beginning of this work there was no commercially available anti-LICOS mAb. Therefore, the next step was to generate an anti-LICOS mAb producing hybridoma, using the LICOS-Ig fusion protein as an antigen for the immunization of mice. Briefly, the mice received a primary injection with an Ag-adjuvant mixture (100 μ g LICOS-Ig in TiterMax Gold Adjuvant), followed by two boosts, with 100 μ g antigen in adjuvant and 50 μ g antigen in PBS, respectively. Three days after the final boost, the mice were euthanized and the spleen was harvested for cell fusion. Further, the technique involved fusing a normal antibody-producing spleen B cells with myeloma cells to produce hybrid cells or hybridoma. The desired antibody-producing hybridomas were identified by cycles of subcloning and expansion of the positive clones, which were selected after screening of their mAb-containing supernatants in ELISA assays, using LICOS-Ig and CTLA4-Ig (negative control) as antigens.

Following three fusions of lymphocytes with myeloma cells and 5 000 primarily screened clones, only one clone was found to be selectively reactive to LICOS-Ig. From this clone, several subcloned hybridoma cells were further reactive to the specific antigen. Eventually, only two clones (HGW1) were stabilized to constantly secrete specific antibodies against

LICOS-Ig. The cell culture supernatant containing anti-LICOS mAb HGW1 from these clones was collected and either used by itself in some assays or subjected to purification. The purified anti-LICOS mAb HGW1 was characterized regarding its isotype and capacity to recognize LICOS antigen in diverse forms: as soluble fusion protein, in ELISA; as membrane-attached form on the cell surface, in FACS analysis; as denatured protein after acetone fixation, in cytospin preparations.

ELISA. To investigate the HGW1 mAb binding specificity for a soluble LICOS antigen, LICOS-Ig fusion protein, an ELISA assay was carried out. LICOS-Ig, along with CTLA4-Ig and B7.1-Ig fusion proteins were immobilized on plates coated with anti-huIgG1, then incubated with serial five-fold dilutions of HGW1 supernatant, and detected with anti-moIgG-POD. The anti-LICOS mAb HIL131 served as a positive control. In ELISA, HGW1 specifically recognized LICOS-Ig, but not the negative controls CTLA4-Ig and B7.1-Ig. The binding of HGW1 was comparable to that of the positive control HIL131 mAb. This result demonstrated that HGW1, in ELISA settings, bound selectively to LICOS and exhibited no cross-reactivity to other members of the CD28 and B7 families, CTLA4 and B7.1 (Fig. 19).

Flow cytometry. To study the HGW1 mAb binding specificity for a membrane-anchored form of LICOS on the cell surface, analysis of SKMel-LICOS, SKMel-wt, SKMel B7.1 and SKMel B7.2 cell lines was performed by flow cytometry (Fig. 20). The SKMel transfectants, adherent human skin melanoma cells expressing on their surface either LICOS, B7.1 or B7.2 were stained with HGW1 supernatant and with secondary antibody anti-moIgG1 FITC (Fig. 20, A) or, alternatively, with the positive control anti-LICOS mAb HIL131 coupled with PE (Fig. 20, B). On each of the histograms, the fluorescence level of stained cells (filled histograms) was compared to that of unstained cells (unfilled histograms). FACS analysis revealed that HGW1 supernatant specifically stained SKMel LICOS cells but not SKMel-wt, SKMel B7.1 or SKMel B7.2 (Fig. 20, A) and the binding was similar to that of the positive control HIL131 (Fig. 20, B). Consequently, HGW1 appeared to be a suitable reagent for flow cytometry.

Immunocytochemistry. To determine whether HGW1 was an appropriate tool for immunocytochemistry, I examined the binding specificity of this antibody for its denatured antigen, after acetone fixation, in cytospin preparations. For this purpose, SKMel LICOS, SKMel wt, SKMel B7.1 and SKMel B7.2 cells were centrifuged onto glass slides, fixed in acetone and stained with HGW1 supernatant and with anti-moIgG1 FITC, as secondary antibody (Fig. 21). In cytospin preparations, HGW1 supernatant displayed a clear positive signal for LICOS presence on SKMel LICOS, while SKMel wt, SKMel B7.1 and SKMel B7.2 were not stained (Fig. 21). For this reason, HGW1 seemed a proper mAb for immunocytochemistry.

Taken together, these results established that HGW1 was a reliable specific tool in detecting LICOS in ELISA, flow cytometry and microscopy.

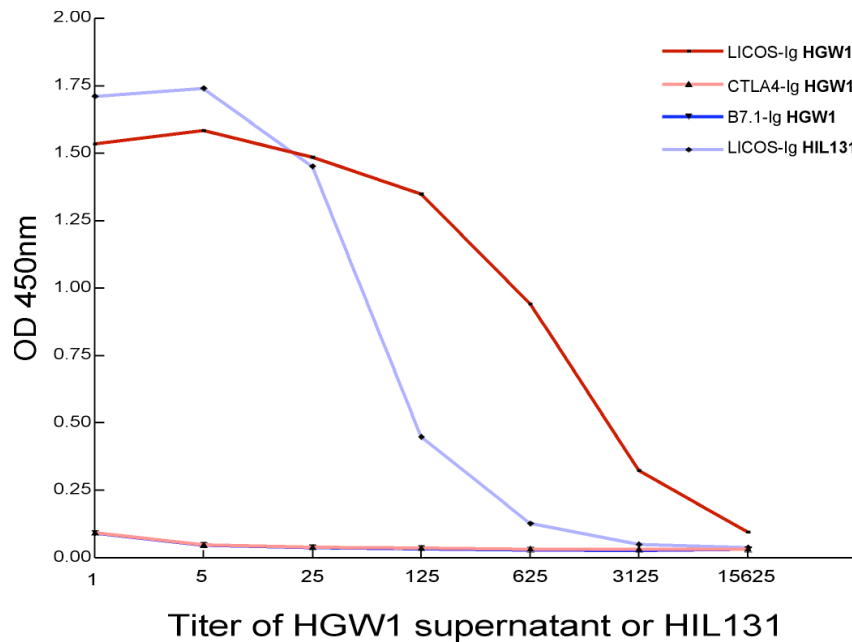


Figure 19. Binding of HGW1 mAb to LICOS-Ig, CTLA4-Ig and B7.1-Ig in ELISA assay. ELISA plates coated with LICOS-Ig, CTLA4-Ig and B7.1-Ig were incubated with serial five-fold dilutions of HGW1 supernatant and detected with anti-molG-POD. The anti-LICOS mAb HIL131 served as a positive control. HGW1 specifically recognized LICOS-Ig and showed no cross-reaction with other members of CD28-B7 family (CTLA4-Ig and B7.1-Ig).

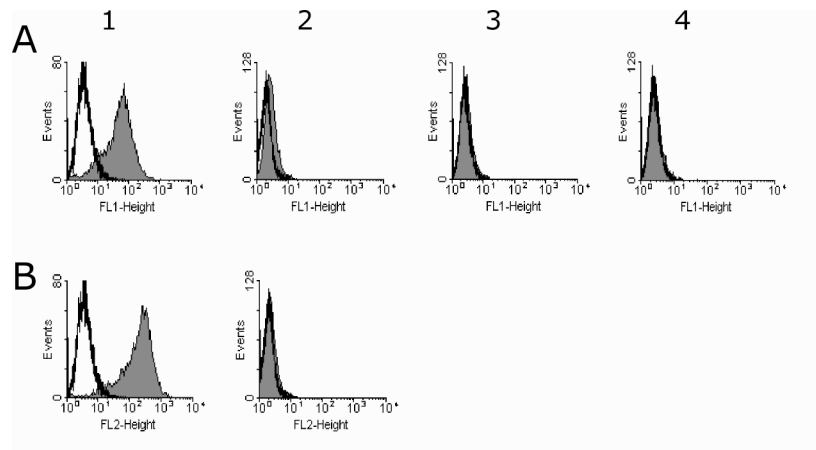


Figure 20. HGW1 binding to SKMel-LICOS, SKMel wt, SKMel B7.1 and SKMel B7.2 in FACS analysis. A, cells stained with HGW1 supernatant; B, cells stained with anti-LICOS mAb HIL131 (positive control). (1) SKMel-LICOS, (2) SKMel wt, (3) SKMel-B7.1, (4) SKMel-B7.2. The cells were stained with HGW1 supernatant and anti-molG1 FITC, as secondary antibody (A, 1, 2, 3, 4,) or, alternatively, with HIL131 PE (B, 1, 2). The fluorescence level of stained cells (filled histograms) was compared to that of unstained cells (unfilled histograms). HGW1 in the supernatant specifically stained SKMel LICOS (A, 1) cells but not SKMel wt (A, 2), SKMel B7.1 (A, 3) or SKMel B7.2 (A, 4) and the binding was similar to that of the positive control (B, 1).

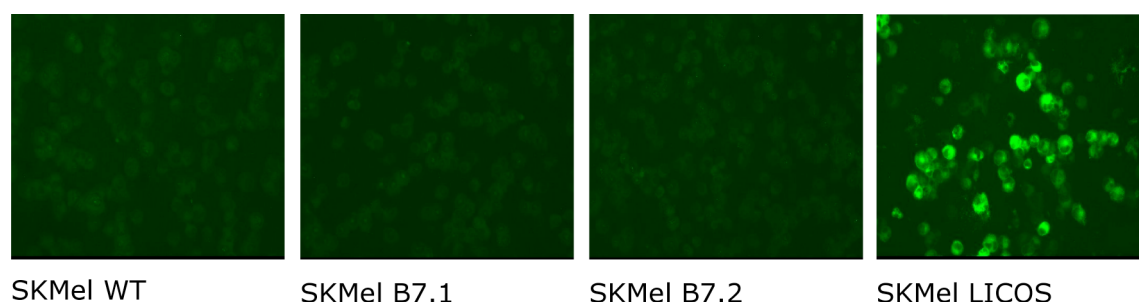


Figure 21. Cytospin preparations of SKMel wt, SKMel B7.1, SKMel B7.2 and SKMel LICOS stained with HGW1 supernatant. SKMel LICOS, SKMel wt, SKMel B7.1 and SKMel B7.2 cells were centrifuged onto glass slides, fixed in acetone and stained with HGW1 supernatant and with anti-moIgG1 FITC as secondary antibody. HGW1 specifically bound to LICOS transfected SKMel cells and did not cross-react with other members of B7 family, B7.1 and B7.2.

The HGW1 antibody was purified from the supernatant by affinity chromatography, and then either biotinylated or labeled with the fluorescent dye Alexa Fluor® 647, as described (sections 2.2.2.3 and 2.2.2.5). The biotinylated (Fig. 22, D) and Alexa 647 labeled (Fig. 22, B) HGW1 mAbs were tested for the ability to stain SKMel LICOS (Fig. 22, 1) and SKMel wt (Fig. 22, 2) by FACS analysis in comparison to HIL131 (Fig. 22, A) and the HGW1 supernatant (Fig. 22, C). The binding of biotinylated HGW1 and unlabeled HGW1 was detected with streptavidin-PE and anti-moIgG FITC, respectively. On the histograms, the fluorescence level of stained cells (filled histograms) was compared to that of unstained cells (Fig. 22, A, C, D) or isotype control (Fig. 22, B) (unfilled histograms). Again, LICOS was specifically recognized by all purified HGW1 preparations.

3.6 Binding of HGW1 Alexa 647 to whole blood cells

Based on the results obtained in the SKMel LICOS system, I proceeded to the staining of B cells and monocytes in whole blood with Alexa 647-labeled HGW1 (Fig. 23). B cells (Fig. 23, top row) were double-stained with anti-CD19 FITC (x-axis) and HIL131 PE (y-axis of the first dot-plot), or different dilutions of HGW1 Alexa 647 (y-axis of the next dot-plots). Monocytes (Fig. 23, bottom row) were double-stained with anti-CD14 FITC (x-axis) and HIL131 PE (y-axis of the first dot-plot), or different dilutions of HGW1 Alexa 647 (y axis of the next dot-plots). Surprisingly, HGW1 Alexa 647 and HIL131 PE presented different binding patterns. Namely, HIL 131 bound strongly to CD19+ B cells (98.2%) and only weakly to CD14+ monocytes (26.61%). The situation was reversed when using HGW1: strong binding to monocytes (51.97% to 93.47%), but only low intensity staining of B cells (8% to 50.2%) (Fig. 23).

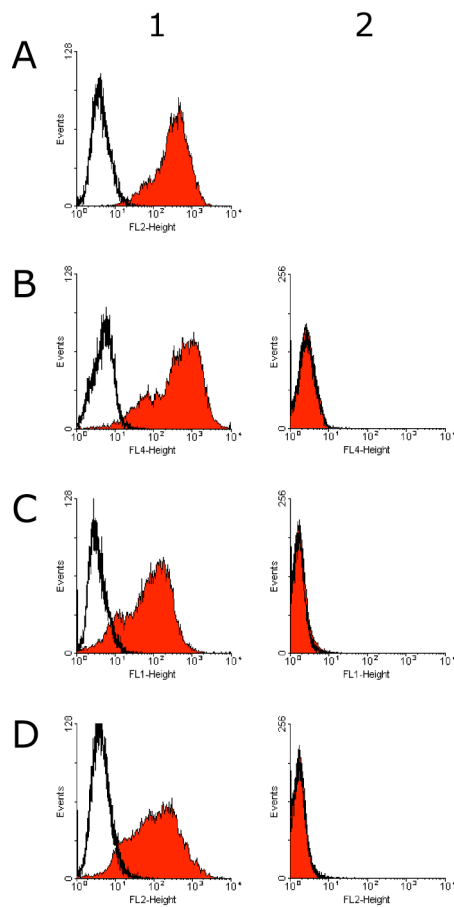


Figure 22. Binding of purified HGW1 preparations to SKMel LICOS and SKMel wt, in FACS analysis. A, HIL131 PE (positive control); B, HGW1 Alexa 647; C, HGW1 supernatant; D, biotinylated HGW1. (1) SKMel LICOS; (2) SKMel wt. The cells were stained with HIL131, Alexa 647 labeled HGW1, unlabeled and biotinylated HGW1 mAbs and the Alexa 647 labeled isotype control. The binding of biotinylated HGW1 and unlabeled HGW1 was detected with streptavidin-PE and anti-molIgG FITC, respectively. The fluorescence level of stained cells (filled histograms) was compared to that of unstained cells (A, C, D) or isotype control (B) (unfilled histograms). LICOS was specifically bound by all purified HGW1 preparations.

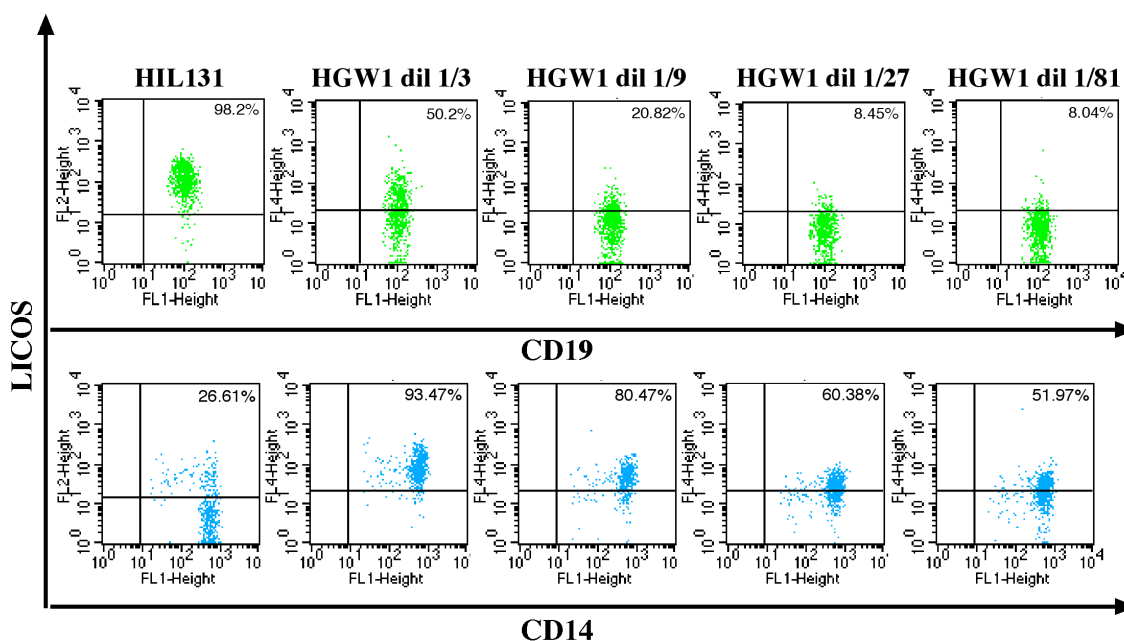


Figure 23. Different binding profiles of HGW1 Alexa 647 and HIL131 PE on whole blood B cells and monocytes (FACS analysis). B cells (top row) were double-stained with anti-CD19 FITC (x-axis) and HIL131PE (y-axis of the first dot-plot), or different dilutions of HGW1 Alexa 647 (y-axis of the next dot-plots). Monocytes (bottom row) were double-stained with anti-CD14 FITC (x-axis) and HIL131PE (y-axis of the first dot-plot), or different dilutions of HGW1 Alexa 647 (y-axis of the next dot-plots). The 1/3 dilution of HGW1-Alexa 647 was optimal as determined by staining of SKMel LICOS cells.

3.7 Competition assays

The different binding profiles of HGW1 Alexa 647 and HIL131 PE raised the questions whether there is a difference between the SKMel LICOS and the whole blood system and whether the two antibodies bind to different epitopes of the LICOS molecule that are differentially expressed by B cells and monocytes. To test this, the relation between the two antibodies vis-à-vis their binding to antigen was assessed in competition experiments.

Competition ELISA assay. Plates, coated with LICOS-Ig or CTLA4-Ig, were preincubated with unlabeled HIL131 in increasing concentrations from 0 to 60 µg/ml (excess) for 15 min. Then, biotinylated HGW1 was added at a suboptimal concentration previously determined and detected with streptavidin-POD (Fig. 24). If the two antibodies had competed for the same epitope, as concentration of the unlabeled antibody increased, the number of free epitopes to be bound later by the labeled antibody would have decreased. Subsequently, the signal developed would have progressively decrease in a descendent curve. If they had not competed for the same epitopes, the increasing concentration of unlabeled antibody would not have influenced the binding of the labeled antibody and subsequently, the signal developed would have depicted a plateau. Surprisingly, the signal developed depicted a bimodal curve: a descending curve down to a certain point, followed by a plateau. In other

words, unlabeled HIL131 competed biotinylated HGW1, but not completely. The plateau suggested the presence of another antibody that bound to a different epitope. Most probably, the biotinylated HGW1 is, de facto, a pool of two or more antibodies, two or more clones, with different specificities: one antibody recognizes the same epitope as HIL131 and the other one(s) binds to a different epitope.

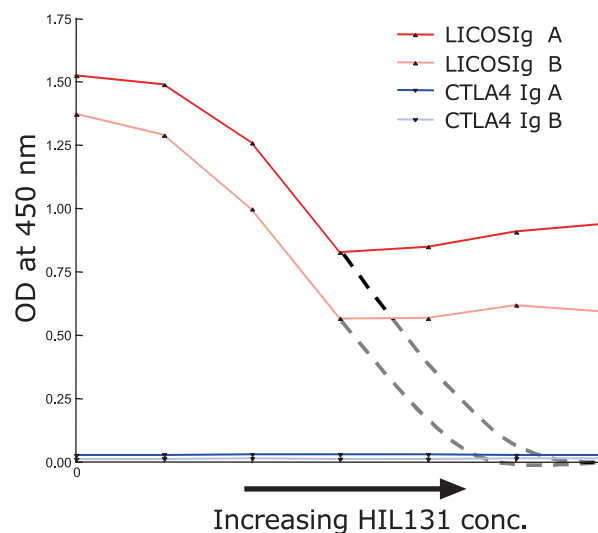


Figure 24. Bimodal curve of biotinylated HGW1 binding, after competition with increasing concentrations of unlabeled HIL131 in ELISA assay. The plates coated with LICOS-Ig (red lines) or CTLA4-Ig (blue lines), were preincubated with unlabeled HIL131 at increasing concentrations. Two different concentrations of biotinylated HGW1 were used (A and B). The descending curve suggests the presence of an antibody that binds the same epitope as HIL131, whereas the plateau corresponds to an antibody with a different specificity than HIL131.

Flow cytometry. In a first experiment, SKMel LICOS cells preincubated with HIL131 PE at increasing concentrations were subsequently stained with HGW1 Alexa 647 at suboptimal concentration. The positive cell populations were determined in both fluorescence channels – FL2 for HIL131 PE and FL4 for HGW1 Alexa 647. The reciprocal experiment was also conducted. If the two antibodies had bound to the same or to overlapping epitopes, the binding of the HGW1 Alexa 647 antibody used at suboptimal concentration would have declined with the increasing concentrations of the competing antibody (HIL131 PE). Subsequently, in the FACS histogram, the increase in the competing antibody concentrations would have resulted in a shift to the right of the corresponding positive population and, more important, a shift to the left of the population stained with the antibody at suboptimal concentration. If the two antibodies had bound to different epitopes, they would not have influenced each other's binding and consequently, no shift to the left of the competed-antibody stained population would have occurred.

In Fig. 25, as the HIL131 PE concentration increased (B, y-axis), the HIL131 population shifted to the right (Fig. 25, B, left column), but no shift to the left of the HGW1 Alexa 647

population was observed (Fig. 25, B, right column). The same result was seen in the reciprocal

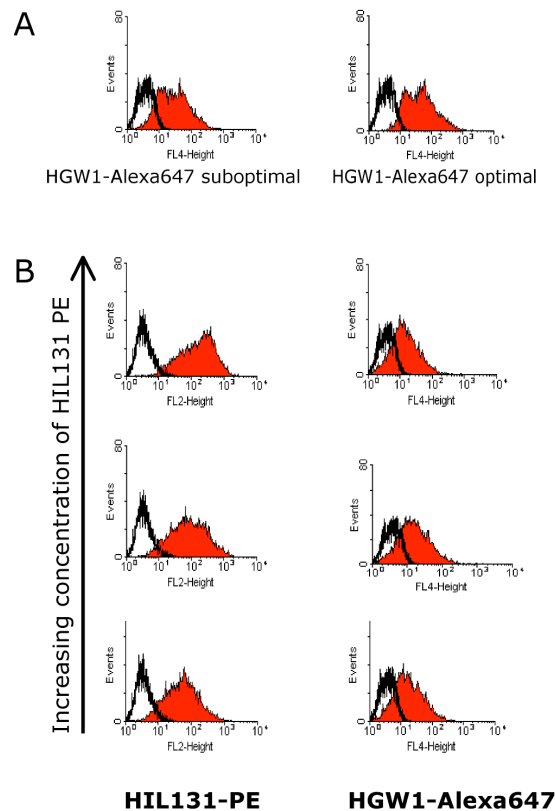


Figure 25. HIL131 PE did not compete HGW1 Alexa 647 in FACS analysis of SKMel LICOS cells. SKMel LICOS cells were preincubated with increasing concentrations of HIL131 PE and stained with suboptimal concentration of HGW1 Alexa 647. A, comparison of positive cell populations at suboptimal and optimal concentration of HGW1 Alexa 647. B, as the concentration of HIL131 PE increased (y-axis), the positive cell populations were determined in both fluorescence channels (x-axis)– FL2 for HIL131 PE (left panels) and FL4 for HGW1 Alexa 647 (right panels). The fluorescence level of stained cells (filled histograms) was compared to that of unstained cells (B, left panels) or isotype control (A, entirely and B, right panels) (unfilled histograms).

experiment (Fig. 26), where as the HGW1 Alexa 647 concentration increased (Fig. 26, B, left column), the HIL131 PE positive population was not affected (Fig. 26, B, right column). These findings suggested that HGW1 and HIL131 detect different epitopes.

To exclude the hypothesis that the apparently contradictory results of FACS analysis obtained with Alexa 647-labeled HGW1 (Fig. 25 and Fig. 26) and of ELISA assay obtained with biotin-labeled HGW1 (Fig. 24) were due to the different labels, biotinylated HGW1 was also employed in a FACS experiment. SKMel LICOS cells preincubated with increasing concentrations of unlabeled HIL131 or unlabeled HGW1 were stained with a suboptimal concentration of biotinylated HGW1 (and streptavidin-PE) or HIL131 PE, respectively (Fig. 27). No reduction in the positive cell population stained with either of the labeled antibodies

was exhibited upon blocking with unlabeled Abs (Fig. 27). This finding was in agreement with the results obtained in FACS analysis with HGW1 Alexa 647, described above (Fig. 25 and Fig. 26) and suggested that biotinylated HGW1 and HIL131 bind different epitopes.

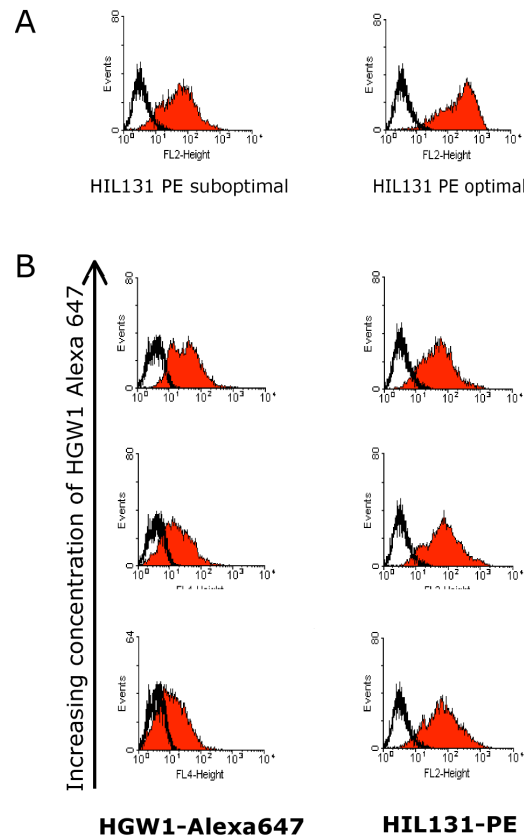


Figure 26. HGW1 Alexa 647 did not compete HIL131 PE in FACS analysis of SKMel LICOS cells. SKMel LICOS cells were preincubated with increasing concentrations of HGW1 Alexa 647, and stained with a suboptimal concentration of HIL131 PE. A, comparison of positive cell populations at suboptimal and optimal concentrations of HIL131 PE. B, as the concentration of HGW1 Alexa 647 increased (y-axis), the positive cell populations were determined on both fluorescence channels (x-axis): FL4 for HGW1 Alexa 647 (left panels) and FL2 for HIL131 PE (right panels). The fluorescence level of stained cells (filled histograms) was compared to that of unstained cells (A, entirely and B, right panels) or isotype control (B, left panels) (unfilled histograms).

In a second experiment, SKMel LICOS cells were preincubated with an excess concentration of unlabeled HGW1, followed by staining with HIL131 PE (Fig. 28, A). The reciprocal experiment was also performed (Fig. 28, B). In this case, if the two antibodies had competed for the same epitope, the excess of unlabeled antibody would have left no free epitopes to be bound later by the labeled antibody. Subsequently, there would have been no positive population detected by the labeled antibody. If they had not competed for the same epitopes, the unlabeled antibody would have not influenced the binding of the labeled antibody and subsequently, the labeled antibody would have stained the cells. Indeed, blocking with an excess of unlabeled HGW1 did not affect the staining of the HIL131 PE positive population

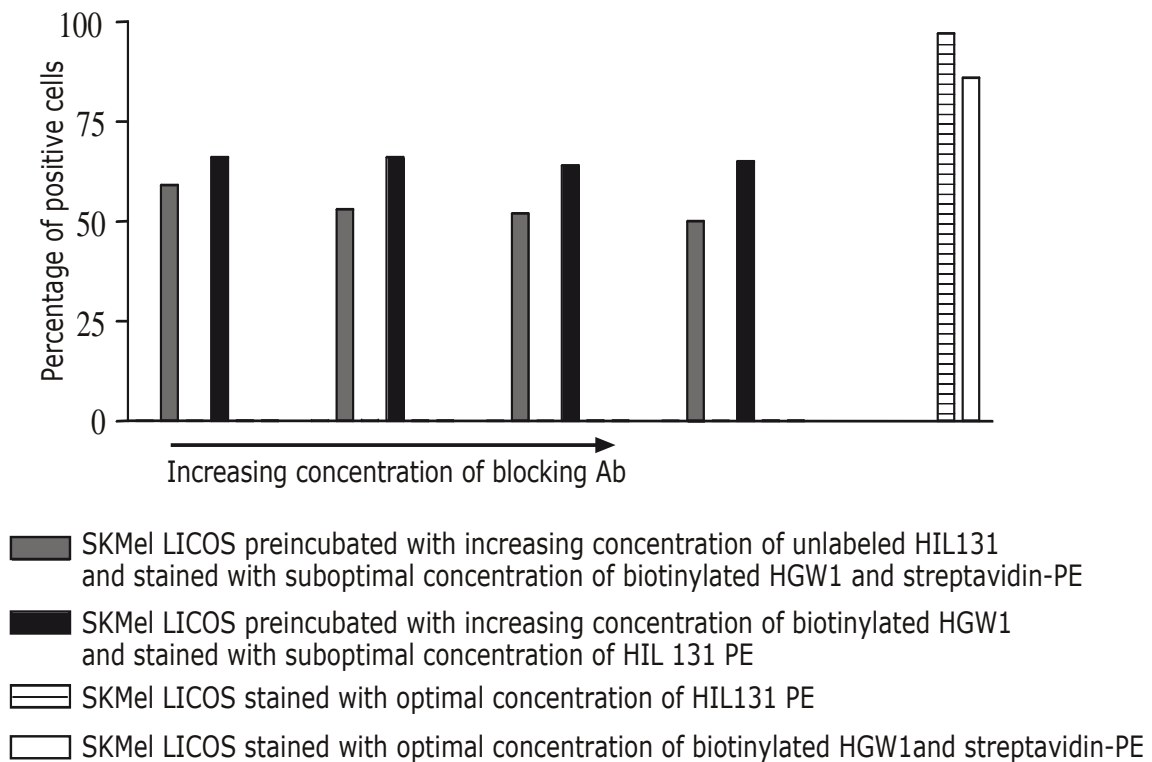


Figure 27. HIL131 PE did not compete biotinylated HGW1 and vice versa in FACS analysis of SKMel LICOS cells. No reduction in the percentage of positive population stained by either antibodies when blocked with the other, was noticed.

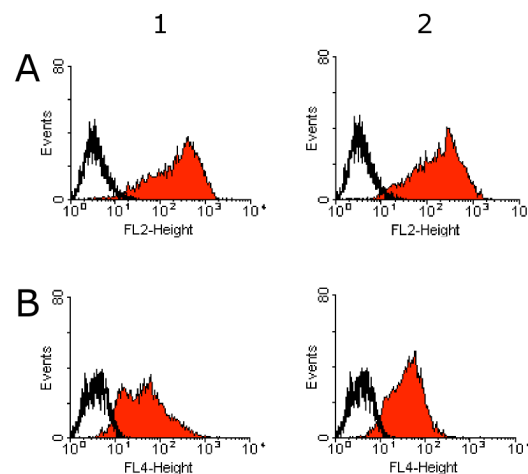


Figure 28. Neither the binding of HIL131 PE or of HGW1 Alexa 647 to SKMel LICOS was affected by blocking with an excess of unlabeled HGW1 or HIL131, respectively. (A) HIL131 PE staining: (1) before unlabeled-HGW1 blocking; (2) after unlabeled-HGW1 blocking. (B) HGW1 Alexa 647 staining: (1) before unlabeled-HIL131 blocking; (2) after unlabeled-HIL131 blocking. The fluorescence level of stained cells (filled histograms) was compared to that of unstained cells (A) or isotype control (B) (unfilled histograms).

(Fig. 28, A). Reciprocally, preincubation with unlabeled HIL131 in excess had no effect on the staining of the HGW1 Alexa 647 positive population (Fig. 28, B).

In a third experiment, SKMel LICOS cells were incubated concomitantly with both HIL131 PE and HGW1 Alexa 647 at optimal concentration. In this case, if the two antibodies had competed for the same epitope, adding them simultaneously would have led to a distribution of the epitopes between the two antibodies, depending on their binding affinity or avidity. Subsequently, the positive population would have been divided accordingly between the labeled antibodies. If they had not competed for the same epitopes, they would not have influenced each other's binding and subsequently, both labeled antibody would have stained the cells as in the absence of the other. Indeed, HIL131 PE and HGW1 Alexa 647, when present together, at optimal concentrations, showed no reduction in their positive population seen previously by separate staining (Fig. 29). This result pointed out that HIL131 PE and HGW1 Alexa 647 bind different epitopes.

Taken together, the results of the competition assays in flow cytometry indicated that there was no competition between the two antibodies. This implied that the two antibodies bind to different epitopes.

3.8 Comparison of HGW1 preparations binding to native LICOS

To assess the binding ability of HGW1 in different preparations – HGW1 Alexa 647, biotin-labeled HGW1 and unlabeled HGW1 – in relation to HIL131, in a native-LICOS expressing system, FACS analyses of the whole blood lymphocytes and purified CD19+ B cells were performed. Although monocytes also express LICOS, lymphocytes were chosen for this test because they are a more homogeneous population than the monocytes in terms of FSC, SSC parameters and unspecific binding of reagents. In addition, LICOS expression on lymphocytes in a healthy donor was compared to that of a critically ill patient in whom B cell number and LICOS expression were increased. This would have helped to make more visible any difference between stainings which otherwise would have not been seen due to a small B cell population with low LICOS expression in the normal whole blood (Fig. 30).

In the whole blood of the patient, HIL131 had an increased LICOS+ population compared to the donor (Fig. 30, A), while biotinylated and unlabeled HGW1 showed no positive population at all (Fig. 30, B and D). However, HGW1 Alexa 647 rendered high background staining in both cases (Fig. 30, C). When donor's purified CD19+ B cells were stained, HIL131 revealed most of the cells LICOS+ (Fig. 30, A bottom). Conversely, HGW1 preparations had a rather unspecific staining (Fig. 30, B, C, D bottom).

To confirm that the binding of HGW1 preparations observed in CD19+ B cells was indeed unspecific staining, the Raji cell line (a Burkitt's lymphoma EBV+) was employed (Fig. 31).

Raji cells were almost 100% LICOS+ when stained with HIL131 (Fig. 31, A), while most preparations of HGW1 – supernatant, purified-unlabeled and biotin-labeled – did not exhibit

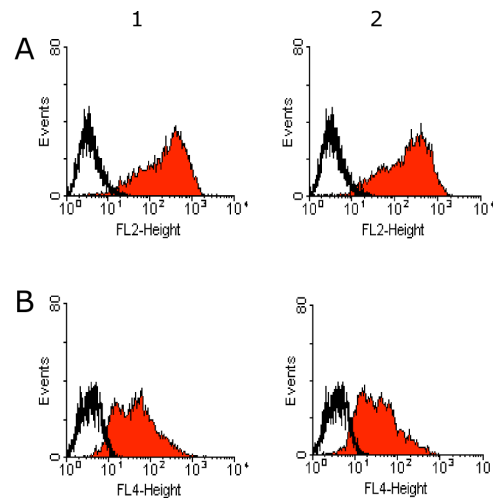


Figure 29. HGW1 Alexa 647 did not compete with HIL131 PE when they stained simultaneously SKMe1 LICOS in FACS analysis. (A) HIL131 PE staining: (1) in the absence of HGW1 Alexa 647; (2) by simultaneous staining with HGW1 Alexa 647. (B) HGW1 Alexa 647 staining: (1) in the absence of HIL131 PE; (2) by simultaneous staining with HIL131 PE. The fluorescence level of stained cells (filled histograms) was compared to that of unstained cells (A) or isotype control (B) (unfilled histograms).

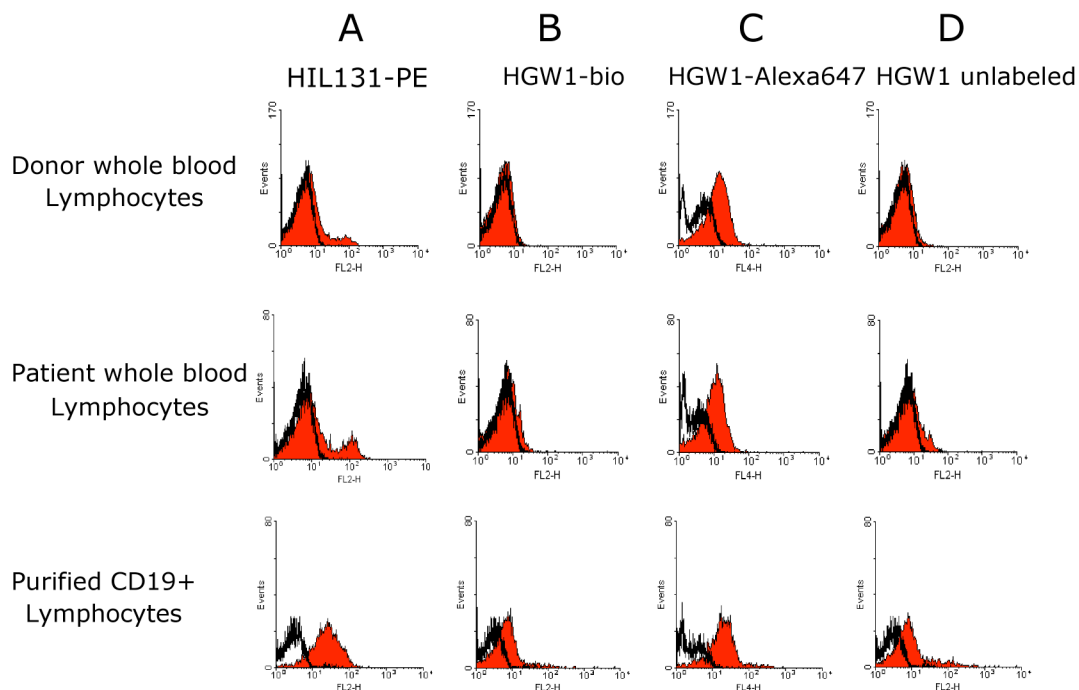


Figure 30. LICOS expression on a healthy-donor and an ICU-patient whole blood lymphocytes and on a healthy-donor purified CD19+ lymphocytes revealed by HGW1 preparations and HIL131 mAb. The fluorescence level of stained cells (filled histograms) was compared to that of unstained cells (A, B, D) or isotype control (C) (unfilled histograms).

any capacity to stain LICOS+ cells in FACS analysis (Fig. 31, B). The ability of HGW1 Alexa 647 to stain whole blood lymphocytes and CD19+ B cells (Fig. 31, C) was also maintained in Raji cells (Fig. 31, C, 1). However, when the Raji cells were preincubated with purified-unlabeled HGW1 in excess, HGW1 Alexa 647 staining was not extinguished. This finding clearly demonstrated that HGW1 Alexa 647 provides an unspecific staining, probably due to the labeling dye (Fig. 31, C).

Altogether, these data showed that HGW1 was in fact a pool of two or more antibodies and it contained an antibody that competed with HIL131 for the antigen. Unfortunately, due to low amounts, its effect was overwhelmed by the presence of other antibody(ies) in the pool. As a consequence, in FACS analysis it seemed that HGW1 and HIL131 bind to different epitopes: HIL131 binds to one that is expressed by both SKMel cells and blood cells, while HGW1 to one that is expressed only on SKMel cells. Therefore, unfortunately, HGW1 was not suitable for detection of LICOS on primary immune cells.

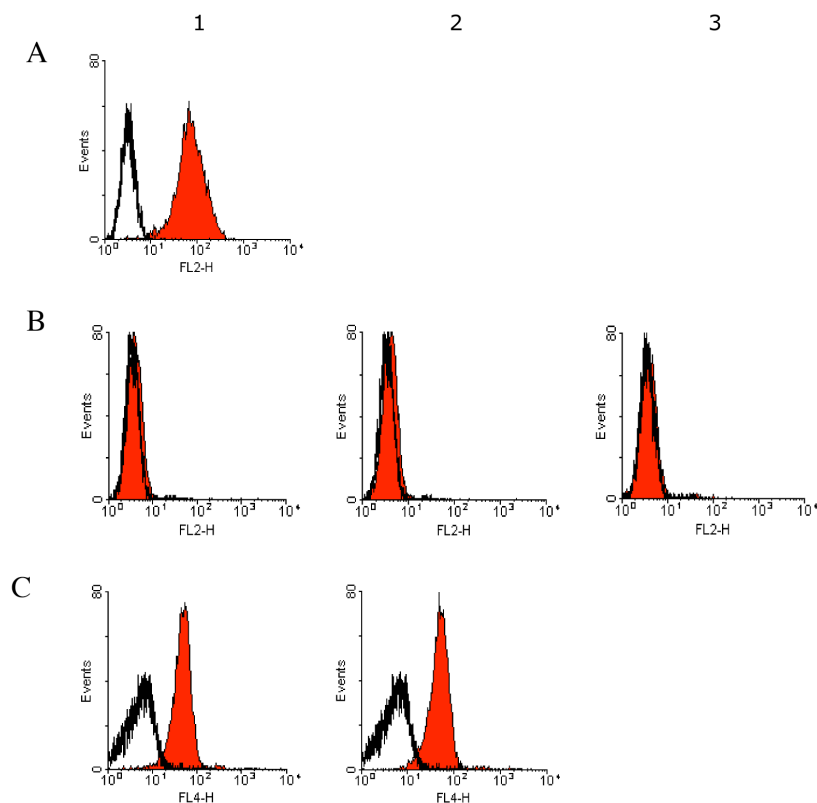


Figure 31. None of the HGW1 preparations specifically stained Raji cell line in FACS analysis. Cells were either stained with HIL131 PE (A, 1), HGW1 purified-unlabeled (B, 1), HGW1 supernatant (B, 2), HGW1 biotinylated (B, 3), HGW1 Alexa 647 (C, 1), or preincubated with HGW1 purified-unlabeled in excess and stained with HGW1 Alexa 647 (C, 2). The fluorescence level of stained cells (filled histograms) was compared to that of unstained cells (A, B, 1,2, 3) or isotype control (C) (unfilled histograms).

During the course of these experiments an anti-LICOS mAb (MIH12) became commercially available and it was used in all subsequent investigations. To evaluate its binding to native LICOS molecules, MIH12 was tested along with HIL131, first on the Raji cell line and then in the whole blood. As depicted in Fig. 32, both antibodies had the same ability to distinguish LICOS+ cells, in both test systems.

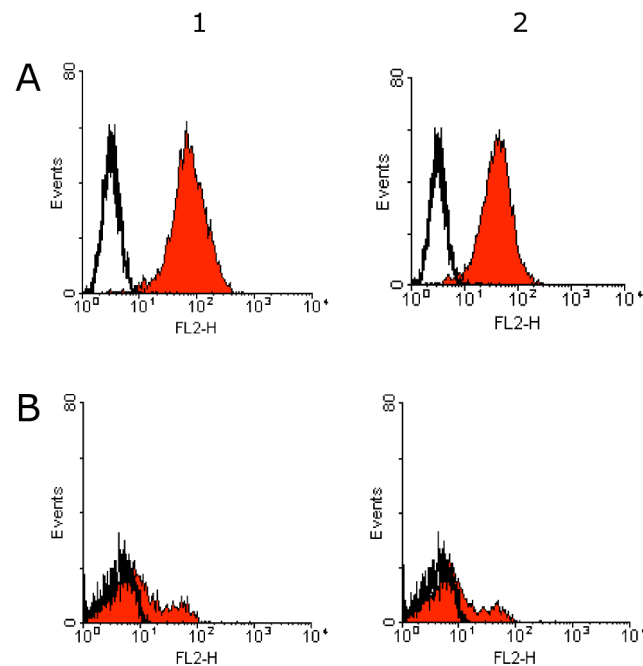


Figure 32. Comparison between the binding of HIL131 PE and that of MIH12 PE to native LICOS. Raji cell line (A) or whole blood cells (B) were stained with either HIL131 PE (1), or MIH12 PE (2) anti-LICOS mAbs. The fluorescence level of stained cells (filled histograms) was compared to that of unstained cells (1) or isotype control (2) (unfilled histograms).

3.9 Expression of HLA-DR, CD86, LICOS and ICOS in patients with major trauma and stroke in a pilot study

Polytrauma, hemorrhage and severe burn injuries are known to suppress T cell function. Immunosuppression predisposes the patients to a high incidence of septic complications. Among others, a shift of a Th1 dominated T cell response towards a TH2 response has been described as a potential mechanism of immune suppression in septic patients.

The ICOS-LICOS axis has an important role in the modulation of Th1 and Th2 differentiation and effector function. However, nothing is known about the level of ICOS expression on T cells and that of LICOS on APCs in critically ill patients.

In this pilot study, six patients with multiple severe injuries, nine stroke patients and 32 healthy donors were investigated for the expression of HLA-DR, CD86, LICOS and ICOS on the surface of CD14+ monocytes and on the CD19+, CD3+, CD4+ subpopulations of lymphocytes, by FACS analysis of whole blood. The clinical and demographic profile of the patients and the donors are shown in Table 1. Detailed characteristics of the trauma and stroke patients are displayed in the Table 2 and Table 3, respectively.

Table 1. Clinical and demographic profile of polytrauma, stroke patients and controls.

Group	Patients with polytrauma	Patients with stroke	Healthy donors Controls
Number of persons	6	9	32
ISS mean	42.33 (SD: 12.12)	-	-
ISS range	29-57	-	-
APACHE II mean	19 (SD: 4.3)	-	-
APACHE II range	13-24	-	-
GCS score mean	-	12 (SD: 4.65)	-
GCS score range	-	6-15	-
NIH score mean	-	6.6 (SD: 0.58)	-
NIH score range	-	6-7	-
Age in years mean	43.33 (SD: 23.95)	62.11 (SD: 13.9)	33.41 (SD: 11.37)
Age in years range	18-70	44-77	19-53
Ratio male:female	4:2	4:5	17:15
Deceased	1	0	0

First, I determined the base line levels of HLA-DR, CD86, LICOS and ICOS expression on the surface of CD14+ monocytes and on the CD19+, CD3+, CD4+ subpopulations of lymphocytes from 32 healthy donors. The positive populations were reported as percentage of corresponding CD14+ monocytes and CD19+, CD3+, CD4+ subpopulations of lymphocytes (Table 4). The expression range for these markers along with the mean \pm SD are displayed in the Table 4.

To illustrate the difference between donors and patients regarding the expression of any of

the surface markers determined, an example is given in the figures 33 and 34. The general trend observed in this figure is the decrease in number of CD19, CD3 and CD4 lymphocytes and the loss of costimulatory molecules on the surface of monocytes. For comparison, for each parameter displayed, the mean value of the donors and standard deviation (SD) were calculated and the value of $MEAN \pm SD$ was plotted. The data for each of the trauma and stroke patients, plotted against the range of surface markers expression in healthy donors are shown in the figures 35 and 38.

Table 2. Detailed clinical characteristics of the trauma patients (T patients).

Patients	ISS score on admission	APACHE II score on admission	Age	Gender	Time point of SIRS/sepsis	Deceased
T patient 1	32	15	70	F	None	No
T patient 2	41	13	68	M	D*1, D7 SIRS	No
T patient 3	57	24	24	F	D1-D7 sepsis D8-D11 SIRS D12-D14 sepsis D15-D18 SIRS D19-D22 sepsis D23-D29 SIRS	No
T patient 4	38	22	18	M	None	No
T patient 5	29	18	56	M	D1, D2, D5, D6 SIRS	No
T patient 6	57	22	24	M	D1 SIRS	Yes

D*=day of hospitalization

Table 3. Detailed clinical characteristics of the stroke patients (S patients).

Patients	GCS score	NIH score	Age	Gender	Time point of SIRS/sepsis	Deceased
S patient 1	6	-	44	F	D*3, D5, D7 SIRS	No
S patient 2	15	-	49	F	None	No
S patient 3	15	-	40	M	None	No
S patient 4	15	-	77	M	None	No
S patient 5	15	-	65	M	None	No
S patient 6	6	-	72	M	D1, D3, D5-D7 SIRS	No
S patient 7	-	7	71	F	None	No
S patient 8	-	7	67	M	None	No
S patient 9	-	6	74	F	None	No

D*=day of hospitalization

Table 4. The expression of the measured markers in range and mean \pm SD in healthy donors.

Marker expression	Range	Mean \pm SD
HLA-DR+/ CD14+	90-100%	97.52 \pm 2.6
CD86+/ CD14+	81-100%	93.08 \pm 5.13
LICOS+/ CD14+	1-12%	7.36 \pm 2.24
CD86+HLA-DR+/ CD14+	82-100%	91.45 \pm 5.86
LICOS+HLA-DR+/ CD14+	1-12%	7.38 \pm 2.24
HLA-DR+/ CD19+	98-100%	99.67 \pm 0.42
CD86+/ CD19+	2-24%	13.68 \pm 5.2
LICOS+/ CD19+	31-93%	72.26 \pm 14.24
CD86+HLA-DR+/ CD19+	2-24%	13.54 \pm 5.16
LICOS+ HLA-DR+/ CD19+	30-92%	72.38 \pm 14.11
HLA-DR+/ CD3+	4-36%	11.43 \pm 6.54
LICOS+/ CD3+	0.1-3%	0.72 \pm 0.63
LICOS+HLA-DR+/ CD3+	0.01-0.8%	0.2 \pm 0.17
ICOS+(dim&bright)/ CD3+	42-78%	64.3 \pm 9.38
ICOS ^{dim} / CD3+	37-78%	63.29 \pm 9.76
ICOS ^{bright} / CD3+	0.7-1.99%	1.36 \pm 0.28
CD4+/ CD3+	37-77%	64.72 \pm 7.66
HLA-DR+/ CD4+	1.5-12%	5.5 \pm 2.63
ICOS+ (dim&bright)/ CD4+	68-96%	84.24 \pm 6.14
ICOS ^{dim} / CD4+	67-90%	82.52 \pm 6.12
ICOS ^{bright} / CD4+	0.9-4%	1.9 \pm 0.62
ICOS+ (dim&bright) HLA-DR+ / CD4+	1-11%	4.94 \pm 2.38

3.9.1 Expression of HLA-DR, CD86 and LICOS on CD14+ monocytes

On the CD14 monocytes, HLA-DR expression was in the range of 90-100% of normal CD14+ cells (mean expression 97.6% \pm 2.6SD) and dramatically reduced in trauma patients, with the lowest values belonging to the patients with the highest ISS score (T patients 3 and 6, both with ISS score 57 on admission) (Fig. 35, A, 1). Correspondingly, stroke patients with the lowest GCS score (S patient 1 and S patient 6) presented low HLA-DR expression on CD14+ monocytes (Fig. 38, A, 1).

Expression of CD86+ was clearly reduced with large variations in all six trauma patients (Fig. 35, A, 2). From these, trauma patients 2 and 3, having the highest ISS scores (41 and 57, respectively), displayed a below-normal range level of expression for a longer time, while the rest of the patients (ISS score 29-38 on admission) recovered normal expression faster. Conversely, most of the stroke patients exhibited a CD86+ level within the healthy donor range (Fig. 38, A, 2). Again, the stroke patients with the lowest GCS score (S patient 1 and S

patient 6) had the most reduced CD86 expression on CD14⁺ monocytes in the first days of hospitalization, which recovered later (Fig. 38, A, 2). CD86 was largely coregulated with HLA-DR in both trauma and stroke patients (Fig. 35, A, 4 and Fig. 38, A, 4). Consequently, the strong downregulation of CD86, in both categories of patients, mirrors that of HLA-DR and provides no additional information.

LICOS⁺ was expressed by a subpopulation of HLA-DR^{bright} monocytes (Fig. 33). In trauma patients, the fraction of LICOS⁺ monocytes was also reduced, but to a more variable extent and could not be correlated to ISS score (Fig. 35, A, 3). Similarly, most of the stroke patients had a low percentage of LICOS⁺ monocytes, except for S patient 6, who displayed a transient upregulation of LICOS on these cells (Fig. 38, A, 3).

Again, LICOS was coregulated with HLA-DR, in trauma patients as well as in stroke patients (Fig. 35, A, 5 and Fig. 38, A, 5).

3.9.2 Expression of HLA-DR, CD86 and LICOS on CD19⁺ lymphocytes

All CD19⁺ lymphocytes expressed HLA-DR in healthy donors and also in trauma and stroke patients (Fig. 35, B, 1 and Fig. 38, B, 1).

CD86 was variably expressed on a subset of CD19⁺ lymphocytes: downregulated in most of the trauma patients and upregulated in the patient with sepsis (Fig. 35, B, 2). On the other hand, in all stroke patients, CD86 level on CD19⁺ lymphocytes resembled that of healthy donors (Fig. 38, B, 2).

Similar to CD86, the expression of LICOS was also variable, although less pronounced than that of CD86 (Fig. 35, B, 3 and Fig. 38, B, 3).

CD86⁺HLA-DR⁺ and LICOS⁺HLA-DR⁺ B cells (Fig. 35, B, 4, 5 and Fig. 38, B, 4, 5) reflected the expression pattern of CD86⁺ and LICOS⁺ B cells, respectively, in both categories of patients.

3.9.3 Expression of HLA-DR and LICOS on CD3⁺ lymphocytes

Patient levels of HLA-DR and LICOS on CD3⁺ lymphocytes were in the normal range of expression exhibited by controls (Fig. 35, C, 1, 3, 5 and Fig. 38, C1, 3, 5).

3.9.4 Expression of ICOS and CD4 on CD3+ lymphocytes

In all patients, ICOS expression as both a proportion of CD3+ lymphocytes or CD4+ lymphocytes was in the same range as for normal donors, except for S patient 7, who showed a decrease in ICOS level (Fig. 35, D, 2 and F, 2; Fig. 38, D, 2, and F, 2).

The frequency of CD4+ T cells among CD3+ lymphocytes was slightly elevated in T patients 3 and 5 (Fig. 35, E, 1), but within the controls' range in stroke patients (Fig. 38, E, 1).

Given that there was no difference between patients and healthy donors regarding ICOS+ CD3+ and ICOS+CD4+ cells (Fig. 35, D, 2 and F, 2; Fig. 38, D, 2, and F, 2), these positive populations were next divided by gating into two subpopulations, namely ICOS^{bright} and ICOS^{dim} (Fig. 36). To determine the dynamic of ICOS expression in the patients' CD3+ and CD4+ lymphocyte populations, ICOS^{bright}, ICOS^{dim} and ICOS⁻ subpopulations were compared (Fig. 37 and Fig. 39). In both categories of patients, in both CD3+ and CD4+ lymphocyte populations, the fraction of ICOS^{dim} and ICOS⁻ cells did not differ significantly from that of controls (Fig. 37, A, B and Fig. 39 A, B). Interestingly, the ICOS^{bright} subpopulation was markedly increased in all trauma patients (Fig. 37, C) and in most of the stroke patients (Fig. 39, C).

3.9.5 Expression of HLA-DR on CD4+ lymphocytes

Patients' HLA-DR expression on CD4+ lymphocytes (T helper cells) remained within the controls' range (Fig. 35, F, 1 and Fig. 38, F, 1) and all HLA-DR+ CD4 lymphocytes coexpressed ICOS (Fig. 35, F, 3 and Fig. 38, F, 3).

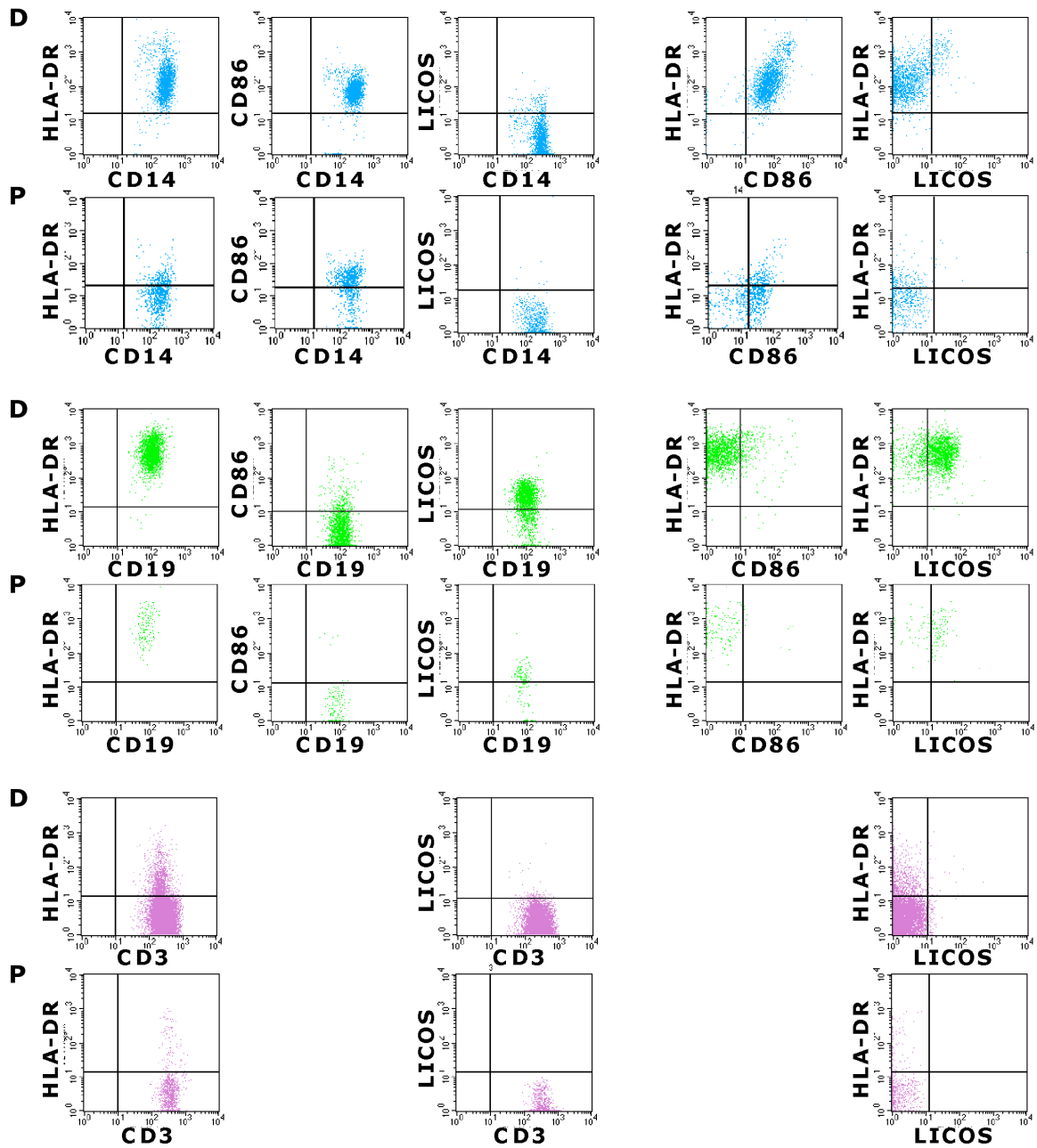


Figure 33. The difference between a donor (D) and T patient 3 (P) regarding the expression of surface markers HLA-DR, CD86 and LICOS on CD14+ monocytes (blue gate), CD19+ lymphocytes (green gate), CD3+ lymphocytes (move gate) (an example).

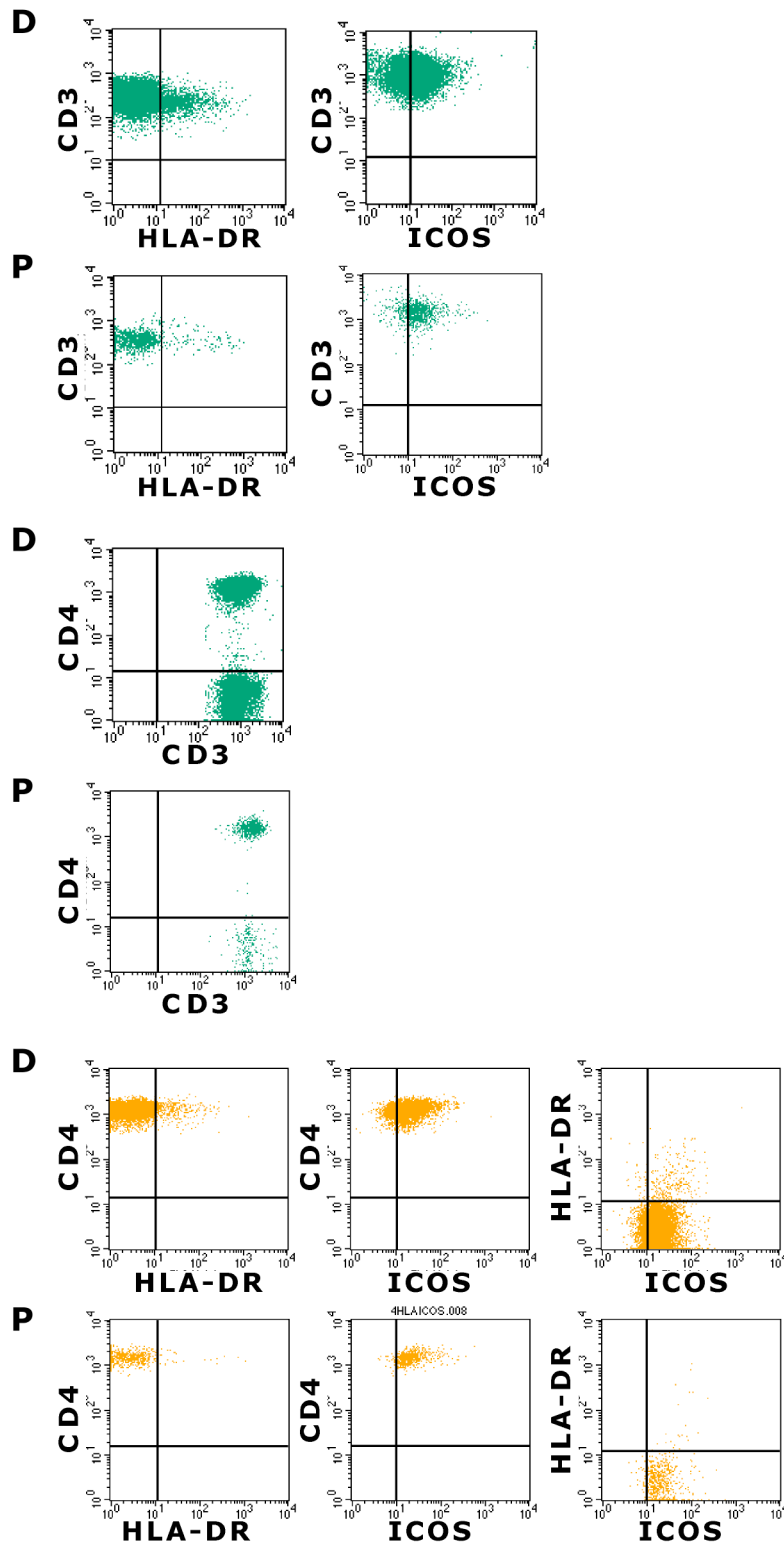


Figure 34. The difference between a donor (D) and T patient 3 (P) regarding the expression of surface markers HLA-DR and ICOS on CD3+ lymphocytes (dark-green gate) and CD4+ lymphocytes (orange gate) (an example).

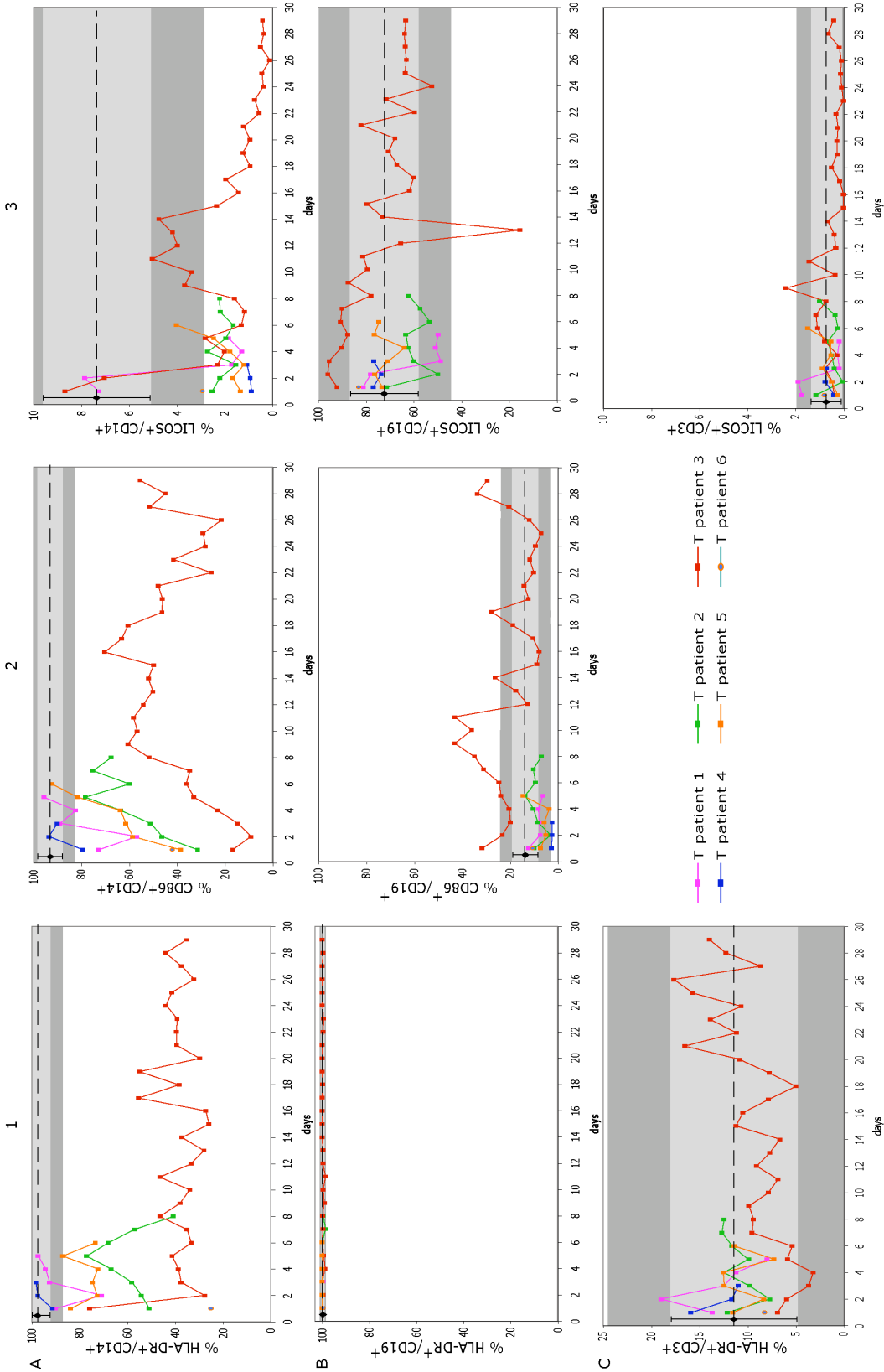


Figure 35. Expression of HLA-DR, CD86 and LICOS on CD14⁺ monocytes as well as on CD19⁺ and CD3⁺ lymphocytes from trauma patients (T patients). A, CD14⁺ monocytes; B, CD19⁺ lymphocytes; C, CD3⁺ lymphocytes. 1, HLA-DR+ cells; 2, CD86+ cells; 3, LICOS+ cells. Mean values of controls (dashed black line) \pm 1SD (grey shaded area) and 2SD (dark grey shaded area) are showed. (continued)

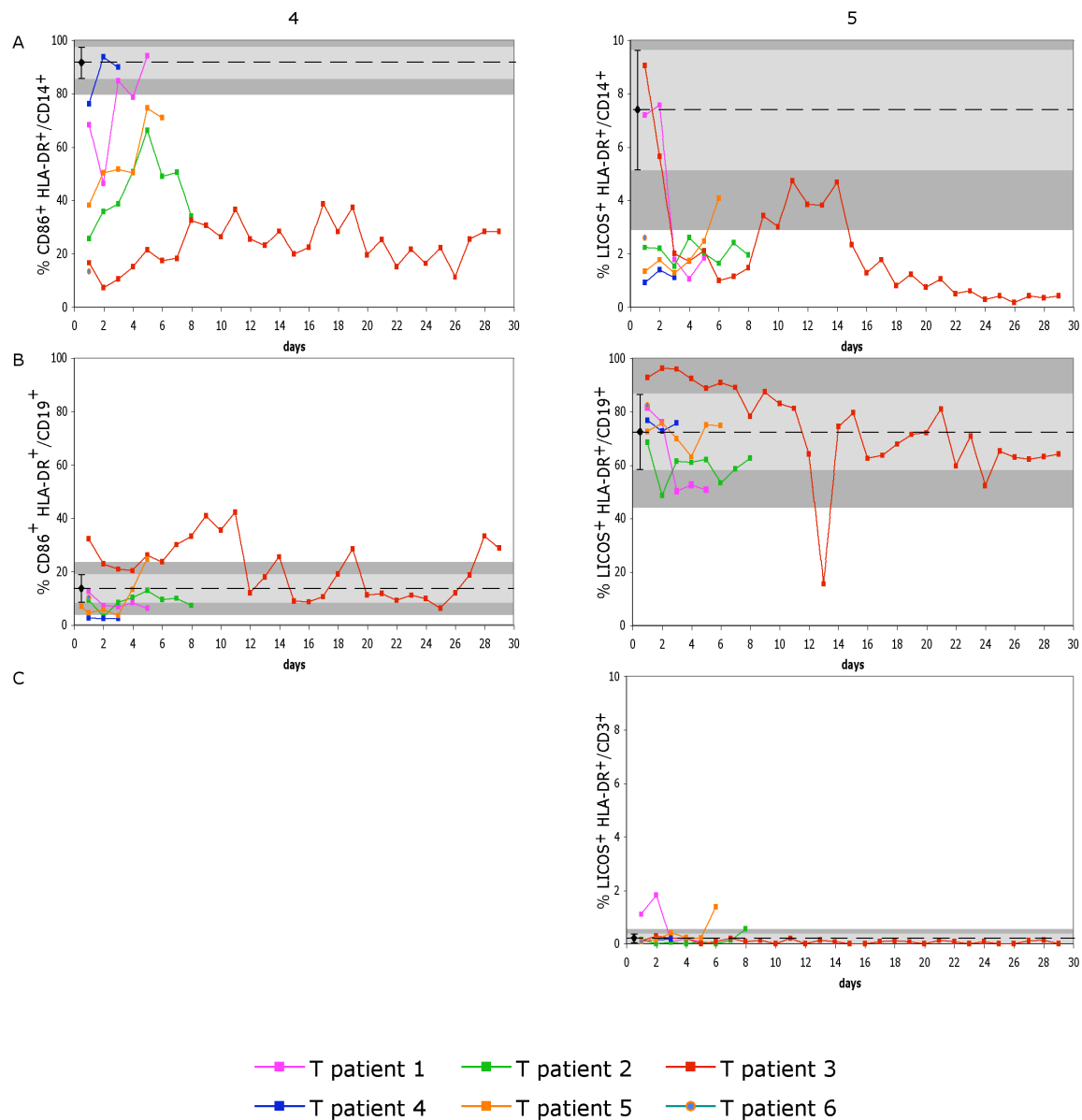
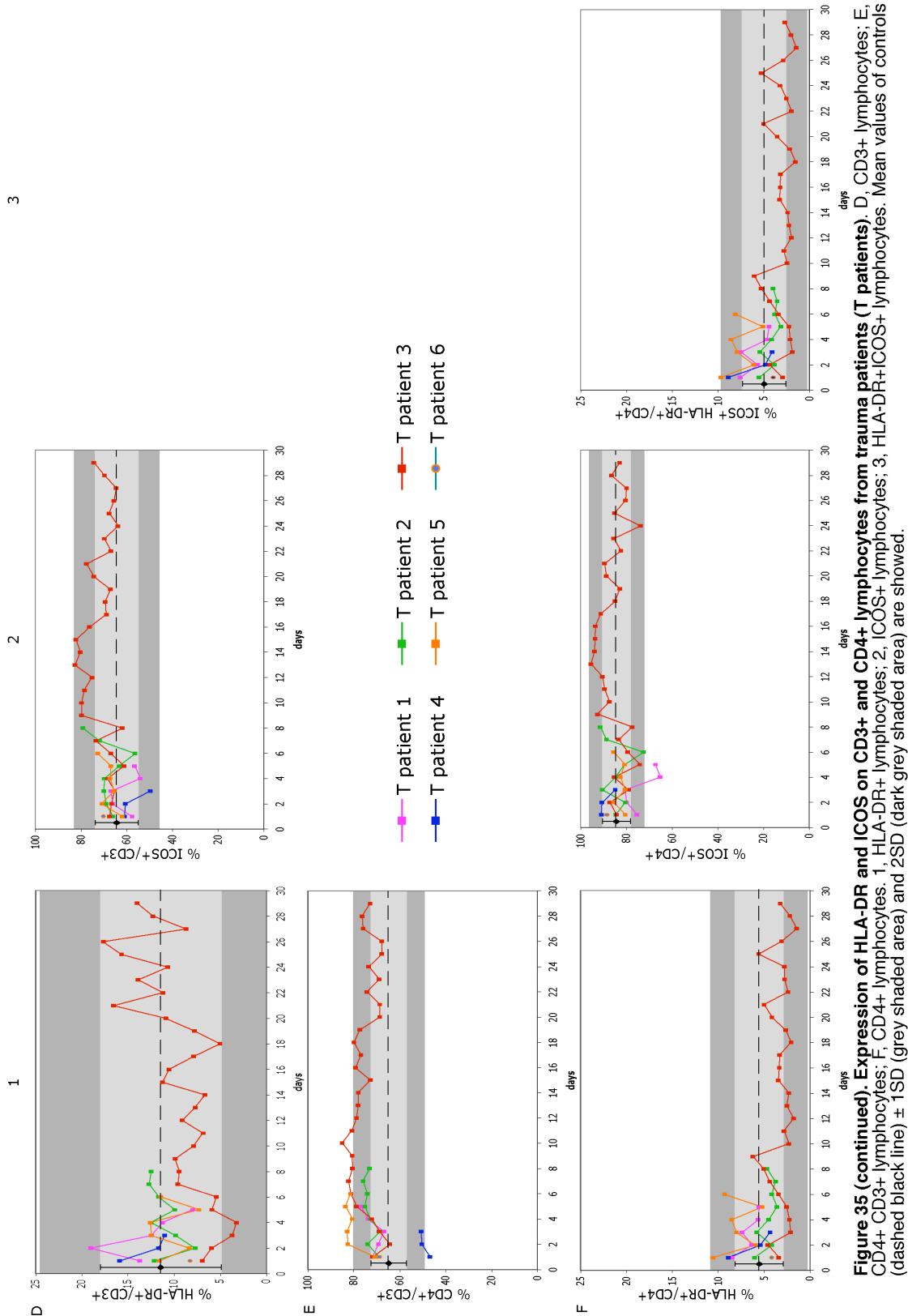


Figure 35 (continued). Expression of HLA-DR, CD86 and LICOS on CD14⁺ monocytes as well as on CD19⁺ and CD3⁺ lymphocytes from trauma patients (T patients). A, CD14⁺ monocytes; B, CD19⁺ lymphocytes; C, CD3⁺ lymphocytes. 4, HLA-DR+CD86⁺ cells; 5, HLA-DR+LICOS⁺ cells. Mean values of controls (dashed black line) $\pm 1SD$ (grey shaded area) and $\pm 2SD$ (dark grey shaded area) are shown. (continued)



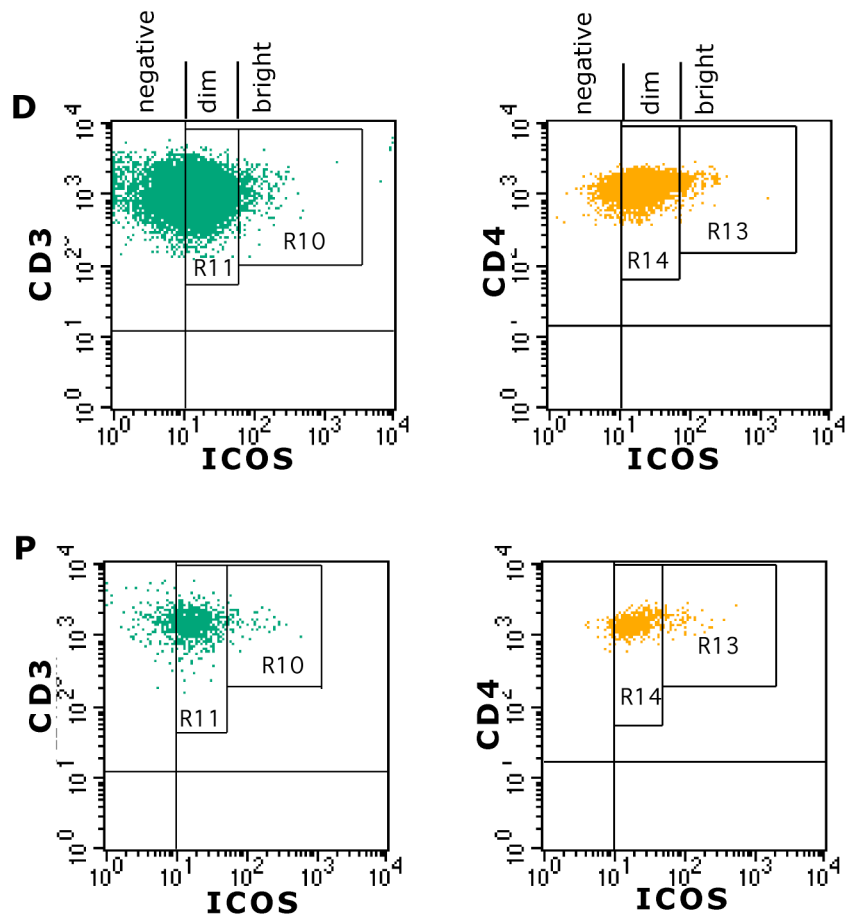


Figure 36. The division of ICOS⁺ CD3⁺ and ICOS⁺CD4⁺ lymphocyte populations into ICOS^{bright} and ICOS^{dim} subpopulations. On the dot plots shown in the Fig. 34, gates were set to delimit ICOS^{bright} from ICOS^{dim} subpopulation.

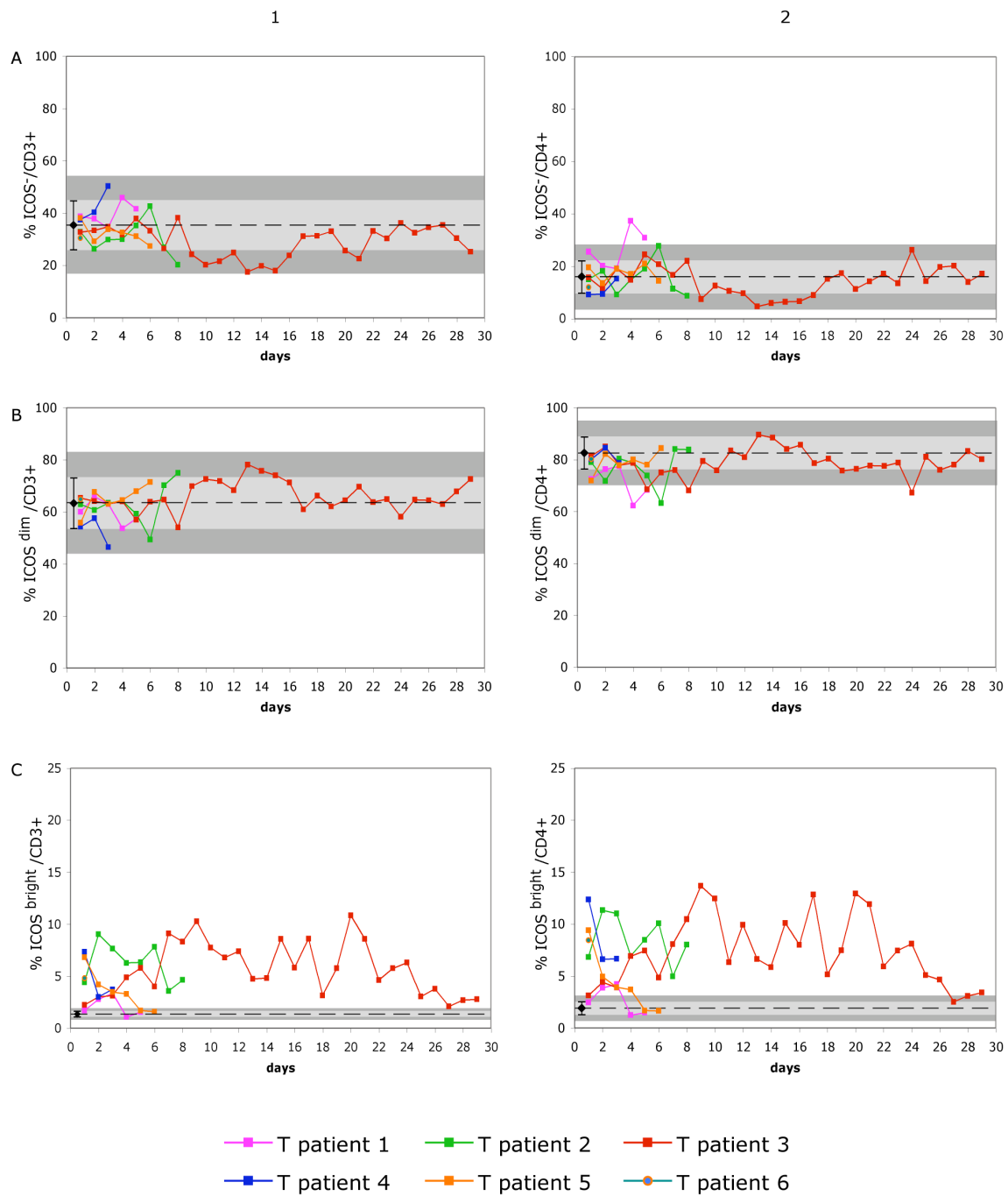


Figure 37. Expression of ICOS^{bright}, ICOS^{dim} and ICOS⁻ subpopulations of CD3⁺ and CD4⁺ lymphocytes in trauma patients (T patients). A, ICOS⁻; B, ICOS^{dim}; C, ICOS^{bright}. 1, CD3⁺ lymphocytes; 2, CD4⁺ lymphocytes. ICOS^{dim} and ICOS⁻ subpopulations were similar to healthy donors (A, B 1, 2). In contrast, the expression of ICOS^{bright} was elevated in patients on a subset of CD3⁺ and CD4⁺ lymphocytes (C, 1, 2). Mean values of controls (dashed black line) ± 1SD (grey shaded area) and 2SD (dark grey shaded area) are shown.

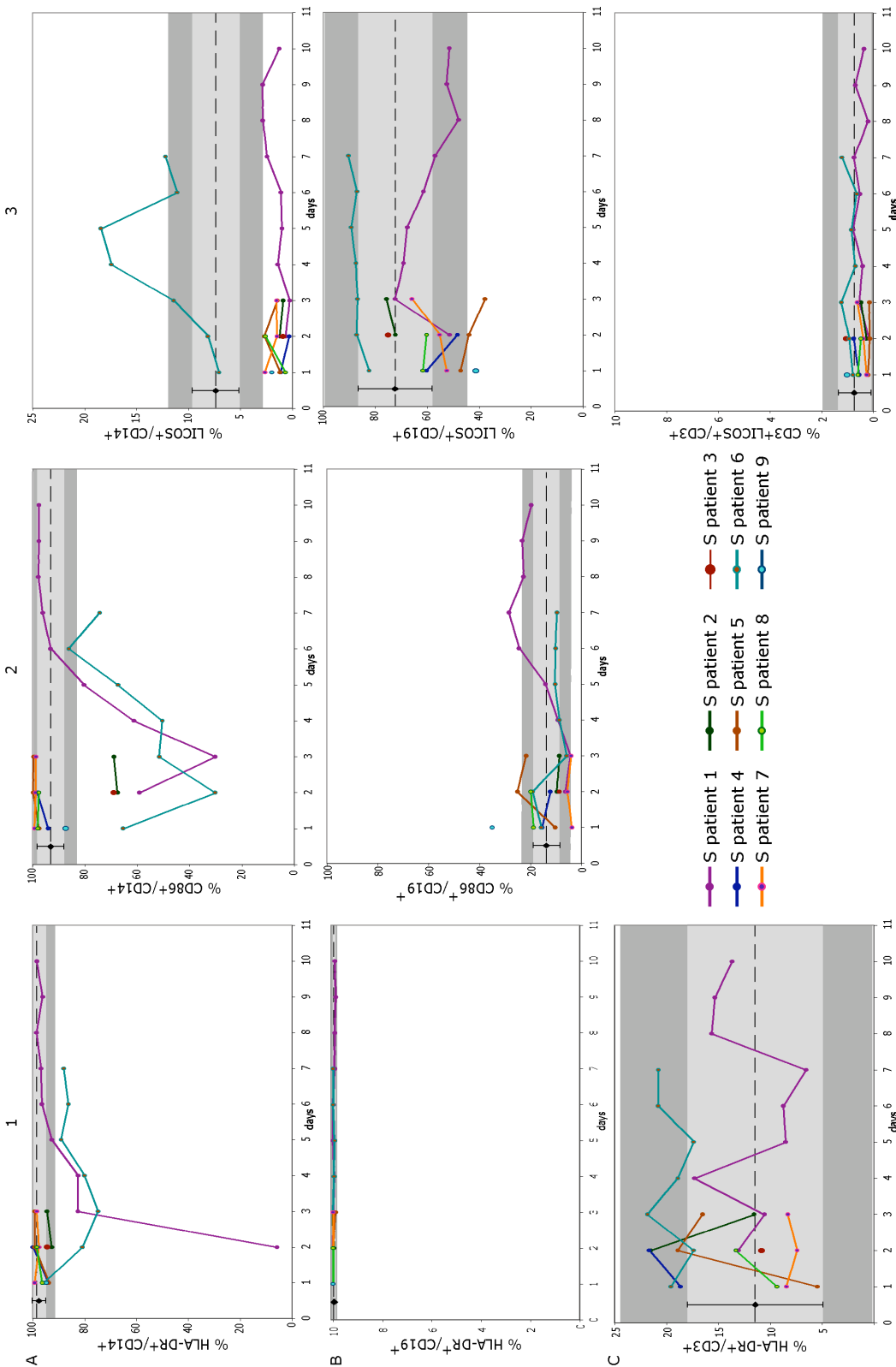


Figure 38. Expression of HLA-DR, CD86 and LICOS on CD14⁺ monocytes as well as on CD19⁺ and CD3⁺ lymphocytes from stroke patients (S patients). A, CD14⁺ monocytes; B, CD19⁺ lymphocytes; C, CD3⁺ lymphocytes. 1, HLA-DR⁺ cells; 2, CD86⁺ cells; 3, LICOS⁺ cells. Mean values of controls (dashed black line) \pm 1SD (grey shaded area) and 2SD (dark grey shaded area) are showed. (continued)

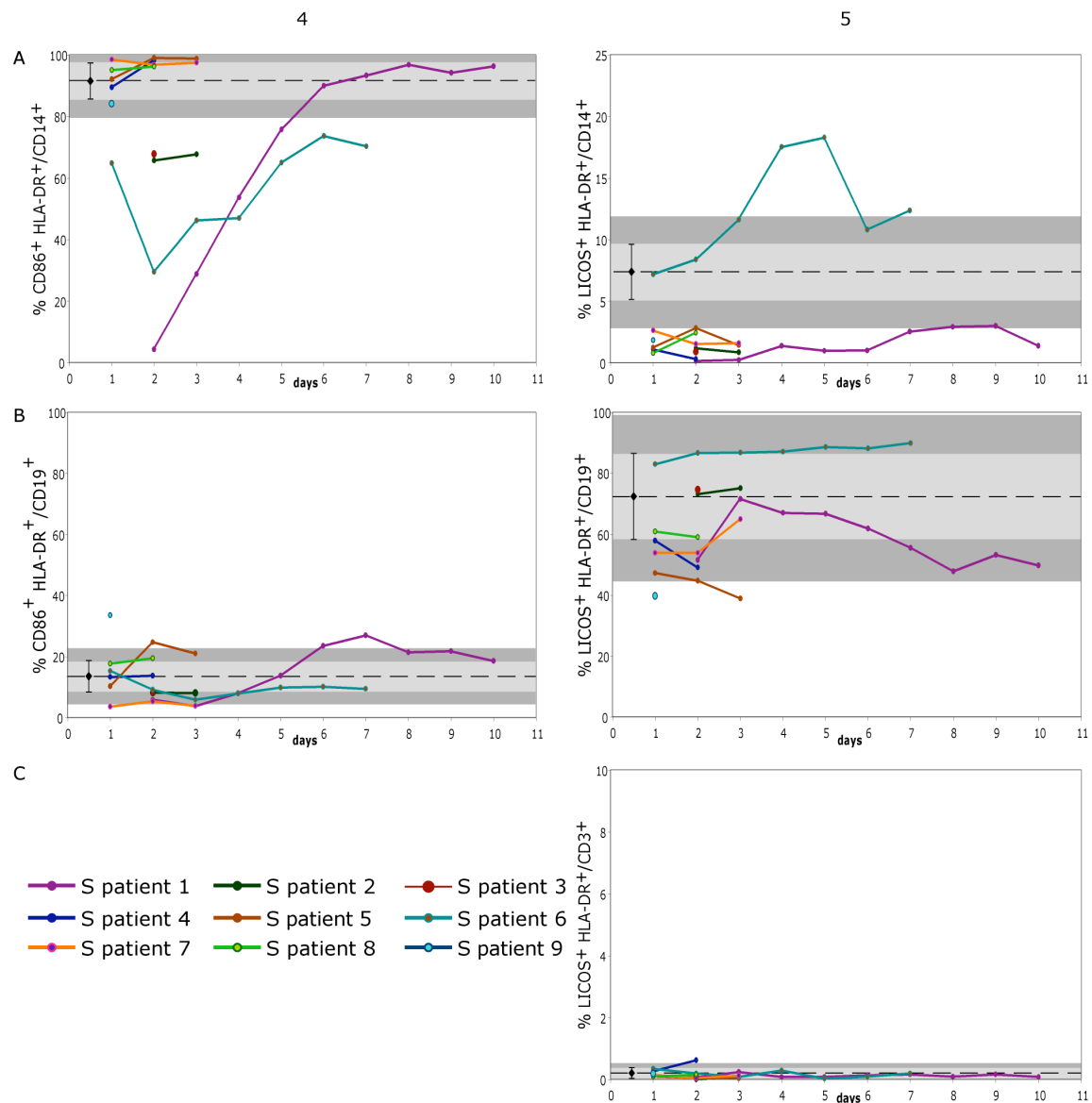


Figure 38 (continued). Expression of HLA-DR, CD86 and LICOS on CD14⁺ monocytes as well as on CD19⁺ and CD3⁺ lymphocytes from stroke patients (S patients). A, CD14⁺ monocytes; B, CD19⁺ lymphocytes; C, CD3⁺ lymphocytes. 4, HLA-DR⁺CD86⁺ cells; 5, HLA-DR⁺LICOS⁺ cells. Mean values of controls (dashed black line) \pm 1SD (grey shaded area) and 2SD (dark grey shaded area) are shown. (continued)

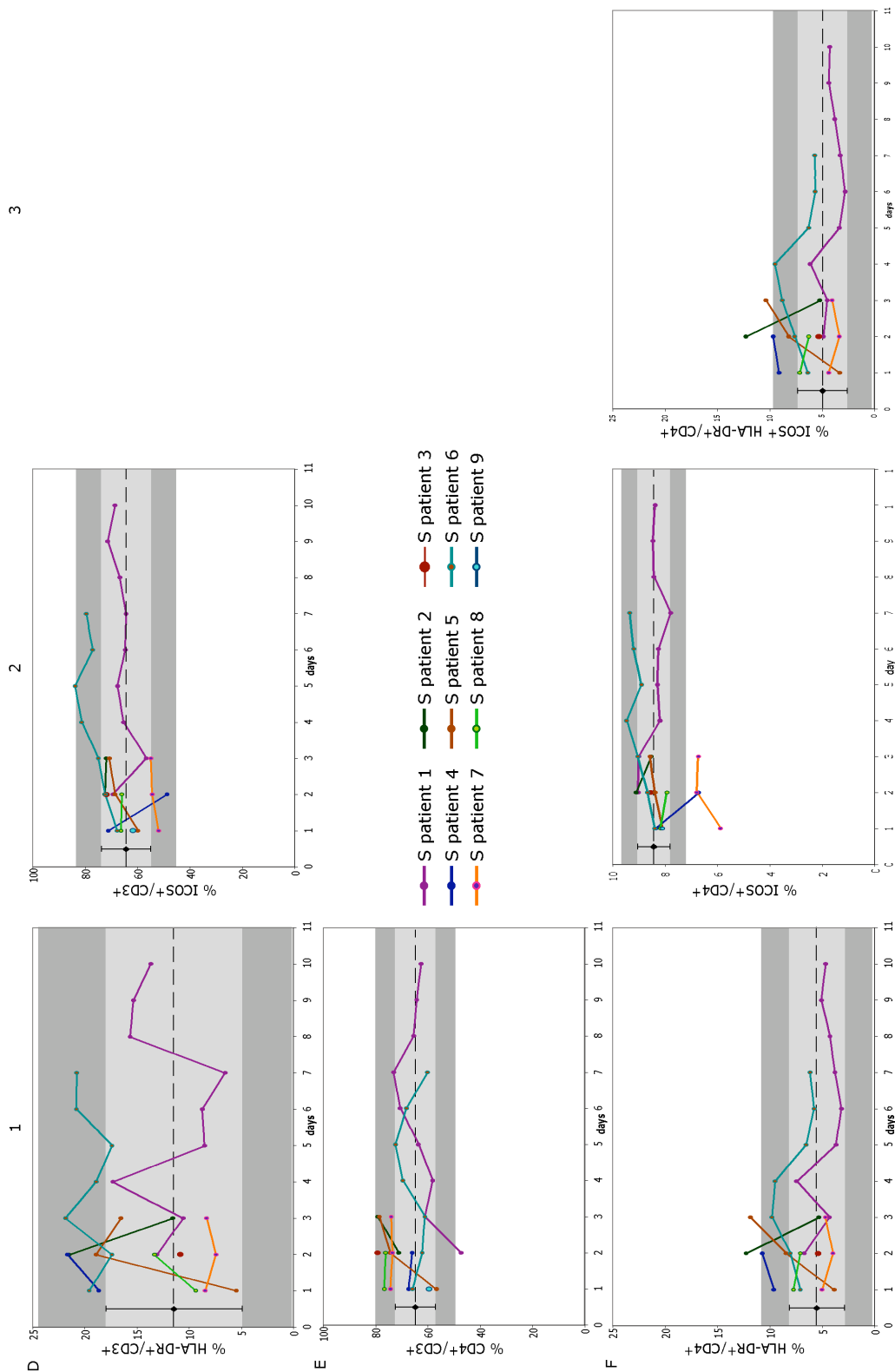


Figure 38 (continued). Expression of HLA-DR and ICOS on CD3+ and CD4+ lymphocytes from stroke patients (S patients). D, CD3+ lymphocytes; E, CD4+ CD3+ lymphocytes; F, CD4+ lymphocytes. 1, HLA-DR+ lymphocytes; 2, ICOS+ lymphocytes; 3, HLA-DR+ICOS+ lymphocytes. Mean values of controls (dashed black line) \pm 1SD (grey shaded area) are shown.

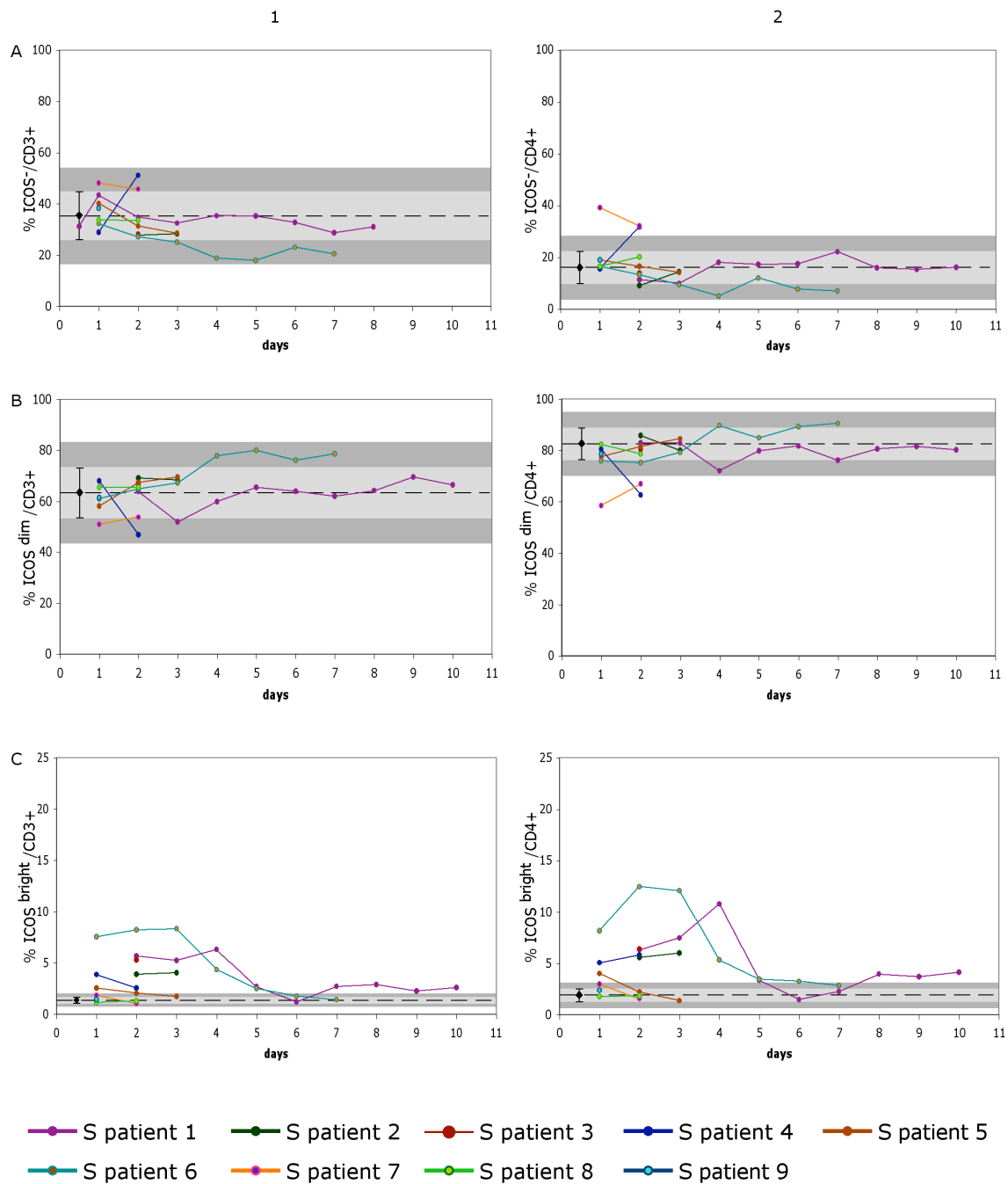


Figure 39. Expression of ICOS^{bright}, ICOS^{dim} and ICOS⁺ subpopulations of CD3⁺ and CD4⁺ lymphocytes in stroke patients (S patients). A, ICOS⁺; B, ICOS^{dim}; C, ICOS^{bright}. 1, CD3⁺ lymphocytes; 2, CD4⁺ lymphocytes. ICOS^{dim} and ICOS⁺ subpopulations were similar to healthy donors (A, B, 1, 2). In contrast, the expression of ICOS^{bright} was elevated in patients on a subset of CD3⁺ and CD4⁺ lymphocytes (C, 1, 2). Mean values of controls (dashed black line) \pm 1SD (grey shaded area) and 2SD (dark grey shaded area) are shown.

4. Discussion

4.1 Generation of the LICOS-Ig fusion protein and of an anti-LICOS mAb (HGW1)

After the discovery of the ICOS/LICOS pathway, many studies have revealed important aspects of its functional implication in T cell activation and effector functions in relation with CD28/CTLA-4/B7.1/B7.2 pathway. The CD28/B7.1(CD80)/B7.2(CD86) pathway influences the Th1/Th2 balance and Th2 differentiation and acts as an attenuator of IL-10 production. In contrast, the ICOS/LICOS pathway is a superinducer of IL-10 production and has a particular role in Th2 differentiation and effector function and in the initiation and maintenance of B cell response.

Predominant Th2 responses associated with high levels of IL-10 as well as loss of antigen-presentation and costimulatory capacity by circulating monocytes were linked to immunosuppression in trauma and subsequent sepsis. Moreover, a state of immunosuppression is associated with increased risk of infection complications after stroke.

In this study the expression level of costimulatory molecules CD86 (B7.2), LICOS and ICOS along with that of HLA-DR, on the surface of circulating T cells, B cells and monocytes in major trauma and stroke patients in comparison to healthy controls was determined. For this purpose, first a LICOS-Ig fusion protein was generated and used for anti-LICOS monoclonal antibodies (mAbs) production. Following three fusions and the screening of 5 000 primary clones, only one primary clone (HGW1) was found to be selectively reactive to LICOS-Ig. From this clone, after cycles of screening and subcloning, only two subclones were shown to constantly secrete specific antibodies against LICOS-Ig and their supernatants were pooled (HGW1 supernatant) and used further.

Considering that the two HGW1 subclones originated in the same master well, deriving from a single hybridoma cell, as efforts to ensure monoclonality were made and only wells containing monoclonal cells were expanded, one could expect to obtain in the end two or more stable subclones of the same specificity. This expectation explains the mixing of the two supernatants. It seems very unlikely that during the screening, subcloning and expansion steps, one cell underwent a mutation and the offspring of that cell was further selected and propagated in the culture. In a hybridoma culture, the chances for a random mutation to occur are as low as of $8.7 \times 10^{-5} \text{ h}^{-1}$ and they usually lead to the loss of antibody production (Kromenaker and Srien 1994). Furthermore, the chances for a mutation that can refine or degenerate antigen recognition are even much lower.

In the production of mAbs the result is influenced by many factors: the species to be immunized, the antigen preparation, the immunization protocol, and the sensitivity of screening assay. Usually, depending on the purity of the antigen and the immunization

protocol, <1 to 5% of the primary wells contain hybridomas of desired specificity (Current Protocols in Immunology, unit 2.5), while, as few as 0.1% of the primary wells were positive in this work. One reason for this could be the amount of spleen used for fusion. A cell suspension representing 3/4 of a mouse spleen was used in the present case. Probably, the fusion efficiency was very high so that the hybridoma of desired specificity together with several hybridomas of other specificities were plated in the same well, resulting in oligoclonality, which was not considered (only approx. 10 wells per plate contained monoclones). On the other hand, when a fusion with 1/4 of a spleen was performed no positive clones were obtained. Another reason for low number of positive primary wells could be the low immunogenicity of human LICOS in mice, due to a high homology between the two orthologous proteins. However, the human and mouse LICOS share only about 50% homology within the extracellular domain (Yoshinaga, Zhang et al. 2000), compared to 67% homology between human and mouse CTLA4 extracellular domain. Moreover, CTLA4-Ig was successfully used to obtain an anti-CTLA4 mAb (Harper, Balzano et al. 1991; Castan, Tenner-Racz et al. 1997). Furthermore, when Khayyamian et al. used huLICOS-rabbit-Ig fusion protein for immunizing BALB/c mice, they obtained 23 different anti-LICOS mAbs (Khayyamian, Hutloff et al. 2002). The lack of activated B cells could also be a reason for the low number of specific clones. The activation status of B cells can be assayed by measuring the antibody titers before the final boost and fusion. Unfortunately, due to technical problems this measurement could not be performed.

HGW1 supernatant stained LICOS expressed by the melanoma cell line SKMel following transfection with full-length LICOS. Other members of the B7 family, CD80 and CD86, were not bound by HGW1.

The staining of lymphocytes and monocytes in whole blood was then compared to that of another anti-LICOS monoclonal antibody (HIL131, a kind gift of R. A. KroczeK). HGW1 and HIL131 showed different binding patterns: HIL131 bound strongly to CD19+ B cells and only weakly to CD14+ monocytes, while HGW1 showed strong binding to monocytes, but only low intensity staining of B cells. This difference raised the questions, whether there was a difference between native LICOS on primary blood cells and recombinant LICOS expressed from a transgene by SKMel and whether the two antibodies bound to different epitopes of LICOS molecule that are differentially expressed by B cells and monocytes.

Competition experiments with ELISA suggested that HGW1 was probably a pool of two different LICOS-binding monoclonal antibodies, one of which competed with HIL131 for the antigen, while the other did not. On the other hand, in FACS analysis, competition for LICOS binding between HGW1 and HIL131 was not evident in whole blood and a B cell line probably due to the low amount of the competing mAb species in the putative HGW1 pool. In other words, the HGW1 was likely a pool of two antibodies with different specificities: one antibody, present in low amounts, recognized the same epitope as HIL131, which was found on both recombinant and native forms of LICOS and the other one(s), present in high

amounts, bound to a different epitope, which was found only on the recombinant form of LICOS. Therefore, due to the predominant clone, which bound with high affinity only to recombinant LICOS, HGW1 was not suitable for the quantification of the native form of LICOS on primary immune cells by flow cytometry. However, in FACS and microscope analysis of LICOS transfected SKMel cells, HGW1 could attest the presence of LICOS molecules on the cell surface, probably due to the predominant clone(s) present in the pool. Thus, HGW1 can be used for ELISA assays, FACS analysis and histochemical stainings that involve LICOS-transfected cells, *in vitro*.

4.2 Expression of HLA-DR, CD86, LICOS and ICOS in patients with major trauma and stroke

In this pilot study, the expression of HLA-DR, CD86, LICOS and ICOS on the surface of CD14⁺ monocytes and on the CD19⁺, CD3⁺, CD4⁺ lymphocytes were investigated, by FACS analysis of whole blood, in six patients with multiple severe injuries and nine stroke patients.

4.2.1 Expression of HLA-DR, CD86 and LICOS on CD14⁺ monocytes

HLA-class II molecules play a critical role in the adaptive immune response of the host against infection. During the initial phase of sepsis, the systemic hyperinflammatory response (SIRS) has been associated with normal or increased monocyte HLA-DR expression (Haveman, Muller Kobold et al. 1999). As the compensatory anti-inflammatory response syndrome (CARS) is initiated immediately after SIRS, monocytes down-regulate HLA-DR expression and become deactivated and unresponsive (Kox, Volk et al. 2000; Hoflich and Volk 2002). The reduction in the number of circulating monocytes was correlated with infection complications, the severity and outcome of sepsis (Cheadle, Hershman et al. 1991; Heumann, Glauser et al. 1998), although some studies have reported the contrary (Oczenski, Krenn et al. 2003; Perry, Mostafa et al. 2003). Whether HLA-DR expression on monocytes is a reliable prognostic parameter for clinical outcome or just a parameter for monocytes immunocompetence is not yet clear (Spittler and Roth 2003). Nevertheless, it is now generally accepted that HLA-DR expression is high in healthy donors and dramatically reduced in critically ill patients. In healthy donors, more than 90% of CD14⁺ monocytes express HLA-DR at very high densities (1-2 decades higher than the isotype control) (Spittler and Roth 2003). In this regard, I also found that HLA-DR was expressed on ca. 97%* of CD14⁺ cells from healthy controls. This level was massively reduced in trauma patients with

* average value

the lowest values belonging to the patients with the highest ISS score (the most severe cases, T patient 3 and T patient 6, in Fig. 35, A, 1 and Table 2). Correspondingly, in stroke patients the lowest CGS score (the most severe state) correlated with low HLA-DR expression on CD14+ monocytes (S patient 1 and S patient 6, in Fig. 38, A, 1 and Table 3).

Normally, CD86 is constitutively expressed on APCs and readily upregulated in response to infection, acting in the early phases of the immune response (Furukawa, Mandelbrot et al. 2000). After *in vitro* LPS priming of human monocytes and also on peritoneal macrophages of septic mice, the expression of CD86 and HLA-DR is down-regulated (Wolk, Docke et al. 2000; Newton, Ding et al. 2004).

In the present study, compared to around 93%* of the monocytes bearing CD86 in healthy donors, the expression of this marker in all six trauma patients was clearly reduced but with large variations (Fig. 35, A, 2). From these, trauma patients with the highest ISS scores displayed the lowest level of CD86 expression for a longer time than the rest of the patients, suggesting that the reduction of CD86 expression was affected by the severity of injury (T patient 3 and T patient 6, Table 2). Again, the stroke patients with the lowest GCS score had the lowest CD86 expression on CD14+ monocytes in the first days of hospitalization, but it recovered afterwards (S patient 1 and S patient 6 in Fig. 38, A, 2 and Table 3). This result, together with that obtained with HLA-DR, showed that, apparently, trauma was a stronger inducer of monocytes dysfunction than stroke – an observation that could be explained by the mild severity of the stroke cases (see Table 3). CD86 was largely coexpressed with HLA-DR in both trauma and stroke patients (Fig. 35, A, 4 and Fig. 38, A, 4) consistent with the findings of Manjuck et al. (Manjuck, Saha et al. 2000).

LICOS is expressed at high levels on myelomonocytic cell lines, but unstimulated peripheral CD14+ monocytes were found to express little or no LICOS, depending on the donor (Aicher, Hayden-Ledbetter et al. 2000). Its expression is upregulated on activation of monocytes through integrin-mediated adhesion or IFN- γ , and not by pro-inflammatory stimuli like LPS, IFN- α or TNF- α . No article was found to report LICOS and ICOS expression in critically ill patients at the time this study was carried out.

In healthy controls, 7.5%* of the monocytes expressed LICOS. This LICOS+ subpopulation was very bright for HLA-DR staining. In trauma patients, the fraction of LICOS+ monocytes was reduced, but to a more variable extent than CD86 and could not be correlated to ISS score (Fig. 35, A, 3). Similarly, most of the stroke patients had a low percentage of LICOS+ monocytes, except for the stroke patient 6, who displayed a transient upregulation of LICOS in these cells (Fig. 38, A, 3). LICOS was coexpressed with HLA-DR, in trauma patients as well as in stroke patients (Fig. 35, A, 5 and Fig. 38, A, 5).). Because of its low signal-noise ratio and basal level of LICOS on monocytes, LICOS expression is not an informative parameter in discrimination between patients with high and low risk of sepsis. In contrast to

* average value

LICOS, and similar to HLA-DR, CD86 expression appeared to discriminate between these two groups of patients.

The downregulation of LICOS and CD86 expression simultaneously with that of HLA-DR reflects the immunoincompetence of monocytes during a major insult to the organism. It was interesting to note that while patients showed the clinical signs of the systemic inflammatory syndrome (SIRS) with hypo/hyperthermia, tachycardia, tachypnea or hyperventilation, leukocytosis or leukopenia (Bone 1991), their monocytes were in a state of immunodysfunction (immunoparalysis) as displayed by low levels of HLA-DR and costimulatory molecules expression. This showed that stresses like trauma or stroke, in the absence of any sign of infection, could induce a mixed antagonistic response syndrome (MARS), consistent with the clinical experience of others (Bone 1996; Kox, Volk et al. 2000; Hoflich and Volk 2002; Tschaikowsky, Hedwig-Geissing et al. 2002).

4.2.2 Expression of HLA-DR, CD86 and LICOS on CD19+ lymphocytes

Apart from monocytes, B cells also express HLA-DR molecules on their surfaces. In healthy controls, I found that the percentage of CD19+ B cells bearing HLA-DR was in the 98-100% range (Fig. 35, B, 1). The majority of these HLA-DR+ B cells (72%*) coexpressed LICOS and only 14%* of them were also CD86+ (Fig. 35, B, 4 and 5). Interestingly, the level of HLA-DR in trauma and stroke patients was very similar to that of healthy donors. However, others have found that mean fluorescence intensity (MFI) of B cell HLA-DR expression was decreased on day 2 after injury and significantly reduced in septic trauma patients on day 6 after admission (Ditschkowski, Kreuzfelder et al. 1999). The difference between the high percentage of CD19+ B cells expressing HLA-DR and low MFI of HLA-DR expression has not been evaluated.

CD80 and CD86 are not expressed by unstimulated B cells. Yet, both molecules can be induced on these cells by ligation of MHC class II, bacterial DNA and LPS and their expression is increased by IL-2, IL-4, and IL-5. Moreover, stimulation with LPS or anti-CD40 induces CD86 more rapidly than CD80, as reviewed in (Lenschow, Walunas et al. 1996; McAdam, Schweitzer et al. 1998). In this study, the frequency of B cells bearing CD86 was around 14%* in healthy donors. CD86 was variably expressed on a subset of CD19+ lymphocytes, which tended to downregulation in most of the trauma patients and upregulation in the patient with sepsis (Fig. 35, B, 2). Similar to HLA-DR expression, in all stroke patients CD86 level on CD19+ lymphocytes resembled that of healthy donors (Fig. 38, B, 2).

Early results obtained with ICOS-Ig fusion protein suggested that unstimulated peripheral blood B cells express variable level of LICOS (0-40%) depending on the donor (Aicher,

* average value

Hayden-Ledbetter et al. 2000). In the present work, the use of a specific anti-LICOS antibody showed that LICOS is constitutively expressed within a range of 31-93% of the CD19+ B cells from healthy donors, but at low surface density. No significant modification in the level of LICOS was recorded after trauma or stroke.

4.2.3 Expression of HLA-DR and LICOS on CD3+ lymphocytes

It was found in mice, that a small subset (15%) of CD3+ splenic cells express LICOS (Ling, Wu et al. 2000). I found in human peripheral blood of healthy controls that only a minority of CD3+ lymphocytes (0.1-3%) was positive for LICOS. Although the exact role of LICOS on T cells is not yet known, it is proposed that it acts in T cell - T cell interactions, which would explain the scarce presence of LICOS on peripheral T cells in humans (Yoshinaga, Whoriskey et al. 1999; Coyle and Gutierrez-Ramos 2001). Both groups of patients investigated in this pilot study showed normal numbers of CD3+ lymphocytes expressing HLA-DR and LICOS (Fig. 35, C, 1, 3, 5, D, 1 and Fig. 38, C, 1, 3, 5, D, 1). This result was in agreement with the work of Wakefield et al.; although they did not compare their results to healthy donors, they did not find any statistically significant differences in the percentage of circulating HLA-DR+ T cells between septic and non-septic patients undergoing major surgery (Wakefield, Carey et al. 1993). Collectively, these results suggested that certain surface markers of T cells, such as LICOS and HLA-DR, seemed to be generally unchanged in the trauma and stroke patients compared to donors.

4.2.4 Expression of ICOS and CD4 on CD3+ lymphocytes

The dysfunction of T cells in sepsis is not yet completely elucidated. Some studies suggest that a reduction in the total number of T cells, with a stable CD4/CD8 ratio, is linked to the immunoaberrations in sepsis (Lin, Astiz et al. 1993). Others reported a change in the CD4/CD8 ratio by a reduction in CD4 lymphocytes (Menges, Engel et al. 1999) or by an increase in number of CD8 lymphocytes (Nishijima, Takezawa et al. 1986). Even though no statement can be made in this regard for the present study, as the CD8 expression was not measured, the percentage of CD4+ T cells was generally within the range of controls in both groups of patients (Fig. 35, E, 1 and Fig. 38, E, 1).

In concordance with the results obtained in the CD3+ population of lymphocytes (Fig. 35, D, 1 and Fig. 38 D, 1), patients' CD4 lymphocytes (T helper cells) expressed HLA-DR within the range of controls (Fig. 35, F, 1 and Fig. 38, F, 1).

ICOS is induced after T cell activation on both CD4+ and CD8+ (Hutloff, Dittrich et al. 1999; Beier, Hutloff et al. 2000; Buonfiglio, Bragardo et al. 2000; Coyle, Lehar et al. 2000; Mages, Hutloff et al. 2000; McAdam, Chang et al. 2000; Tezuka, Tsuji et al. 2000; Wang, Zhu et al. 2000) and it is present on effector and memory T cells (Yoshinaga, Whoriskey et

al. 1999; Coyle, Lehar et al. 2000). In the present study, the ICOS level measured on CD3 lymphocytes or CD4 lymphocytes from healthy donors (64% and 48%, respectively), did not change after stroke or trauma. However, within the ICOS⁺ T cell population two subpopulations could be discriminated: ICOS^{bright}, ICOS^{dim} T cells (Fig. 36). Interestingly, the ICOS^{bright} fraction was markedly increased in all trauma patients (Fig. 37, C) and in most of the stroke patients (Fig. 39, C). This did not hold true for ICOS^{dim} and ICOS⁻ cells, which in both CD3⁺ and CD4⁺ lymphocytes did not differ significantly from that of controls (Fig. 37, A, B and Fig. 39 A, B). These findings are compatible with the results of Krocze et al. obtained in a model of unbiased immune system of non-manipulated mice (Lohning, Hutloff et al. 2003; Krocze, Mages et al. 2004). In this model, characterization at single cell level of ICOS-expressing T cells obtained directly ex-vivo showed that high levels of ICOS on T cells strongly correlated with secretion of IL-10, while intermediate levels of ICOS on the large majority of ICOS⁺ T cells *in vivo* were involved in the release of the Th2 cytokines IL-4, IL-5, IL-13 and these cells showed strong inflammatory effects *in vivo*. In contrast, low levels of ICOS were linked to IL-2, IL-3, IL-6 and IFN- γ secretion. In this model, it is proposed that ICOS cell surface density, depending on LICOS availability, regulates the release of different cytokines: plentiful LICOS expression triggers cytokine secretion from all ICOS⁺ T cells, while scarce LICOS expression induces cytokine production, predominantly IL-10, from high-ICOS-density T cells (Lohning, Hutloff et al. 2003; Krocze, Mages et al. 2004). The authors claim that the tight connection between ICOS and IL-10 seen in the mouse immune system is also valid in the human system (Lohning, Hutloff et al. 2003). There, presumably, stresses like trauma or stroke do not affect the overall ratio of ICOS⁺:ICOS⁻ T cells, but within this ICOS⁺ population, they might modify ICOS density on the cell surface. This results in an increased number of T cells that express high levels of ICOS that could in turn trigger an increased release of IL-10. The release of IL-10 from ICOS^{bright} cells could contribute to the high serum levels of IL-10 seen in these patients. The contribution of IL-10 to the aberrant immune response in trauma and septic patients is well documented (reviewed in (Oberholzer, Oberholzer et al. 2002). In patients with severe trauma, increased IL-10 produced by stimulated CD4⁺ T cells has correlated with subsequent septic events (Lyons, Kelly et al. 1997; Murphy, Paterson et al. 2003). The anti-inflammatory cytokine IL-10 was involved in HLA-DR downregulation on monocytes and persistent high levels of IL-10 negatively correlated with HLA-DR expression during hospitalization of septic trauma patients (Cheadle, Hershman et al. 1991; de Waal Malefyt, Abrams et al. 1991; Klava, Windsor et al. 1997; Giannoudis, Smith et al. 2000). Therefore, simultaneous intracellular cytokine staining for IL-10 and quantification of the surface density of ICOS on T cells from trauma patients could directly show whether there is a connection between the increase of ICOS density on the cell surface and the secretion of this cytokine.

In addition, a number of articles suggest that ICOS is critically involved in induction of T_{reg} and controlling IL-10-producing T_{reg} functions in tolerance and autoimmune disease (Akbari, Freeman et al. 2002; Herman, Freeman et al. 2004; Kohyama, Sugahara et al. 2004). T cell

activation by allogeneic costimulation-deficient APCs resulted in the expression of ICOS on a subpopulation of T cells which after restimulation, remained anergic, but they produced IL-10. This IL-10 suppressed the response of ICOS⁺ cells and the activation of naïve or primed T cells in response to allogeneic triggering (Vermeiren, Ceuppens et al. 2004). Moreover, the study of a T_{reg} role in the immunological events that characterize trauma and sepsis syndromes is just beginning (Murphy, Choileain et al. 2005). It might not take very long until the relationship between IL-10, ICOS and T_{reg} in the context of trauma-induced T cells dysfunction will be deciphered.

5. Conclusions

This pilot study provides leads for further study, but because of the low number of patients it does not allow definitive statements.

CD86 was strictly co-regulated with HLA-DR on monocytes. Therefore, assessment of CD86 expression will not provide additional information compared to the measurement of HLA-DR alone, which is already well established as a diagnostic parameter. LICOS expression on monocytes was low and regulated in a similar way to HLA-DR and CD86, but differences between patients and controls were much smaller and did not correlate with the severity of the injury. While downregulation of HLA-DR, CD86 and, to a lesser extent, LICOS expression on monocytes reflects the immuno-incompetence of monocytes after a major insult to the organism, the lower levels of HLA-DR and CD86 in trauma patients compared to stroke patients suggest that polytrauma is a stronger inducer of monocyte dysfunction than stroke. An alternative explanation would be that most of the stroke patients were mild cases.

B cells appeared not to be affected by immunosuppression, as they did not reduce their antigen-presenting capacities and costimulatory molecules.

The levels of HLA-DR and LICOS on T cells in trauma and stroke patients were not changed compared to those of healthy donors.

In CD4⁺ T cells, the proportion of cells expressing high level of ICOS was markedly increased in all trauma patients and in most of the stroke patients. As ICOS expression is tightly connected to IL-10 secretion, this suggests that in such patients the IL-10 production by T cells may be increased, contributing to their immunosuppression. Therefore, simultaneous intracellular cytokine staining for IL-10 and quantification of the surface density of ICOS on T cells could directly show whether there is a connection between the increase of ICOS density on the cell surface and the secretion of this cytokine. Moreover, the enumeration of ICOS^{bright} T cells in a larger cohort of patients would be needed to establish whether this molecule could serve as an independent prognostic marker or as an indicator of immunosuppression. Furthermore, the correlation of ICOS^{bright} T cells with septic complications after trauma and stroke might disclose a role for ICOS in the immunological events that facilitate generalized bacterial infections. Since it has been shown that inducible regulatory T cells (T_{reg}, e.g. T_R1), which are characterized by abundant IL-10 secretion, can develop from the naïve T cells in the periphery, it would be of interest to test whether this ICOS^{bright} population has regulatory properties.

6. Summary

General bacterial infections, which can lead to the clinical picture of sepsis, are a major concern in intensive care units (ICU) and mortality remains high.

Recent data have shown that, besides an overreaction of the immune system, also immunosuppression also plays a role in the pathogenesis of sepsis. Immunosuppression has been documented in patients with polytrauma, stroke and burn wounds, which all confer a high risk of severe bacterial infection. Moreover, it has been shown that T cells have an important role in sepsis. A shift of a Th1 dominated T cell response towards a Th2 response has been described as a potential mechanism of immune suppression in patients with sepsis. One of the molecules on the surface of T cells that is involved in the Th2-mediated immune response is the Inducible Costimulator of T cells (ICOS). Its ligand, LICOS, is expressed on the surface of B cells and monocytes. ICOS ligation induces the production of anti-inflammatory cytokines, especially of IL-10. However, nothing is known about the expression of ICOS on T cells and that of LICOS on APCs in patients with severe trauma and stroke.

Therefore, in the present study, in a first step, a recombinant human LICOS-Ig fusion protein was generated, which was then used as an antigen for the generation of anti-LICOS monoclonal antibodies. In three fusion experiments, 5 000 primay clones were screened and a single hybridoma was obtained, which produced monoclonal antibodies that specifically reacted with recombinant LICOS, both in form of the LICOS-Ig fusion protein and on the surface of a cell line transfected with a full-length LICOS transgene. Since, it turned out that the antibodies did not bind with high affinity to wild type LICOS, as it is expressed on primary human blood cells, phenotypic analyses were carried out with another anti-LICOS monoclonal antibody, which had become commercially available.

Next, the expression of HLA-DR, CD86, LICOS, and ICOS, on the surface of monocytes (CD14+), B cells (CD19+) and T cells (CD3+, CD4+) in whole blood was measured by flow cytometry. Six patients with severe trauma and nine stroke patients were compared with 32 healthy donors.

On CD14+ monocytes from healthy donors, the expression levels of HLA-DR and CD86 were over 90%, while the expression of LICOS was much lower (7,5%). In critically ill patients, HLA-DR, CD86 and LICOS expression were strongly reduced. CD86 and HLA-DR were co-regulated, while HLA-DR and LICOS were not.

In healthy donors, virtually all B cells expressed HLA-DR and the majority of them co-expressed LICOS (72%), while only a small fraction were CD86+ (14%). After trauma and stroke, HLA-DR, as well as LICOS expression on these cells remained normal; CD86 had a tendency towards being downregulated in most of the trauma patients, while most of the stroke patients exhibited normal CD86+ levels.

The levels of HLA-DR and LICOS on T cells in trauma and stroke patients were low and very similar to those of healthy donors.

The fraction of CD3+ T lymphocytes or their CD4+ subpopulation, which expressed measurable levels of ICOS (64% and 48%, respectively), did not change after stroke or trauma. However, within the ICOS+ T cell population two subpopulations could be distinguished: ICOS^{bright} and ICOS^{dim} T cells. Interestingly, the ICOS^{bright} subpopulation, but not the ICOS^{dim} and ICOS^{negative} subpopulations, was markedly increased in all trauma patients and in most of the stroke patients.

Given that CD86 was co-regulated with HLA-DR on monocytes it appears that, similar to HLA-DR, CD86 expression could discriminate between patients with a low and high risk of sepsis. In contrast, because of its low basal expression on monocytes and its low signal-noise ratio, LICOS expression levels are not informative.

Since ICOS expression on T cells is tightly connected to IL-10 secretion, the high proportion of ICOS^{bright} cells in critically ill patients might contribute to the high IL-10 serum concentrations, which have been reported to be linked to immunosuppression in these patients.

7. Bibliography

- Abraham, E. (1999). "Why immunomodulatory therapies have not worked in sepsis." *Intensive Care Med* **25**(6): 556-66.
- Aicher, A., M. Hayden-Ledbetter, et al. (2000). "Characterization of human inducible costimulator ligand expression and function." *J Immunol* **164**(9): 4689-96.
- Akbari, O., G. J. Freeman, et al. (2002). "Antigen-specific regulatory T cells develop via the ICOS-ICOS-ligand pathway and inhibit allergen-induced airway hyperreactivity." *Nat Med* **8**(9): 1024-32.
- Angele, M. K. and E. Faist (2002). "Clinical review: immunodepression in the surgical patient and increased susceptibility to infection." *Crit Care* **6**(4): 298-305.
- Angus, D. C., W. T. Linde-Zwirble, et al. (2001). "Epidemiology of severe sepsis in the United States: analysis of incidence, outcome, and associated costs of care." *Crit Care Med* **29**(7): 1303-10.
- Arimura, Y., H. Kato, et al. (2002). "A co-stimulatory molecule on activated T cells, H4/ICOS, delivers specific signals in T(h) cells and regulates their responses." *Int Immunol* **14**(6): 555-66.
- Aslanyan, S., C. J. Weir, et al. (2004). "Pneumonia and urinary tract infection after acute ischaemic stroke: a tertiary analysis of the GAIN International trial." *Eur J Neurol* **11**(1): 49-53.
- Bach, J. F. (2003). "Regulatory T cells under scrutiny." *Nat Rev Immunol* **3**(3): 189-98.
- Beier, K. C., A. Hutloff, et al. (2000). "Induction, binding specificity and function of human ICOS." *Eur J Immunol* **30**(12): 3707-17.
- Beier, K. C., A. Hutloff, et al. (2004). "Inducible costimulator-positive T cells are required for allergen-induced local B-cell infiltration and antigen-specific IgE production in lung tissue." *J Allergy Clin Immunol* **114**(4): 775-82.
- Belkaid, Y. and B. T. Rouse (2005). "Natural regulatory T cells in infectious disease." *Nat Immunol* **6**(4): 353-60.
- Bertram, E. M., A. Tafuri, et al. (2002). "Role of ICOS versus CD28 in antiviral immunity." *Eur J Immunol* **32**(12): 3376-85.
- Birnboim, H. C. and J. Doly (1979). "A rapid alkaline extraction procedure for screening recombinant plasmid DNA." *Nucleic Acids Res* **7**(6): 1513-23.
- Bluestone, J. A. (2005). "Regulatory T-cell therapy: is it ready for the clinic?" *Nat Rev Immunol* **5**(4): 343-9.
- Bone, R. C. (1991). "The pathogenesis of sepsis." *Ann Intern Med* **115**(6): 457-69.
- Bone, R. C. (1996). "Sir Isaac Newton, sepsis, SIRS, and CARS." *Crit Care Med* **24**(7): 1125-8.
- Bone, R. C., R. A. Balk, et al. (1992). "Definitions for sepsis and organ failure and guidelines for the use of innovative therapies in sepsis. The ACCP/SCCM Consensus Conference Committee. American College of Chest Physicians/Society of Critical Care Medicine." *Chest* **101**(6): 1644-55.
- Bone, R. C., C. J. Fisher, Jr., et al. (1989). "Sepsis syndrome: a valid clinical entity. Methylprednisolone Severe Sepsis Study Group." *Crit Care Med* **17**(5): 389-93.
- Bonhagen, K., O. Liesenfeld, et al. (2003). "ICOS+ Th cells produce distinct cytokines in different mucosal immune responses." *Eur J Immunol* **33**(2): 392-401.
- Bown, M. J., T. Horsburgh, et al. (2004). "Cytokines, their genetic polymorphisms, and outcome after abdominal aortic aneurysm repair." *Eur J Vasc Endovasc Surg* **28**(3): 274-80.
- Brenner, M. B., J. McLean, et al. (1986). "Identification of a putative second T-cell receptor." *Nature* **322**(6075): 145-9.
- Brodie, D., A. V. Collins, et al. (2000). "LICOS, a primordial costimulatory ligand?" *Curr Biol* **10**(6): 333-6.
- Brun-Buisson, C. (2000). "The epidemiology of the systemic inflammatory response." *Intensive Care Med* **26 Suppl 1**: S64-74.
- Brunner, M., C. Krenn, et al. (2004). "Increased levels of soluble ST2 protein and IgG1 production in patients with sepsis and trauma." *Intensive Care Med* **30**(7): 1468-73.
- Buonfiglio, D., M. Bragardo, et al. (2000). "The T cell activation molecule H4 and the CD28-like molecule ICOS are identical." *Eur J Immunol* **30**(12): 3463-7.
- Carreno, B. M. and M. Collins (2002). "The B7 family of ligands and its receptors: new pathways for costimulation and inhibition of immune responses." *Annu Rev Immunol* **20**: 29-53.

- Castan, J., K. Tenner-Racz, et al. (1997). "Accumulation of CTLA-4 expressing T lymphocytes in the germinal centres of human lymphoid tissues." *Immunology* **90**(2): 265-71.
- Cheadle, W. G., M. J. Hershman, et al. (1991). "HLA-DR antigen expression on peripheral blood monocytes correlates with surgical infection." *Am J Surg* **161**(6): 639-45.
- Chernoff, A. E., E. V. Granowitz, et al. (1995). "A randomized, controlled trial of IL-10 in humans. Inhibition of inflammatory cytokine production and immune responses." *J Immunol* **154**(10): 5492-9.
- Cochran, J. R., T. O. Cameron, et al. (2000). "The relationship of MHC-peptide binding and T cell activation probed using chemically defined MHC class II oligomers." *Immunity* **12**(3): 241-50.
- Collins, A. V., D. W. Brodie, et al. (2002). "The interaction properties of costimulatory molecules revisited." *Immunity* **17**(2): 201-10.
- Coyle, A. J. and J. C. Gutierrez-Ramos (2001). "The expanding B7 superfamily: increasing complexity in costimulatory signals regulating T cell function." *Nat Immunol* **2**(3): 203-9.
- Coyle, A. J. and J. C. Gutierrez-Ramos (2004). "The role of ICOS and other costimulatory molecules in allergy and asthma." *Springer Semin Immunopathol* **25**(3-4): 349-59.
- Coyle, A. J., S. Lehar, et al. (2000). "The CD28-related molecule ICOS is required for effective T cell-dependent immune responses." *Immunity* **13**(1): 95-105.
- Dariavach, P., M. G. Mattei, et al. (1988). "Human Ig superfamily CTLA-4 gene: chromosomal localization and identity of protein sequence between murine and human CTLA-4 cytoplasmic domains." *Eur J Immunol* **18**(12): 1901-5.
- Davenport, R. J., M. S. Dennis, et al. (1996). "Complications after acute stroke." *Stroke* **27**(3): 415-20.
- Dawson, C. W., A. M. Ledgerwood, et al. (1982). "Anergy and altered lymphocyte function in the injured patient." *Am Surg* **48**(8): 397-401.
- De, A. K., K. M. Kodys, et al. (2000). "Induction of global anergy rather than inhibitory Th2 lymphokines mediates posttrauma T cell immunodepression." *Clin Immunol* **96**(1): 52-66.
- De Maio, A., M. B. Torres, et al. (2005). "Genetic determinants influencing the response to injury, inflammation, and sepsis." *Shock* **23**(1): 11-7.
- de Waal Malefyt, R., J. Abrams, et al. (1991). "Interleukin 10(IL-10) inhibits cytokine synthesis by human monocytes: an autoregulatory role of IL-10 produced by monocytes." *J Exp Med* **174**(5): 1209-20.
- DeFranco, A. L. (1997). "The complexity of signaling pathways activated by the BCR." *Curr Opin Immunol* **9**(3): 296-308.
- Deitch, E. A. (1998). "Animal models of sepsis and shock: a review and lessons learned." *Shock* **9**(1): 1-11.
- Ditschkowski, M., E. Kreuzfelder, et al. (1999). "Reduced B cell HLA-DR expression and natural killer cell counts in patients prone to sepsis after injury." *Eur J Surg* **165**(12): 1129-33.
- Dong, C., A. E. Juedes, et al. (2001). "ICOS co-stimulatory receptor is essential for T-cell activation and function." *Nature* **409**(6816): 97-101.
- Dong, C., U. A. Temann, et al. (2001). "Cutting edge: critical role of inducible costimulator in germinal center reactions." *J Immunol* **166**(6): 3659-62.
- Fink, M. P. and S. O. Heard (1990). "Laboratory models of sepsis and septic shock." *J Surg Res* **49**(2): 186-96.
- Fontenot, J. D. and A. Y. Rudensky (2005). "A well adapted regulatory contrivance: regulatory T cell development and the forkhead family transcription factor Foxp3." *Nat Immunol* **6**(4): 331-7.
- Frizzell, J. P. (2005). "Acute stroke: pathophysiology, diagnosis, and treatment." *AACN Clin Issues* **16**(4): 421-40; quiz 597-8.
- Fumeaux, T. and J. Pugin (2002). "Role of interleukin-10 in the intracellular sequestration of human leukocyte antigen-DR in monocytes during septic shock." *Am J Respir Crit Care Med* **166**(11): 1475-82.
- Furukawa, Y., D. A. Mandelbrot, et al. (2000). "Association of B7-1 co-stimulation with the development of graft arterial disease. Studies using mice lacking B7-1, B7-2, or B7-1/B7-2." *Am J Pathol* **157**(2): 473-84.
- Gennari, R., J. W. Alexander, et al. (1994). "Effects of antimurine interleukin-6 on bacterial translocation during gut-derived sepsis." *Arch Surg* **129**(11): 1191-7.
- Giannoudis, P. V., R. M. Smith, et al. (2000). "Immediate IL-10 expression following major orthopaedic trauma: relationship to anti-inflammatory response and subsequent development of sepsis." *Intensive Care Med* **26**(8): 1076-81.

- Giannoudis, P. V., R. M. Smith, et al. (1999). "Monocyte human leukocyte antigen-DR expression correlates with intrapulmonary shunting after major trauma." *Am J Surg* **177**(6): 454-9.
- Goebel, A., E. Kavanagh, et al. (2000). "Injury induces deficient interleukin-12 production, but interleukin-12 therapy after injury restores resistance to infection." *Ann Surg* **231**(2): 253-61.
- Gonzalo, J. A., T. Delaney, et al. (2001). "Cutting edge: the related molecules CD28 and inducible costimulator deliver both unique and complementary signals required for optimal T cell activation." *J Immunol* **166**(1): 1-5.
- Gonzalo, J. A., J. Tian, et al. (2001). "ICOS is critical for T helper cell-mediated lung mucosal inflammatory responses." *Nat Immunol* **2**(7): 597-604.
- Greenwald, R. J., G. J. Freeman, et al. (2005). "The B7 family revisited." *Annu Rev Immunol* **23**: 515-48.
- Greenwald, R. J., A. J. McAdam, et al. (2002). "Cutting edge: inducible costimulator protein regulates both Th1 and Th2 responses to cutaneous leishmaniasis." *J Immunol* **168**(3): 991-5.
- Grimbacher, B., A. Hutloff, et al. (2003). "Homozygous loss of ICOS is associated with adult-onset common variable immunodeficiency." *Nat Immunol* **4**(3): 261-8.
- Guo, J., M. Stolina, et al. (2001). "Stimulatory effects of B7-related protein-1 on cellular and humoral immune responses in mice." *J Immunol* **166**(9): 5578-84.
- Hanchaiphiboolkul, S. (2005). "Risk factors for early infection after an acute cerebral infarction." *J Med Assoc Thai* **88**(2): 150-5.
- Harada, H., A. D. Salama, et al. (2003). "The role of the ICOS-B7h T cell costimulatory pathway in transplantation immunity." *J Clin Invest* **112**(2): 234-43.
- Harada, Y., D. Ohgai, et al. (2003). "A single amino acid alteration in cytoplasmic domain determines IL-2 promoter activation by ligation of CD28 but not inducible costimulator (ICOS)." *J Exp Med* **197**(2): 257-62.
- Harper, K., C. Balzano, et al. (1991). "CTLA-4 and CD28 activated lymphocyte molecules are closely related in both mouse and human as to sequence, message expression, gene structure, and chromosomal location." *J Immunol* **147**(3): 1037-44.
- Haveman, J. W., A. C. Muller Kobold, et al. (1999). "The central role of monocytes in the pathogenesis of sepsis: consequences for immunomonitoring and treatment." *Neth J Med* **55**(3): 132-41.
- Hawrylowicz, C. M. and A. O'Garra (2005). "Potential role of interleukin-10-secreting regulatory T cells in allergy and asthma." *Nat Rev Immunol* **5**(4): 271-83.
- Heidecke, C. D., T. Hensler, et al. (1999). "Selective defects of T lymphocyte function in patients with lethal intraabdominal infection." *Am J Surg* **178**(4): 288-92.
- Heidecke, C. D., H. Weighardt, et al. (2000). "[Immune paralysis of T-lymphocytes and monocytes in postoperative abdominal sepsis. Correlation of immune function with survival]." *Chirurg* **71**(2): 159-65.
- Hensler, T., H. Hecker, et al. (1997). "Distinct mechanisms of immunosuppression as a consequence of major surgery." *Infect Immun* **65**(6): 2283-91.
- Herman, A. E., G. J. Freeman, et al. (2004). "CD4+CD25+ T regulatory cells dependent on ICOS promote regulation of effector cells in the prediabetic lesion." *J Exp Med* **199**(11): 1479-89.
- Hershman, M. J., W. G. Cheadle, et al. (1990). "Monocyte HLA-DR antigen expression characterizes clinical outcome in the trauma patient." *Br J Surg* **77**(2): 204-7.
- Heumann, D., M. P. Glauser, et al. (1998). "Molecular basis of host-pathogen interaction in septic shock." *Curr Opin Microbiol* **1**(1): 49-55.
- Hilker, R., C. Poetter, et al. (2003). "Nosocomial pneumonia after acute stroke: implications for neurological intensive care medicine." *Stroke* **34**(4): 975-81.
- Hoflich, C. and H. D. Volk (2002). "[Immunomodulation in sepsis]." *Chirurg* **73**(11): 1100-4.
- Hotchkiss, R. S., K. C. Chang, et al. (2003). "Adoptive transfer of apoptotic splenocytes worsens survival, whereas adoptive transfer of necrotic splenocytes improves survival in sepsis." *Proc Natl Acad Sci U S A* **100**(11): 6724-9.
- Hotchkiss, R. S. and I. E. Karl (2003). "The pathophysiology and treatment of sepsis." *N Engl J Med* **348**(2): 138-50.
- Hotchkiss, R. S., K. W. Tinsley, et al. (2001). "Sepsis-induced apoptosis causes progressive profound depletion of B and CD4+ T lymphocytes in humans." *J Immunol* **166**(11): 6952-63.
- Howard, R. J. and R. L. Simmons (1974). "Acquired immunologic deficiencies after trauma and surgical procedures." *Surg Gynecol Obstet* **139**(5): 771-82.

- Hubbard, V. M., J. M. Eng, et al. (2005). "Absence of inducible costimulator on alloreactive T cells reduces graft-versus-host disease and induces Th2 deviation." Blood.
- Hung, J. W., T. H. Tsay, et al. (2005). "Incidence and risk factors of medical complications during inpatient stroke rehabilitation." Chang Gung Med J **28**(1): 31-8.
- Hutloff, A., K. Buchner, et al. (2004). "Involvement of inducible costimulator in the exaggerated memory B cell and plasma cell generation in systemic lupus erythematosus." Arthritis Rheum **50**(10): 3211-20.
- Hutloff, A., A. M. Dittrich, et al. (1999). "ICOS is an inducible T-cell co-stimulator structurally and functionally related to CD28." Nature **397**(6716): 263-6.
- Iwai, H., Y. Kozono, et al. (2002). "Amelioration of collagen-induced arthritis by blockade of inducible costimulator-B7 homologous protein costimulation." J Immunol **169**(8): 4332-9.
- Janeway Jr, C. A. (2002). Immunobiology **5**, Garland.
- Jiang, G. and T. Hunter (1999). "Receptor signaling: when dimerization is not enough." Curr Biol **9**(15): R568-71.
- Johnston, K. C., J. Y. Li, et al. (1998). "Medical and neurological complications of ischemic stroke: experience from the RANTTAS trial. RANTTAS Investigators." Stroke **29**(2): 447-53.
- Kalra, L., G. Yu, et al. (1995). "Medical complications during stroke rehabilitation." Stroke **26**(6): 990-4.
- Katzan, I. L., R. D. Cebul, et al. (2003). "The effect of pneumonia on mortality among patients hospitalized for acute stroke." Neurology **60**(4): 620-5.
- Kearney, J. F., A. Radbruch, et al. (1979). "A new mouse myeloma cell line that has lost immunoglobulin expression but permits the construction of antibody-secreting hybrid cell lines." J Immunol **123**(4): 1548-50.
- Kelly, J. L., A. Lyons, et al. (1997). "Anti-interleukin-10 antibody restores burn-induced defects in T-cell function." Surgery **122**(2): 146-52.
- Kelly, J. L., C. B. O'Suilleabhain, et al. (1999). "Severe injury triggers antigen-specific T-helper cell dysfunction." Shock **12**(1): 39-45.
- Kelly, J. L., C. O'Sullivan, et al. (1997). "Is circulating endotoxin the trigger for the systemic inflammatory response syndrome seen after injury?" Ann Surg **225**(5): 530-41; discussion 541-3.
- Khayyamian, S., A. Hutloff, et al. (2002). "ICOS-ligand, expressed on human endothelial cells, costimulates Th1 and Th2 cytokine secretion by memory CD4+ T cells." Proc Natl Acad Sci U S A **99**(9): 6198-203.
- Klava, A., A. C. Windsor, et al. (1997). "Interleukin-10. A role in the development of postoperative immunosuppression." Arch Surg **132**(4): 425-9.
- Klingenberg, R., F. Autschbach, et al. (2005). "Endothelial inducible costimulator ligand expression is increased during human cardiac allograft rejection and regulates endothelial cell-dependent allo-activation of CD8+ T cells in vitro." Eur J Immunol **35**(6): 1712-21.
- Kobayashi, H., M. Kobayashi, et al. (1999). "Therapeutic protective effects of IL-12 combined with soluble IL-4 receptor against established infections of herpes simplex virus type 1 in thermally injured mice." J Immunol **162**(12): 7148-54.
- Kohyama, M., D. Sugahara, et al. (2004). "Inducible costimulator-dependent IL-10 production by regulatory T cells specific for self-antigen." Proc Natl Acad Sci U S A **101**(12): 4192-7.
- Kopf, M., A. J. Coyle, et al. (2000). "Inducible costimulator protein (ICOS) controls T helper cell subset polarization after virus and parasite infection." J Exp Med **192**(1): 53-61.
- Kox, W. J., T. Volk, et al. (2000). "Immunomodulatory therapies in sepsis." Intensive Care Med **26 Suppl 1**: S124-8.
- Kroczyk, R. A., H. W. Mages, et al. (2004). "Emerging paradigms of T-cell co-stimulation." Curr Opin Immunol **16**(3): 321-7.
- Kromenaker, S. J. and F. Srienc (1994). "Stability of producer hybridoma cell lines after cell sorting: a case study." Biotechnol Prog **10**(3): 299-307.
- Lafage-Pochitaloff, M., R. Costello, et al. (1990). "Human CD28 and CTLA-4 Ig superfamily genes are located on chromosome 2 at bands q33-q34." Immunogenetics **31**(3): 198-201.
- Le Tulzo, Y., C. Pangault, et al. (2002). "Early circulating lymphocyte apoptosis in human septic shock is associated with poor outcome." Shock **18**(6): 487-94.
- Lederer, J. A., M. L. Rodrick, et al. (1999). "The effects of injury on the adaptive immune response." Shock **11**(3): 153-9.

- Lenschow, D. J., T. L. Walunas, et al. (1996). "CD28/B7 system of T cell costimulation." Annu Rev Immunol **14**: 233-58.
- Levine, B. L., W. B. Bernstein, et al. (1997). "Effects of CD28 costimulation on long-term proliferation of CD4+ T cells in the absence of exogenous feeder cells." J Immunol **159**(12): 5921-30.
- Liang, L., E. M. Porter, et al. (2002). "Constitutive expression of the B7h ligand for inducible costimulator on naive B cells is extinguished after activation by distinct B cell receptor and interleukin 4 receptor-mediated pathways and can be rescued by CD40 signaling." J Exp Med **196**(1): 97-108.
- Liew, F. Y. (2002). "T(H)1 and T(H)2 cells: a historical perspective." Nat Rev Immunol **2**(1): 55-60.
- Lin, R. Y., M. E. Astiz, et al. (1993). "Altered leukocyte immunophenotypes in septic shock. Studies of HLA-DR, CD11b, CD14, and IL-2R expression." Chest **104**(3): 847-53.
- Ling, V., P. W. Wu, et al. (2000). "Cutting edge: identification of GL50, a novel B7-like protein that functionally binds to ICOS receptor." J Immunol **164**(4): 1653-7.
- Ling, V., P. W. Wu, et al. (2001). "Differential expression of inducible costimulator-ligand splice variants: lymphoid regulation of mouse GL50-B and human GL50 molecules." J Immunol **166**(12): 7300-8.
- Liu, X., X. F. Bai, et al. (2001). "B7H costimulates clonal expansion of, and cognate destruction of tumor cells by, CD8(+) T lymphocytes in vivo." J Exp Med **194**(9): 1339-48.
- Livingston, D. H., S. H. Appel, et al. (1988). "Depressed interferon gamma production and monocyte HLA-DR expression after severe injury." Arch Surg **123**(11): 1309-12.
- Lohning, M., A. Hutloff, et al. (2003). "Expression of ICOS in vivo defines CD4+ effector T cells with high inflammatory potential and a strong bias for secretion of interleukin 10." J Exp Med **197**(2): 181-93.
- Loke, P., X. Zang, et al. (2005). "Inducible costimulator is required for type 2 antibody isotype switching but not T helper cell type 2 responses in chronic nematode infection." Proc Natl Acad Sci U S A **102**(28): 9872-7.
- Lyons, A., A. Goebel, et al. (1999). "Protective effects of early interleukin 10 antagonism on injury-induced immune dysfunction." Arch Surg **134**(12): 1317-23; discussion 1324.
- Lyons, A., J. L. Kelly, et al. (1997). "Major injury induces increased production of interleukin-10 by cells of the immune system with a negative impact on resistance to infection." Ann Surg **226**(4): 450-8; discussion 458-60.
- MacLean, L. D., J. L. Meakins, et al. (1975). "Host resistance in sepsis and trauma." Ann Surg **182**(3): 207-17.
- Mages, H. W., A. Hutloff, et al. (2000). "Molecular cloning and characterization of murine ICOS and identification of B7h as ICOS ligand." Eur J Immunol **30**(4): 1040-7.
- Maghsudi, M. and M. Nerlich (1998). "[Polytrauma]." Internist (Berl) **39**(2): 188-94.
- Mak, T. W., A. Shahinian, et al. (2003). "Costimulation through the inducible costimulator ligand is essential for both T helper and B cell functions in T cell-dependent B cell responses." Nat Immunol **4**(8): 765-72.
- Maloy, K. J. and F. Powrie (2001). "Regulatory T cells in the control of immune pathology." Nat Immunol **2**(9): 816-22.
- Manjuck, J., D. C. Saha, et al. (2000). "Decreased response to recall antigens is associated with depressed costimulatory receptor expression in septic critically ill patients." J Lab Clin Med **135**(2): 153-60.
- McAdam, A. J., T. T. Chang, et al. (2000). "Mouse inducible costimulatory molecule (ICOS) expression is enhanced by CD28 costimulation and regulates differentiation of CD4+ T cells." J Immunol **165**(9): 5035-40.
- McAdam, A. J., R. J. Greenwald, et al. (2001). "ICOS is critical for CD40-mediated antibody class switching." Nature **409**(6816): 102-5.
- McAdam, A. J., A. N. Schweitzer, et al. (1998). "The role of B7 co-stimulation in activation and differentiation of CD4+ and CD8+ T cells." Immunol Rev **165**: 231-47.
- McHugh, R. S., M. J. Whitters, et al. (2002). "CD4(+)CD25(+) immunoregulatory T cells: gene expression analysis reveals a functional role for the glucocorticoid-induced TNF receptor." Immunity **16**(2): 311-23.
- Menger, M. D. and B. Vollmar (2004). "Surgical trauma: hyperinflammation versus immunosuppression?" Langenbecks Arch Surg **389**(6): 475-84.
- Menges, T., J. Engel, et al. (1999). "Changes in blood lymphocyte populations after multiple trauma: association with posttraumatic complications." Crit Care Med **27**(4): 733-40.

- Mills, K. H. (2004). "Regulatory T cells: friend or foe in immunity to infection?" Nat Rev Immunol **4**(11): 841-55.
- Mittrucker, H. W., M. Kursar, et al. (2002). "Inducible costimulator protein controls the protective T cell response against *Listeria monocytogenes*." J Immunol **169**(10): 5813-7.
- Molloy, R. G., M. O'Riordain, et al. (1993). "Mechanism of increased tumor necrosis factor production after thermal injury. Altered sensitivity to PGE2 and immunomodulation with indomethacin." J Immunol **151**(4): 2142-9.
- Muckart, D. J. and S. Bhagwanjee (1997). "American College of Chest Physicians/Society of Critical Care Medicine Consensus Conference definitions of the systemic inflammatory response syndrome and allied disorders in relation to critically injured patients." Crit Care Med **25**(11): 1789-95.
- Mueller, A., E. Kreuzfelder, et al. (2003). "Human leukocyte antigen-DR expression in peripheral blood mononuclear cells from healthy donors influenced by the sera of injured patients prone to severe sepsis." Intensive Care Med **29**(12): 2285-90.
- Munford, R. S. and J. Pugin (2001). "Normal responses to injury prevent systemic inflammation and can be immunosuppressive." Am J Respir Crit Care Med **163**(2): 316-21.
- Murphey, E. D., C. Y. Lin, et al. (2004). "Diminished bacterial clearance is associated with decreased IL-12 and interferon-gamma production but a sustained proinflammatory response in a murine model of postseptic immunosuppression." Shock **21**(5): 415-25.
- Murphy, T., H. Paterson, et al. (2003). "Use of intracellular cytokine staining and bacterial superantigen to document suppression of the adaptive immune system in injured patients." Ann Surg **238**(3): 401-10; discussion 410-1.
- Murphy, T. J., N. N. Choileain, et al. (2005). "CD4+CD25+ regulatory T cells control innate immune reactivity after injury." J Immunol **174**(5): 2957-63.
- Natanson, C., W. D. Hoffman, et al. (1994). "Selected treatment strategies for septic shock based on proposed mechanisms of pathogenesis." Ann Intern Med **120**(9): 771-83.
- Newton, S., Y. Ding, et al. (2004). "Sepsis-induced changes in macrophage co-stimulatory molecule expression: CD86 as a regulator of anti-inflammatory IL-10 response." Surg Infect (Larchmt) **5**(4): 375-83.
- Nishijima, M. K., J. Takezawa, et al. (1986). "Serial changes in cellular immunity of septic patients with multiple organ-system failure." Crit Care Med **14**(2): 87-91.
- Noel, P. J., L. H. Boise, et al. (1996). "CD28 costimulation prevents cell death during primary T cell activation." J Immunol **157**(2): 636-42.
- Nurieva, R. I., J. Duong, et al. (2003). "Transcriptional regulation of th2 differentiation by inducible costimulator." Immunity **18**(6): 801-11.
- Nurieva, R. I., X. M. Mai, et al. (2003). "B7h is required for T cell activation, differentiation, and effector function." Proc Natl Acad Sci U S A **100**(24): 14163-8.
- O'Sullivan, S. T., J. A. Lederer, et al. (1995). "Major injury leads to predominance of the T helper-2 lymphocyte phenotype and diminished interleukin-12 production associated with decreased resistance to infection." Ann Surg **222**(4): 482-90; discussion 490-2.
- Oberholzer, A., C. Oberholzer, et al. (2001). "Sepsis syndromes: understanding the role of innate and acquired immunity." Shock **16**(2): 83-96.
- Oberholzer, A., C. Oberholzer, et al. (2002). "Interleukin-10: A complex role in the pathogenesis of sepsis syndromes and its potential as an anti-inflammatory drug." Crit Care Med **30**(1 Supp): S58-S63.
- Oczenski, W., H. Krenn, et al. (2003). "HLA-DR as a marker for increased risk for systemic inflammation and septic complications after cardiac surgery." Intensive Care Med **29**(8): 1253-7.
- Ogasawara, K., S. K. Yoshinaga, et al. (2002). "Inducible costimulator costimulates cytotoxic activity and IFN-gamma production in activated murine NK cells." J Immunol **169**(7): 3676-85.
- Osborn, T. M., J. K. Tracy, et al. (2004). "Epidemiology of sepsis in patients with traumatic injury." Crit Care Med **32**(11): 2234-40.
- Ozkaynak, E., W. Gao, et al. (2001). "Importance of ICOS-B7RP-1 costimulation in acute and chronic allograft rejection." Nat Immunol **2**(7): 591-6.
- Paterson, H. M., T. J. Murphy, et al. (2003). "Injury primes the innate immune system for enhanced Toll-like receptor reactivity." J Immunol **171**(3): 1473-83.
- Paust, S., L. Lu, et al. (2004). "Engagement of B7 on effector T cells by regulatory T cells prevents autoimmune disease." Proc Natl Acad Sci U S A **101**(28): 10398-403.

- Pellegrini, J. D., A. K. De, et al. (2000). "Relationships between T lymphocyte apoptosis and anergy following trauma." *J Surg Res* **88**(2): 200-6.
- Pentcheva-Hoang, T., J. G. Egen, et al. (2004). "B7-1 and B7-2 selectively recruit CTLA-4 and CD28 to the immunological synapse." *Immunity* **21**(3): 401-13.
- Perry, S. E., S. M. Mostafa, et al. (2003). "Is low monocyte HLA-DR expression helpful to predict outcome in severe sepsis?" *Intensive Care Med* **29**(8): 1245-52.
- Podojil, J. R., N. W. Kin, et al. (2004). "CD86 and beta2-adrenergic receptor signaling pathways, respectively, increase Oct-2 and OCA-B Expression and binding to the 3'-IgH enhancer in B cells." *J Biol Chem* **279**(22): 23394-404.
- Podojil, J. R. and V. M. Sanders (2003). "Selective regulation of mature IgG1 transcription by CD86 and beta 2-adrenergic receptor stimulation." *J Immunol* **170**(10): 5143-51.
- Prass, K., C. Meisel, et al. (2003). "Stroke-induced immunodeficiency promotes spontaneous bacterial infections and is mediated by sympathetic activation reversal by poststroke T helper cell type 1-like immunostimulation." *J Exp Med* **198**(5): 725-36.
- Radhakrishnan, S., L. T. Nguyen, et al. (2003). "Naturally occurring human IgM antibody that binds B7-DC and potentiates T cell stimulation by dendritic cells." *J Immunol* **170**(4): 1830-8.
- Reth, M. (1992). "Antigen receptors on B lymphocytes." *Annu Rev Immunol* **10**: 97-121.
- Reth, M. (2001). "Oligomeric antigen receptors: a new view on signaling for the selection of lymphocytes." *Trends Immunol* **22**(7): 356-60.
- Rice, T. W. and G. R. Bernard (2005). "Therapeutic intervention and targets for sepsis." *Annu Rev Med* **56**: 225-48.
- Richter, G., M. Hayden-Ledbetter, et al. (2001). "Tumor necrosis factor-alpha regulates the expression of inducible costimulator receptor ligand on CD34(+) progenitor cells during differentiation into antigen presenting cells." *J Biol Chem* **276**(49): 45686-93.
- Riedemann, N. C., R. F. Guo, et al. (2003). "The enigma of sepsis." *J Clin Invest* **112**(4): 460-7.
- Riley, J. L., P. J. Blair, et al. (2001). "ICOS costimulation requires IL-2 and can be prevented by CTLA-4 engagement." *J Immunol* **166**(8): 4943-8.
- Rottman, J. B., T. Smith, et al. (2001). "The costimulatory molecule ICOS plays an important role in the immunopathogenesis of EAE." *Nat Immunol* **2**(7): 605-11.
- Rutitzky, L. I., E. Ozkaynak, et al. (2003). "Disruption of the ICOS-B7RP-1 costimulatory pathway leads to enhanced hepatic immunopathology and increased gamma interferon production by CD4 T cells in murine schistosomiasis." *Infect Immun* **71**(7): 4040-4.
- Saenz, J. J., J. J. Izura, et al. (2001). "Early prognosis in severe sepsis via analyzing the monocyte immunophenotype." *Intensive Care Med* **27**(6): 970-7.
- Salomon, B., D. J. Lenschow, et al. (2000). "B7/CD28 costimulation is essential for the homeostasis of the CD4+CD25+ immunoregulatory T cells that control autoimmune diabetes." *Immunity* **12**(4): 431-40.
- Samelson, L. E. (2002). "Signal transduction mediated by the T cell antigen receptor: the role of adapter proteins." *Annu Rev Immunol* **20**: 371-94.
- Schreiner, B., J. Wischhusen, et al. (2003). "Expression of the B7-related molecule ICOSL by human glioma cells in vitro and in vivo." *Glia* **44**(3): 296-301.
- Schwacha, M. G., L. T. Holland, et al. (2005). "Genetic variability in the immune-inflammatory response after major burn injury." *Shock* **23**(2): 123-8.
- Shahbazian, L. M., M. Jeevanandam, et al. (1999). "Release of proinflammatory cytokines by mitogen-stimulated peripheral blood mononuclear cells from critically ill multiple-trauma victims." *Metabolism* **48**(11): 1397-401.
- Sharpe, A. H. and G. J. Freeman (2002). "The B7-CD28 superfamily." *Nat Rev Immunol* **2**(2): 116-26.
- Shimizu, J., S. Yamazaki, et al. (2002). "Stimulation of CD25(+)CD4(+) regulatory T cells through GITR breaks immunological self-tolerance." *Nat Immunol* **3**(2): 135-42.
- Smail, N., A. Messiah, et al. (1995). "Role of systemic inflammatory response syndrome and infection in the occurrence of early multiple organ dysfunction syndrome following severe trauma." *Intensive Care Med* **21**(10): 813-6.
- Smith, K. M., J. M. Brewer, et al. (2003). "Inducible costimulatory molecule-B7-related protein 1 interactions are important for the clonal expansion and B cell helper functions of naive, Th1, and Th2 T cells." *J Immunol* **170**(5): 2310-5.

- Spittler, A. and E. Roth (2003). "Is monocyte HLA-DR expression predictive for clinical outcome in sepsis?" *Intensive Care Med* **29**(8): 1211-2.
- Sporici, R. A., R. L. Beswick, et al. (2001). "ICOS ligand costimulation is required for T-cell encephalitogenicity." *Clin Immunol* **100**(3): 277-88.
- Suh, W. K., A. Tafuri, et al. (2004). "The inducible costimulator plays the major costimulatory role in humoral immune responses in the absence of CD28." *J Immunol* **172**(10): 5917-23.
- Swallow, M. M., J. J. Wallin, et al. (1999). "B7h, a novel costimulatory homolog of B7.1 and B7.2, is induced by TNFalpha." *Immunity* **11**(4): 423-32.
- Tafuri, A., A. Shahinian, et al. (2001). "ICOS is essential for effective T-helper-cell responses." *Nature* **409**(6816): 105-9.
- Tang, Q., K. J. Henriksen, et al. (2003). "Cutting edge: CD28 controls peripheral homeostasis of CD4+CD25+ regulatory T cells." *J Immunol* **171**(7): 3348-52.
- Taylor, P. A., C. J. Lees, et al. (2004). "B7 expression on T cells down-regulates immune responses through CTLA-4 ligation via T-T interactions [corrections]." *J Immunol* **172**(1): 34-9.
- Tesciuba, A. G., S. Subudhi, et al. (2001). "Inducible costimulator regulates Th2-mediated inflammation, but not Th2 differentiation, in a model of allergic airway disease." *J Immunol* **167**(4): 1996-2003.
- Tezuka, K., T. Tsuji, et al. (2000). "Identification and characterization of rat AILIM/ICOS, a novel T-cell costimulatory molecule, related to the CD28/CTLA4 family." *Biochem Biophys Res Commun* **276**(1): 335-45.
- Tschaikowsky, K., M. Hedwig-Geissing, et al. (2002). "Coincidence of pro- and anti-inflammatory responses in the early phase of severe sepsis: Longitudinal study of mononuclear histocompatibility leukocyte antigen-DR expression, procalcitonin, C-reactive protein, and changes in T-cell subsets in septic and postoperative patients." *Crit Care Med* **30**(5): 1015-23.
- Tsiagbe, V. K., G. Inghirami, et al. (1996). "The physiology of germinal centers." *Crit Rev Immunol* **16**(4): 381-421.
- Van Amersfoort, E. S., T. J. Van Berkel, et al. (2003). "Receptors, mediators, and mechanisms involved in bacterial sepsis and septic shock." *Clin Microbiol Rev* **16**(3): 379-414.
- van Berkel, M. E., E. H. Schrijver, et al. (2005). "ICOS contributes to T cell expansion in CTLA-4 deficient mice." *J Immunol* **175**(1): 182-8.
- van der Poll, T. (2001). "Immunotherapy of sepsis." *Lancet Infect Dis* **1**(3): 165-74.
- van Dissel, J. T., P. van Langevelde, et al. (1998). "Anti-inflammatory cytokine profile and mortality in febrile patients." *Lancet* **351**(9107): 950-3.
- Vella, A. T., T. Mitchell, et al. (1997). "CD28 engagement and proinflammatory cytokines contribute to T cell expansion and long-term survival in vivo." *J Immunol* **158**(10): 4714-20.
- Vermeiren, J., J. L. Ceuppens, et al. (2004). "Human T cell activation by costimulatory signal-deficient allogeneic cells induces inducible costimulator-expressing anergic T cells with regulatory cell activity." *J Immunol* **172**(9): 5371-8.
- Villegas, E. N., L. A. Lieberman, et al. (2002). "A role for inducible costimulator protein in the CD28-independent mechanism of resistance to *Toxoplasma gondii*." *J Immunol* **169**(2): 937-43.
- Wahl, P., R. Schoop, et al. (2002). "Renal tubular epithelial expression of the costimulatory molecule B7RP-1 (inducible costimulator ligand)." *J Am Soc Nephrol* **13**(6): 1517-26.
- Wakefield, C. H., P. D. Carey, et al. (1993). "Changes in major histocompatibility complex class II expression in monocytes and T cells of patients developing infection after surgery." *Br J Surg* **80**(2): 205-9.
- Wallin, J. J., L. Liang, et al. (2001). "Enhancement of CD8+ T cell responses by ICOS/B7h costimulation." *J Immunol* **167**(1): 132-9.
- Wang, S., G. Zhu, et al. (2000). "Costimulation of T cells by B7-H2, a B7-like molecule that binds ICOS." *Blood* **96**(8): 2808-13.
- Wang, S., G. Zhu, et al. (2002). "Ligand binding sites of inducible costimulator and high avidity mutants with improved function." *J Exp Med* **195**(8): 1033-41.
- Wassink, L., P. L. Vieira, et al. (2004). "ICOS expression by activated human Th cells is enhanced by IL-12 and IL-23: increased ICOS expression enhances the effector function of both Th1 and Th2 cells." *J Immunol* **173**(3): 1779-86.
- Weighardt, H., C. D. Heidecke, et al. (2000). "Sepsis after major visceral surgery is associated with sustained and interferon-gamma-resistant defects of monocyte cytokine production." *Surgery* **127**(3): 309-15.

- Wiendl, H., M. Mitsdoerffer, et al. (2003). "Human muscle cells express a B7-related molecule, B7-H1, with strong negative immune regulatory potential: a novel mechanism of counterbalancing the immune attack in idiopathic inflammatory myopathies." *Faseb J* **17**(13): 1892-4.
- Wiendl, H., M. Mitsdoerffer, et al. (2003). "Muscle fibres and cultured muscle cells express the B7.1/2-related inducible co-stimulatory molecule, ICOSL: implications for the pathogenesis of inflammatory myopathies." *Brain* **126**(Pt 5): 1026-35.
- Wilfinger, W. W., K. Mackey, et al. (1997). "Effect of pH and ionic strength on the spectrophotometric assessment of nucleic acid purity." *Biotechniques* **22**(3): 474-6, 478-81.
- Wolfe, J. H., A. V. Wu, et al. (1982). "Anergy, immunosuppressive serum, and impaired lymphocyte blastogenesis in burn patients." *Arch Surg* **117**(10): 1266-71.
- Wolk, K., W. D. Docke, et al. (2000). "Impaired antigen presentation by human monocytes during endotoxin tolerance." *Blood* **96**(1): 218-23.
- Wong, S. C., E. Oh, et al. (2003). "Impaired germinal center formation and recall T-cell-dependent immune responses in mice lacking the costimulatory ligand B7-H2." *Blood* **102**(4): 1381-8.
- Wu, J. Z., C. K. Ogle, et al. (1995). "The increased potential for the production of inflammatory cytokines by Kupffer cells and splenic macrophages eight days after thermal injury." *Inflammation* **19**(5): 529-41.
- Yoshinaga, S. K., J. S. Whoriskey, et al. (1999). "T-cell co-stimulation through B7RP-1 and ICOS." *Nature* **402**(6763): 827-32.
- Yoshinaga, S. K., M. Zhang, et al. (2000). "Characterization of a new human B7-related protein: B7RP-1 is the ligand to the co-stimulatory protein ICOS." *Int Immunol* **12**(10): 1439-47.
- Zang, Y., S. M. Dolan, et al. (2004). "Burn injury initiates a shift in superantigen-induced T cell responses and host survival." *J Immunol* **172**(8): 4883-92.
- Zuberek, K., V. Ling, et al. (2003). "Comparable in vivo efficacy of CD28/B7, ICOS/GL50, and ICOS/GL50B costimulatory pathways in murine tumor models: IFNgamma-dependent enhancement of CTL priming, effector functions, and tumor specific memory CTL." *Cell Immunol* **225**(1): 53-63.

Eidesstattliche Erklärung

Hiermit erkläre ich, dass ich die vorliegende Dissertation selbständig verfaßt und keine anderen als die angegebenen Hilfsmittel benutzt habe.

Die Dissertation ist bisher keiner anderen Fakultät vorgelegt worden.

Ich erkläre, dass ich bisher kein Promotionverfahren erfolglos beendet habe und dass eine Aberkennung eines bereits erworbenen Doktorgrades nicht vorliegt.

Datum
30.11.2006

Unterschrift

Curriculum vitae

Ionela Moanta

Date of birth: 10.03.1976

Place of birth: Craiova, Romania

Educational Background:

1990-1994 "Nicolae Balcescu" Theoretical High School, Craiova, Romania

1994-1998 B.S. Biology, University of Bucharest, Romania

1999-2001 M.S. Genetics, University of Bucharest and Center of Immunology, Institute of Virology, Bucharest, Romania

2002-2005 PhD Immunology, Ernst-Moritz Arndt University of Greifswald, Germany

Professional experience

2000-2002 Research Asst., Institute of Genetics, University of Bucharest, Romania

2002-2005 Research Asst., Institute of Immunology and Transfusion Medicine, Ernst-Moritz Arndt University of Greifswald

Publications:

- L. Popa, **Ionela Moanta**, Florina Raicu, D. Cimponeriu, Gabriela Bordeianu, Pompilia Apostol, Letitia Dan, Olivia Popa, *Human Genome Organization*, Advances in Biotechnology, Vol.3, 285-303, Bucharest, 2001
- L. Popa, **Ionela Moanta**, Florina Raicu, D. Cimponeriu, Gabriela Bordeianu, Pompilia Apostol, Letitia Dan, Olivia Popa, *Hemoglobinopathies and Thalassemias*, Advances in Biotechnology, Vol.3, 285-303, Bucharest, 2001
- Pompilia Apostol, Florina Raicu, Gabriela Bordeianu, **Ionela Moanta**, Danut Cimponeriu, Luis O. Popa, *The ethiology of prionic diseases*, Advances in Biotechnology, Vol.2, 91-99, Bucharest, 2002
- **Ionela Moanta**, *Nucleic acids and protein electrophoresis*, in **Genomics** (Lucian Gavrilă ed.), Romanian Academy Publishing House, Bucharest, 2003
- M. Dumitrescu, R. Ion, **I. Moanta**, P. Apostol, D. Cimponeriu, *DNA conformations*, in **Genomics**, (Lucian Gavrilă ed.), Romanian Academy Publishing House, Bucharest, 2003

Poster presentations:

- Baiu D.C., **Moanta I.**, Van den Herik Oudijk, *Intracellular signal sequences of FcR*, Annual Scientific Meeting of The Institute of Biochemistry, Bucharest, Romania, September, 2000
- Luis Popa, **Ionela Moanta**, Florina Raicu, Dan Cimponeriu, Olivia Popa, *The alphoid heteroduplex polymorphism in sample populations from South Moldavia (Romania)*, The Second National Symposium (with international participation): "Bioethical and scientific implications in genome analysis and manipulation", Bucharest, October 2-3, 2001

- Gabriela Bordeianu, Lucian Gavrilă, Luis Popa, **Ionela Moanta**, Florina Raicu, *Gene therapy for chronic myelogenous leukemia*, The Second National Symposium (with international participation): "Bioethical and scientific implications in genome analysis and manipulation", Bucharest, October 2-3, 2001
- Florina Raicu, Lucian Gavrilă, Gabriela Bordeianu, Luis Popa, **Ionela Moanta**, Dan Cimponeriu, Pompilia Apostol, Letitia Dan, *Males with idiopathic sterility: analysis of the genes controlling spermatogenesis located on the human Y chromosome*, The Second National Symposium (with international participation): "Bioethical and scientific implications in genome analysis and manipulation", Bucharest, October 2-3, 2001
- Luis Popa, **Ionela Moanta**, Florina Raicu, Dan Cimponeriu, Pompilia Apostol, Gabriela Bordeianu, Lucian Gavrilă. *Alphoid Heteroduplex polymorphism in sample population of Romania*, Human Genome Meeting, Shanghai, China, April 14-17, 2002.
- **I Moanta**, A. Sulica, D. C. Baiu. *FcγIIb receptors on Jurkat T cells*. Euroconference, Goehren-Lebbin, Germany, June 5-8, 2002
- **I Moanta**, A. Dressel, M. Gruendling, U. Grunwald, S.O. Kuhn, B. M. Broeker. *Involvement of ICOS/ICOS-L in immunosuppression in ICU patients*. Euroconference, Joachimstahl, Germany, June 2-5, 2005.

Datum

30.11.2006

Unterschrift